

**Large-scale Separation and Wake
Closure/Reattachment -- The Cascade Problem¹**

F.T. Smith²
Research Report YALEU/CSD/RR-281
August 1983

¹Published simultaneously by United Technologies Research Center as report UTRC83-13

²Mathematics Department, Imperial College, London. This work was done while at the Yale Research Center for Scientific Computation and the United Technologies Research Center. It was supported in part by the U.S. Office of Naval Research contracts #N000014-82-K-0184 and #N000014-81-C-0381.

Large-Scale Separation and Wake
Closure/Reattachment - The Cascade Problem

TABLE OF CONTENTS

	<u>Page</u>
FOREWORD	1
ABSTRACT	2
<u>PART I - THE FINITE-SPREAD CASCADE</u>	
I-1 INTRODUCTION	3
I-2 THEORETICAL FLOW DEVELOPMENT	5
I-3 NUMERICAL TREATMENT OF CLOSURE/REATTACHMENT	12
I-4 RESULTS AND DISCUSSION	14
<u>PART II - THE WIDE-SPREAD CASCADE AND EXTERNAL FLOW</u>	
II-1 INTRODUCTION	17
II-2 ON LENGTH SCALES FOR THE WIDE-SPREAD CASCADE	19
II-3 THE LONG EDDY	24
II-4 SHORTER EDDIES	26
II-5 ON PRESSURE-FREE VISCOUS WAKES	33
II-6 ON MASSIVE EDDY CLOSURE AND REATTACHMENT ONTO A SOLID SURFACE	39
II-7 CONNECTION FROM WIDESPREAD CASCADE TO EXTERNAL FLOW; AND HOW FAR CAN THE KIRCHHOFF PARABOLA LAST?	42
II-8 NON-ENTRAINING SHEAR LAYERS	51
II-9 FURTHER COMMENTS	58
REFERENCES	60

TABLE OF CONTENTS (Cont'd)

	<u>Page</u>
APPENDIX A - A MECHANISM FOR UPSTREAM INFLUENCE	61
APPENDIX B - FURTHER UPSTREAM INFLUENCE	64
APPENDIX C - SIGNIFICANT VISCOUS INFLUENCE IN LARGE-SCALE REVERSED FLOW . .	66
APPENDIX D - EXPONENTIAL BEHAVIOR IN REVERSED MOTIONS	68
APPENDIX E - VISCOUS WAKE CLOSURE WITH PRESSURE FORCING	70

FOREWORD

The majority of this work was performed at United Technologies Research Center, East Hartford, Connecticut, during the summer of 1981 while the author was on leave from the Mathematics Department, Imperial College, London, SW7 2BZ, U.K., and at Imperial College and the Research Center for Computational Science, Yale University, during the summer of 1982. Thanks are due to Dr. M. J. Werle for his encouragement, interest and valuable comments concerning this work; to Dr. R. E. Whitehead for his interest and support under ONR Contract N00014-81-C-0381; to the United Technologies Research Center for their support of portions of this work; and to Professor M. Schultz and the Yale Research Center for Computer Science for further support, interest and helpful comments.

ABSTRACT

This work aims at application in both internal and external flows. An analytical and computational study is described which attempts ultimately to uncover the nature of the flow structure surrounding the wake closure region of a long recirculatory eddy following separation off an isolated aerodynamic element. This problem area forms a critical element in the development of a formally rational model for a massive separation eddy at large Reynolds number. An approach is developed here for addressing the external aerodynamic problem through a family of internal, cascade flow, solutions with increasing gap spacing. Each element of this family is formally correct, thus providing a basis for systematic study of the desired limit case of an infinite gap spacing.

The study is in two parts. Part I presents the structure for finite gap spacing and the corresponding computational results. Part II discusses the possible flow structures emerging for widely spaced cascades and their connection with, and implications for, the external aerodynamic flow.

PART I - THE FINITE-SPREAD CASCADE

I-1. INTRODUCTION

The study of the fluid flow at high Reynolds number through a cascade of bluff bodies is useful, it is believed, for two major reasons. First, the resultant predictions should have some relevance to the performance of the cascade itself, serving in some sense as a model for flow past compressor and turbine blades, in heat exchangers, and in other interactive body configurations. In practice, the resulting breakdown of mainly attached flow can have severe consequences and so the predicted drag and eddy lengths, among other things, are of immediate concern. The second major reason for considering the cascade configuration is that it provides an alternative means of gaining extra insight into the properties of external motions. The main such properties are attained when the cascade becomes widely spaced apart. Since, as shown here, the understanding of the separated flow structure produced by the cascade configuration can be completed, this establishes a firm basis, therefore, for advancing gradually toward an understanding of the still not fully known structure of external flow past a bluff body (whereas direct analysis is hounded by nonuniqueness and nonlinearity). In the latter case the most puzzling issue concerns reattachment, or the closure of the recirculating eddy or eddies behind the body; fortunately, the nature of the reattachment(s) behind a cascade is one of the most important issues of the cascade problem, too.

The present theoretical work supposes the Reynolds number Re to be large, the fluid to be incompressible and its motion to be steady, laminar and two-dimensional. There is a possible application [1981, M. J. Werle, private communications] of the theory to turbulent flow also, however, with regard to the reattachment process. The whole cascade is taken to be infinite in extent, and symmetric, so that only the flow past the upper half of one body needs to be discussed provided the relevant lines of symmetry are present (see Fig. 1). In nondimensional terms the chord of the bluff body is 1, the given cascade spacing H_c is finite, of $O(1)$, the uniform freestream speed is $u = 1$, and the velocities, corresponding Cartesian coordinates, stream function, flow speed and pressure are (u,v) , (x,y) , ψ , q , p , respectively. The pressure level far upstream is normalized to zero. The body is "bluff" in the sense that its typical thickness is allowed to be $O(1)$ and its trailing edge, possibly wedged or blunt, is not cusped.

The separated flow structure is described in Section I-2 below and consists of the body scale flow and the long eddy or reattachment scale flow, considered in turn. The Kirchhoff free streamline solution with a slowly moving eddy gives the dominant self-consistent account of the body scale flow, which leads to a constant $O(1)$ eddy width H_w downstream. The eddy is then closed, yielding reattachment, on a longer $O(Re)$

length scale downstream. There, across the whole flow, the boundary layer equations with unknown pressure control matters, with the viscous forces preventing any strong backward jet from arising, and so overall self-consistency is achieved. The reattachment problem depends only on the ratio $H \equiv H_w/H_c$ (see Fig. 1) and its numerical treatment is outlined in Section I-3. The treatment involves a three-regioned scheme, designed to acknowledge the three-layered form of the starting solution where the initial velocity profile is discontinuous, and windward-differencing to accommodate the upstream influence within the reversed flow. The main results obtained are presented for a range of values of $H = H_w/H_c$, the nondimensional eddy half thickness. Finally, Section I-4 presents our interim comments, preparatory for Part II, including the connection with external flow obtained when H tends to zero and certain possibilities regarding upstream influence in shear layers.

It is worth remarking here that the present reattachment problem opens probably one of the most direct ways of approaching the puzzle of large-scale external reattachment: see also Part II. The way seems easier or more direct than in triple-deck calculations for instance. At the same time, the results for finite cascade spacing could provide some helpful applications.

I-2. THEORETICAL FLOW DEVELOPMENT

On the body scale, where x, y are $O(1)$, the separated flow structure is of the inviscid Kirchhoff, free-streamline, type to leading order with appropriate extensions (see Refs. 1, 2) to include the effects of viscosity. So the following properties (a) - (i) hold.

- (a) The relative error in the dominant inviscid solution is $O(\text{Re}^{-1/16})$; see also (e) below. Thus,

$$(u, \psi, p) = (u_0, \psi_0, p_0) + \text{Re}^{-1/16} (u_1, \psi_1, p_1) + \dots \quad (\text{I-2.1})$$

where u_0, ψ_0, p_0 is the Kirchhoff from (see sketch in Fig. 1).

- (b) The dominant solution u_0, ψ_0, p_0 then satisfies the condition of uniform pressure on the separating streamline $\psi = 0, y = S_0(x)$ (Fig. 1), so that

$$P_0 = C_0 \text{ on } y = S_0(x) \quad (\text{I-2.2})$$

Here $2C_0 = [1 - ((H_c/H_w) / (H_c/H_w - 1))^2]$ is a negative constant, from Bernoulli's theorem and mass conservation considerations, with H_w being defined in Fig. 1 and in (g) below.

- (c) Within the eddy between the separating streamline and the x -axis, the velocities are small, $|q| \ll 1$, and in particular $u_0 = \psi_0 \equiv 0, P_0 \equiv C_0$. It is possible that in fact $|q|$ is as low as $O(\text{Re}^{-1/2})$ in the eddy but that is the least value possible, due to entrainment, and the principal contention of the theory does not yet need to be made more specific than $u_0 \equiv 0$.
- (d) On the body, between the front stagnation point and the separation point, the pressure gradient is favorable, forcing automatically an attached $O(\text{Re}^{-1/2})$ boundary layer there.
- (e) The viscous separation process is local, of the interactive triple-deck form (see Refs. 1-3), and that is responsible (Ref. 1) for the relatively large correction required in Eq. (I-2.1).

- (f) The viscous shear layer surrounding the separating streamline has thickness $O(\text{Re}^{-1/2})$ and is subjected to uniform external velocities of $q \approx H_c / (H_c - H_w)$ and $q \approx 0$ at its upper and low extremes, respectively. At its start, immediately beyond the separation point, it matches (Ref. 1) with the interactive separation process of (e). At its other end, as $x \rightarrow \infty$, its $O(\text{Re}^{-1/2})$ thickness grows like $x^{1/2}$ as the Chapman similarity form is acquired.
- (g) The eddy width $S_o(x)$ tends to a constant H_w downstream as $x \rightarrow \infty$: c.f. the unbounded growth of external flow (Refs. 1, 2). Here H_w depends only on the cascade spacing H_c , for a given body shape, and is related to the principal drag C_D on the body.
- (h) If H_c is large for a given body shape, then the dominant inviscid solution effectively subdivides. First, for $O(1)$ values of x, y the Kirchhoff form for external flow is retrieved as the presence of all the other bodies becomes negligible, to leading order. So the unbounded growth $S_o(x) \sim (4 C_D / \pi)^{1/2} x^{1/2}$ is retrieved downstream as $x \rightarrow \infty$ on that inner subscale. Second, however, the presence of the $O(H_c)$ distant confinement reasserts itself on an outer subscale when x is $O(H_c)$, with $S_o(x)$ then being $O(H_c^{1/2})$ for consistency. The adjustment there is similar to that described in the appendix of Ref. 1, the earlier unbounded growth is gradually halted and as a result the constant eddy width H_w is achieved when $x \gg H_c$. See also Part II. The property found is that

$$H_w \propto H_c^{1/2} \text{ when } H_c \text{ is large.} \quad (\text{I-2.3})$$

A like feature holds in effect if the cascade spacing H_c is kept fixed and the body size is reduced appreciably instead.

- (i) Some inviscid aspects of the above structure are considered in some textbooks (see, for example, Ref. 9).

The structure of the body scale flow above is believed to be entirely self-consistent with regard to the Navier-Stokes equations. We are left now with the task of describing the ultimate wake closure process further downstream, beyond the body scale, as the recirculatory eddy has to close and the motion then returns to its uniform state eventually. The closure or reattachment takes place on the longer $O(\text{Re})$ length scale in x downstream, since then the shear layer thickness of (f) above grows to $O(1)$. So the expressions

$$(u, \psi, p) = (U^*, \psi^*, p^*) + \dots, \text{ with } x = \text{Re } X^*, y = O(1) \quad (\text{I-2.4})$$

hold in the closure phase, with the Navier-Stokes equations thereby reducing to the classical boundary layer equations (as in Refs. 4-6), for $X^* > 0$,

$$U^* = \frac{\partial \psi^*}{\partial y}, \quad U^* \frac{\partial U^*}{\partial X^*} - \frac{\partial \psi^*}{\partial X^*} \frac{\partial U^*}{\partial y} = - \frac{dP^*}{dX^*} + \frac{\partial^2 U^*}{\partial y^2}, \quad (\text{I-2.5a})$$

with P^* dependent only on X^* . The formal relative error involved in Eq. (I-2.5a) is remarkably small, of the order Re^{-2} . The starting conditions required are those of a step-like velocity profile initially:

$$\text{at } X^* = 0+, \quad U^* = \begin{cases} 0 & \text{for } 0 \leq y < H_W \\ H_c / (H_c - H_W) & \text{for } H_W < y \leq H_c, \end{cases} \quad (\text{I-2.5b})$$

to match with the slow eddy velocity and the Kirchhoff solution closer to the body. The boundary conditions in y are

$$\psi^* = \partial U^* / \partial y = 0 \text{ at } y = 0 \quad (\text{I-2.5c})$$

$$\psi^* = H_c, \quad \partial U^* / \partial y = 0 \text{ at } y = H_c, \quad (\text{I-2.5d})$$

for $X^* \geq 0$, from the cascade symmetry. The induced pressure $P^*(X^*)$ is unknown.

The basic closure problem is totally contained in Eqs. (I-2.5a-d), which require a numerical solution. The present standpoint is that the overall theory is complete since the presence of significant viscous forces, in Eq. (I-2.5a), during the closure is always sufficient to allow the constraint of Eq. (I-2.5b) to be met. This constraint is necessary to prevent a strong backward jet from entering the body scale flow and provided that is satisfied the earlier structure then remains intact. The crucial action of viscosity here is due to the flow confinement caused by the cascade symmetry, which in turn restricts the lateral distance y to $O(1)$ values. This is in direct contrast to the extensive dimensions reached by external eddies (according to the same theory) where the influence of viscosity is correspondingly much less clear and where in consequence our understanding has still to be completed (see also Section I-4 and Part II for further discussion of the point). Five main features of the current closure problem can be delineated, in (1)-(5) below, in terms of the renormalized form of the governing equations

$$U = \frac{\partial \psi}{\partial Y}, \quad U \frac{\partial U}{\partial X} - \frac{\partial \psi}{\partial X} \frac{\partial U}{\partial Y} = - \frac{dP^*}{dX} + \frac{\partial U^2}{\partial Y^2} \quad (\text{I-2.6a})$$

$$\text{at } X = 0+, \quad P^* = C_0, \quad U = \begin{cases} 0 & \text{for } 0 \leq Y < H \\ 1/(1-H) & \text{for } H < Y \leq 1 \end{cases} \quad (\text{I-2.6b})$$

$$\psi = \partial U / \partial Y = 0 \text{ at } Y = 0 \quad (\text{I-2.6d})$$

$$\psi = 1, \quad \partial U / \partial Y = 0 \text{ at } Y = 1 \quad (\text{I-2.6e})$$

obtained by setting, in Eq. (I-2.5ad),

$$(U^*, \psi^*, P^*, X^*, y) = (U, H_c \psi, P^*, H_c^2 X, H_c Y), \quad (\text{I-2.7})$$

with

$$H \equiv H_w / H_c. \quad (\text{I-2.8})$$

defining the governing parameter H.

- (1) The solution depends only on the parameter H, the ratio of the incoming eddy width to the cascade spacing.
- (2) Because of the initial discontinuous profile in Eqs. (I-2.6b,c) the solution is singular as $X \rightarrow 0+$, with the Chapman similarity form being recovered then. Thus, near $Y = H$, for small X,

$$\psi \sim X^{1/2} f_c(\eta) + \dots, \quad \text{with } \eta = (Y-H)/X^{1/2}, \quad (\text{I-2.9a})$$

where from Eqs. (I-2.6a-c) f_c satisfies the Blasius equation but with shear layer conditions:

$$f_c'''' + \frac{1}{2} f_c f_c'' = 0, \quad f_c'(\infty) = 1/(1-H), \quad f_c'(-\infty) = 0 \quad (\text{I-2.9b})$$

The solution of Eq. (I-2.9b) gives

$$f_c(-\infty) = -\kappa (1-H)^{-1/2} \quad (\text{I-2.9c})$$

where $\kappa = 1.24$, although there is an uncertainty in the origin for η (see also point (3) below).

- (3) The initial development of the solution for small X is three-layered but is not uniquely determined by local considerations. Generally, Eq. (I-2.9b) yields the property

$$f_c \sim (\eta - \eta_0) / (1-H) \text{ as } \eta \rightarrow \infty \quad (\text{I-2.9d})$$

where η_0 is an unknown constant origin shift. As a result, above the Chapman layer

$$\psi = \left(\frac{Y-H}{1-H} \right) + X^{1/2} \psi_{1/2}(Y) + \dots \quad (\text{I-2.10a})$$

for $H < Y < 1$, with Eqs. (I-2.6a,e) requiring

$$\psi_{1/2}(Y) = -(1-H) P_{1/2}(1-Y); P^* = C_0 - P_{1/2} X^{1/2} + \dots \quad (\text{I-2.10b})$$

Hence, from merging with Eq. (I-2.9d), we have

$$P_{1/2} = + \eta_0 / (1-H)^3 \quad (\text{I-2.10c})$$

Then, from the form of $P^*(X)$ in Eq. (I-2.10b), the solution below the Chapman layer has the expansion

$$\psi = X^{1/4} G(Y) + \dots \quad (\text{I-2.11a})$$

for $0 < Y < H$, since Eq. (I-2.6b) holds. Substituting Eqs. (I-2.11a) and (I-2.10b) into Eqs. (I-2.6a,d) and imposing $G(H-) = 0$ in view of Eq. (I-2.9a,c), it is found that

$$G(Y) = \pm (2 P_{1/2})^{1/2} \frac{H}{n\pi} \sin(n\pi Y/H) \quad (\text{I-2.11b})$$

where n is a positive integer. Physical sense and other considerations (see Ref. 5) suggest that $n = 1$ here and then the $-$ sign is the appropriate one. The constant η_0 remains undetermined throughout; moreover, an even larger origin shift in Y itself is possible in Eq. (I-2.9a). If $\eta_0 = 0$ then nonuniqueness can still arise in higher order terms of the three-layered expansion Eqs. (I-2.9a), (I-2.10a) and (I-2.11a). A special case however is that with $\eta_0 = 0$ and with the flow below the Chapman layer being forced by the entrainment conditions, Eq. (I-2.9c), giving

$$\psi = -\kappa X^{1/2} (1-H)^{-1/2} Y/H + \dots \quad (\text{I-2.12a})$$

there, which requires the pressure expansion to be

$$P^* = C_0 - \frac{1}{2} \frac{\kappa^2}{(1-H)H^2} X + \dots \quad (\text{I-2.12b})$$

Along with Eq. (I-2.12a,b) we then have

$$\psi = \left(\frac{Y-H}{1-H} \right) + X \frac{\kappa^2 (Y-1)}{2 H^2} + \dots \quad (\text{I-2.12c})$$

above the Chapman layer.

- (4) It follows from point (3) above that reversed flow is present immediately in $X > 0$, below the Chapman layer. This feature also seems in line with the nonuniqueness arising above since the governing equations are locally parabolic in the flow direction, yielding upstream influence throughout $0 < X < X_{\text{reatt}}$ where $X = X_{\text{reatt}}$ is the closure position.
- (5) Downstream, as $X \rightarrow \infty$, the uniform state is recovered with $U \rightarrow 1$. But for all X the integrated momentum balance

$$P^*(X) + \int_0^1 U^2(X, Y) dY = C_0 + 1/(1-H) \quad (\text{I-2.13})$$

holds, from Eq. (I-2.6a-3). Therefore the asymptotes

$$U \rightarrow 1, P^* \rightarrow -\frac{1}{2} \left(\frac{H}{1-H} \right)^2 \text{ as } X \rightarrow \infty \quad (\text{I-2.14})$$

give the far downstream behavior.

Henceforth we deal with the modified pressure $P \equiv P^* - C_0$, for convenience.

I-3. NUMERICAL TREATMENT OF CLOSURE/REATTACHMENT

The aspects of points (2), (3) and (4) noted above - the singularity due to the discontinuous initial profile, the initial three-layered structure and the upstream influence in the reversed flow - would seem to be so fundamental to the closure problem that a satisfactory numerical treatment must acknowledge them ultimately. Perhaps the most important aspect however is that of point (4), which requires a numerical treatment to be not solely forward-marching. To accommodate reversed flow we used a windward-differencing approach (see e.g., Ref. 7). This was used within three progressively more refined schemes I, II, III: scheme I adopted uniform differencing in X, Y; scheme II adopted differencing in coordinates sketched in the X, Y directions; and scheme III applied a three-region technique (Refs. 5 and 8) to allow also for the features of points (2), (3) above. All three schemes proved convergent with the windward differences included, but we focus henceforth on the nominally most accurate one, scheme III.

The computational domain was split into three regions A-C, in line with point (3) above. Region A was taken to be in effect below the middle Chapman region B and Region C was taken above it (see Fig. 2). A new variable $\xi \equiv X^{1/2}$ is defined in A, with $\psi = g(\xi, Y)$, $U = c(\xi, Y)$, $\partial U / \partial Y = e(\xi, Y)$, leaving the first order governing equations as

$$c = \frac{\partial g}{\partial Y}, \quad e = \frac{\partial c}{\partial Y}, \quad c \frac{\partial c}{\partial \xi} - \frac{\partial g}{\partial \xi} e = -\frac{dP}{d\xi} + 2\xi \frac{\partial e}{\partial Y} \quad (\text{I-3.1a})$$

from Eq. (I-2.6a), with the boundary conditions from Eq. (I-2.6d) as

$$g = e = 0 \text{ at } Y = 0 \quad (\text{I-3.1b})$$

In B, the variables were written $\psi = \xi f(\xi, \eta)$, $U = s(\xi, \eta)$, $\partial U / \partial Y = \xi^{-1} t(\xi, \eta)$ because of Eq. (I-2.9a), so that here the equations become

$$s = \frac{\partial f}{\partial \eta}, \quad t = \frac{\partial s}{\partial \eta}, \quad \frac{\partial t}{\partial \eta} + \frac{1}{2} f t = \frac{1}{2} \xi \left[s \frac{\partial s}{\partial \xi} - t \frac{\partial f}{\partial \xi} + dP/d\xi \right]. \quad (\text{I-3.2})$$

Then in C the solution has the same structure as in A, giving Eq. (I-3.1a) again but with the boundary conditions from Eq. (I-2.6e) as

$$g = 1, \quad e = 0 \text{ at } Y = 1. \quad (\text{I-3.3})$$

At any station ξ the three regions are inter-linked (Ref. 8) by ensuring that ψ , U , $\partial U/\partial Y$ are all continuous at the upper and lower boundaries $\eta = \eta_{\pm\infty}$, $Y = H + \eta_{\pm\infty} \cdot \xi$, of region B. Uniform differencing in η or Y as appropriate is applied to Eqs. (I-3.1a) and (I-3.2) and, with the 4 conditions of Eqs. (I-3.1b) and (I-3.3) and the 6 inter-linking relations, sufficient information exists to determine the solution at that ξ station upon applying (Ref. 8) Newton iteration, matrix inversion and knowing the solution at the stations $\xi \pm \Delta\xi$. The differencing in the ξ direction is allowed to account for the local flow direction however, consistent with the reversed local influence. If $U > 0$ then the value of U is made to depend on the value at $\xi - \Delta\xi$, as obtained with differences for $U\partial U/\partial X$ centered at $\xi - \Delta\xi/2$. If $U < 0$ then the latest known values at ξ , $\xi + \Delta\xi$ are used instead with a forward difference for $U\partial U/\partial X$. The starting solution at $\xi = 0$ is set in the obvious way for regions A, C whereas that for region B requires solving Eq. (I-3.2) at $\xi = 0$, i.e., solving the Chapman form of Eq. (I-2.9b) there.

The domain is swept and updated N times, each sweep passing from $\xi = 0$ to a sufficiently far downstream location $\xi = \xi_{\infty}$ where Eq. (I-2.14) is effectively obtained, until the system converges. The convergence rate was accelerated in later trials by sweeping back and forth, marching from $\xi = 0$ to $\xi = \xi_{\infty}$, then marching back from ξ_{∞} to 0, and so on, which admits the upstream influence faster. The upstream influence enters the solution sweep-by-sweep through the windward-differencing of the term $U\partial U/\partial X$; note that the term in $\partial\psi/\partial X$ is not windward-differenced, thus allowing Eq. (I-2.6c) to have its necessary influence also. Various appropriate values of $\eta_{\pm\infty}, \Delta\xi$, of the steplengths $\Delta\eta$, ΔY in η , Y and of the Newton iterative tolerance were taken and tests on the accuracy of the results were made. Typically, satisfactory overall convergence is achieved when $N = 10$ for moderate values of H , although this increases for smaller values of H . Further comments are given in the next section.

I-4. RESULTS AND DISCUSSION

The main results obtained for various values of H between 0.9 and 0.2 are shown in Fig. 3-5. In most cases the constant η_0 of Eq. (I-2.9d) was chosen to be zero, with nonzero values having but a very small overall effect.

Figure 3(a) provides an overview of the flow behavior by monitoring the center line velocity, U_{CL} , and the top edge velocity, U_T , for relatively large values of H, corresponding to small cascade gap spacing. In all cases considered the closure process is seen to occur quite rapidly, with the normalized position of the centerline flow reversal always within half a gap width of the initial plane.

It is immediately striking from Figs. 3(a) and 3(b) that as H decreases the closure distance X_{reatt} shrinks very fast and that the minimum centerline velocity U_{min} decreases but less rapidly, while the flow properties near closure become more abrupt. For larger values of H the features are rather milder, in keeping with an asymptotic analysis which shows that

$$X_{reatt} \propto (1-H)^{-1/2}, \quad U_{min} \propto (1-H)^{-1/2}, \quad \text{as } H \rightarrow 1 -. \quad (\text{I-4.1})$$

The extreme smallness of X_{reatt} once H is less than about 1/3 is more clearly shown in Fig. 3(b) in terms of the centerline velocity behavior. This aspect of the flow adds to the computational task of course and in practice it was found to limit the applicability of the first two numerical schemes I, II noted in Section 3. It also emphasized the overriding need for accuracy in the calculations, for checks to be made on the effects of mesh size (see Figs.) and for the proper notice to be taken of the significant upstream influence. This last is more clearly demonstrated in Fig. 3(c) which compares the centerline velocity distributions with and without* upwind differencing in the reversed flow region.

The computational method and program appeared to work satisfactorily for moderate values of H but difficulties became pronounced as H decreased. This was due mainly to the relatively fast change in the solution near wake closure then and the resultant switching between forward and backward differences there, which led to characteristic oscillations from sweep-to-sweep of the flowfield. Incorporating relaxation in the updating per sweep, or fixing the choice of directional differencing for several sweeps, or refining/stretching the mesh near wake closure, all alleviated the problem somewhat but not permanently, and the same was found for other modifications made in view of certain analytical features for small H suggested

*This result is actually achieved in the first sweep of the iterative algorithm by zeroing out the longitudinal convective term for reversed flow, an idea originally introduced by Reyhner and Flügge-Lotz (Ref. 16).

by Part II below. The flow properties are better viewed perhaps in the streamline patterns and velocity profiles of Figs. 4(a)-(e), showing the increasingly rapid turning of the flow toward the wake closure point as H decreases from 0.9 to 0.25. Obviously as H decreases the computational difficulty is aggravated, raising serious concerns for the proper numerical modelling of the convective processes then.

The pressure response P and closure distance X_{reatt} are given in Fig. 5 for various values of H . It is noteworthy that $P(X_{reatt})$ is close to H and X_{reatt} is closely proportional to H^3 [see log-log plot] at the smaller values of H : c.f. Part II.

As regards the hope that an inkling of the unknown structure for external flow past a bluff body should emerge as H becomes small, the major questions perhaps concern the behavior of X_{reatt} and X_{min} (the position at which $U = U_{min}$), as $H \rightarrow 0$. We might expect both to tend to zero rapidly then, in line with the present numerical results (Figs. 3-5), but what matters is the rate of these trends*. Suppose, for instance, that $X_{reatt} \propto H^4$ as $H \rightarrow 0$. Then the unscaled closure distance, which is $x_{reatt} = Re H_c^2 X_{reatt}$ from Eqs. (I-2.4) and (I-2.7), remains $O(Re)$ as $H_c \rightarrow \infty$ with the body fixed, since Eqs. (I-2.8) and (I-2.3) link H to H_c then. Accordingly, the eddy length remains $O(Re)$ and that leads directly to the extended Kirchhoff account of external bluff body flow. If instead $X_{reatt} \propto H^6$ as $H \rightarrow 0$, however, then $x_{reatt} \propto Re H_c^2 H^6 \propto Re H_c^{-1}$ for $H_c \gg 1$ by similar reasoning. So then X_{reatt} falls to $O(1)$ as H_c is increased to $O(Re)$ (the order required for external flow properties to be most relevant: see Ref. 1) and that points strongly to the alternative Prandtl-Batchelor account for external flows. See also Part II.

Again, therefore, there is a call for sufficient accuracy in any further calculations at even smaller values of H , to help settle the matter of the external closure properties.

In the meantime, it is interesting that, on the body scale, the Kirchhoff solution for external flow does emerge as H_c becomes large and the maximum eddy width H_w increases without bound then. It would be remarkable if this process could be reversed, at greater cascade spacing, by the change in closure properties considered above. This issue is amplified in Part II.

Various features of the limit structure for the closure problem as $H \rightarrow 0$ are considered in Part II. A relatively thin detached shear layer tends to be promoted from the Chapman region then but the means of reversal of its entrained fluid (where $\psi < 0$) during closure at $X = X_{reatt}$ has to be established, given the requirement of effectively zero backflow at $X = 0+$. The means may involve a

*A less sensitive quantity to examine may be the ratio X_{min}/X_{reatt} which defines to some extent how local the reattachment process is for a given H . However, any indication of the correct limiting form for $H \rightarrow 0$ is useful.

localized strong interaction near the closure point, in view of the above discussion, which requires the detached shear layer to admit some upstream influence ahead of the closure. One kind of upstream influence studied is discussed in detail in Appendix A. There it is shown that upstream influence is possible (see Eqs. A-4a-f) and an interaction between the oncoming shear layer and the motion beneath it can start. The interaction is found to become nonlinear as \bar{X} becomes finite and it involves the setting up (due to \bar{U}_B) of a significant motion beneath the shear layer. The ultimate properties of this interaction could be significant and might enable the shear layer to rid itself of all the entrained fluid eventually, in readiness for the closure, for instance. Again further study of the consequences of the upstream interaction of Eqs. (A-1 - A-4g) below should be well worthwhile. Appendices B and C summarize other means of upstream influence. Like Appendix A they bring viscosity into play, the importance of which is stressed in Part II. They also have certain repercussions for separated flow stability. Another form of upstream influence which is currently under consideration and may be relevant is that occurring in separated flow as studied in Ref. 10, on the airfoil trailing edge stall/separation problem.

Whatever the limiting form of the present closure problem is as $H \rightarrow 0$, all the above serves to emphasize a major point: the resolution of the puzzle concerning large-scale external closure is contained within the standard boundary layer equations. We believe that still further examination on both the numerical and the analytical sides of the present basic topic could be very rewarding, therefore.

Part II below addresses the limit problem for $H \rightarrow 0$ and its connection with external flow.

PART II: THE WIDE-SPREAD CASCADE AND EXTERNAL FLOW

II-1. INTRODUCTION

Given the basic structure, results and guidelines for cascades of finite spread H^{-1} in Part I, our concern henceforth is with understanding the wake closure in a wide-spread cascade ($H \rightarrow 0$) and then its connection with the external motion past an isolated bluff body. There are two main contenders for the wake flow description, the Kirchhoff free-streamline solution (extended) and the Prandtl-Batchelor model. The latter tends to flounder for any slender wake, however, due to the lack of a sustained pressure gradient, whereas Kirchhoff's description already works apparently for the long slender wake of the finite-spread cascade. So the essential matter is whether or not the Kirchhoff solution continues to hold good for wide-spread cascades also.

Wide-spread cascades require analysis of just the boundary layer equations, from Part I, for wake closure as $H \rightarrow 0$, like the flow beyond a step-like trailing edge. This is started in Section II-2 below, which considers the underlying scales and sublayers implied. The Prandtl-Batchelor model can soon be ruled out. Indeed, near the wake centerline $Y = 0$ all inviscid mechanics fails to maintain consistency at wake closure, thus calling for significant viscous action. Section II-2 also stresses the $O(H)$ pressure rise P and $O(H^3)$ length scale in X suggested by the Part I calculations although the need for wake closure then is not definite. On the contrary, Section II-3 shows that self-consistency is apparently maintained by wake closure on the $O(1)$ scale in X , where the required viscous action comes into play accompanied by a significant pressure gradient. Alternative accounts present themselves, however, due to the nonlinear, recirculating, nature of the earlier eddy motion, as discussed in Section II-4. The Section II-4 findings lead on to the work in Sections II-5 and II-8 in fact.

Section II-5 considers viscous wake closure occurring with negligible pressure gradient, unlike the closure in Section II-3. Similarity wake solutions are found which yield algebraic dependence at the edge of a shear layer on the verge of closure. Other similarity solutions exist, one showing that Goldstein's (Ref. 11) form of the near-wake of an aligned flat plate is not unique: see also Ref. 17.

Another spin-off from Section II-5 concerns reattachment onto a solid surface. The reattachment may be achievable with negligible pressure response, a desirable property, and secondary separation can be induced further upstream. Applications of wide interest exist, to flow past ramps, over bluff bodies with splitter plates, or in wind-tunnels, and these matters are considered in Section II-6.

In Section II-7, external flow and its relation to the wide-spread cascade are studied. The linear dependence of eddy length on Reynolds number Re , as indicated

by previous studies (Refs. 4-6), is supported by an examination of certain exponentially small terms provoked by Kirchhoff's solution. In turn, the earlier limit forms for $H \rightarrow 0$ all support the emergence of Kirchhoff's solution for external flows, on the body scale.

A proposed mechanism for the subsequent lengthy wake closure is provided by non-entraining viscous shear layers, implied by Sections II-4, II-5 and addressed in Section II-8. Their four main attributes are: first, they yield algebraic decay of the velocity in the lower reaches of the shear layer; second, they show that Chapman's solution for a shear layer far downstream is nonunique; third, they avoid the severe difficulties associated with supplying entrainment to classical shear layers; fourth, they suggest a means for massive eddy closure to take place without provoking a strong backward jet along the wake centerline. Final comments are presented in Section II-9.

II-2. ON LENGTH SCALES FOR THE WIDE-SPREAD CASCADE

From Part I, the wake of the cascade with finite spread is governed by the boundary layer equations

$$U = \frac{\partial \psi}{\partial Y}, \quad U \frac{\partial U}{\partial X} - \frac{\partial \psi}{\partial X} \frac{\partial U}{\partial Y} = -P'(X) + \frac{\partial^2 U}{\partial Y^2} \quad (\text{II-2.1a})$$

subject to

$$\psi = \frac{\partial U}{\partial Y} = 0 \text{ at } Y = 0, X > 0 \quad (\text{II-2.1b})$$

$$\psi = 1, \frac{\partial U}{\partial Y} = 0 \text{ at } Y = 1, X > 0 \quad (\text{II-2.1c})$$

$$U = \begin{cases} (1-H)^{-1} & \text{for } H < Y \leq 1 \\ 0 & \text{for } 0 \leq Y < H \end{cases} \text{ at } X = 0. \quad (\text{II-2.1d})$$

Our present concern is with the flow behavior for wide-spread cascades, where $H \rightarrow 0$. The following tentative arguments (see also Fig. 6) may be made then.

At sufficiently small distances $X \sim \Delta$ from the start a thin viscous shear layer is present, originating from the Chapman form and positioned a distance $O(H)$ (at $Y = H\bar{S}(X/\Delta) + \dots$, say) from the center line $Y = 0$, in view of (II-2.1d). The characteristic velocity, mass flux and width of the shear layer are of the orders 1, $\Delta^{1/2}$, $\Delta^{1/2}$ in turn. The pressure force has negligible effect here since, above the shear layer, on a Y scale of $O(1)$, inviscid linearized properties hold, yielding the pressure-displacement law of one-dimensional channel flow, $P = H - H\bar{S}$, for mass conservation.

Hence, on this scale we have

$$X = \Delta \bar{X}, \quad P = H\bar{P}(\bar{X}) + \dots \quad (\text{II-2.2a})$$

with $\bar{P}(0) = 0$ and in the shear layer I, where $Y = H\bar{S}(\bar{X}) + \Delta^{1/2} Y_o$, $(\psi, U) = (\Delta^{1/2} \psi_o, U_o) + \dots$, the pressure-free boundary layer equations

$$U_o = \frac{\partial \psi_o}{\partial Y_o}, \quad U_o \frac{\partial U_o}{\partial \bar{X}} - \frac{\partial \psi_o}{\partial \bar{X}} \frac{\partial U_o}{\partial Y_o} = \frac{\partial^2 U_o}{\partial Y_o^2} \quad (\text{II-2.2b})$$

apply. Here and below the Y-coordinate could be displaced further if necessary because of Prandtl's transformation. The constraints here are the familiar ones for detached shear layers,

$$U_o(\bar{X}, \infty) = 1, U_o(\bar{X}, -\infty) = 0, U_o(0, Y_o) = \begin{cases} 1 & \text{for } Y_o > 0 \\ 0 & \text{for } Y_o < 0 \end{cases}, \quad (\text{II-2.2c})$$

essentially from the starting form (II-2.1d). The Chapman singularity

$$\psi_o \sim \bar{X}^{-1/2} f_c(\eta), \quad \bar{X} \rightarrow 0, \quad \eta = Y_o / \bar{X}^{1/2} \quad (\text{II-2.2d})$$

holds at the start. Above the shear layer where Y is O(1) (region II) we have

$$(\psi, U) = [Y + H(1-\bar{P})(Y-1), 1 + H(1-\bar{P})] + O(H) \quad (\text{II-2.3})$$

for mass and momentum conservation, from (II-2.1a, c, d). Matching with layer I as $Y \rightarrow H \bar{S}(\bar{X}) +$ then gives

$$\bar{P}(\bar{X}) = 1 - \bar{S}(\bar{X}), \quad (\text{II-2.4})$$

as anticipated above. Further terms in the expansions of regions I, II, and III below, may be written down in principle but the balancing of the leading order contributions sets the major task.

A complete solution for the shear layer of (II-2.2b-d) is the Chapman form (II-2.2d) but holding for all $\bar{X} > 0$. We take that as the solution for now (although it is found later to be nonunique: see Section II-8) and follow its implications.

The main point then is that, since $f_c(-\infty) = -\kappa < 0$, a finite fraction of the viscous shear layer I contains fluid entrained from below I, with $\psi_o < 0$. This fluid must be ejected further downstream before reattachment/closure of the wake eddy or eddies can occur. The viscous entrainment forces the condition

$$\psi \rightarrow -\kappa \bar{X}^{-1/2} \Delta^{1/2} (= \psi_E) \text{ as } Y \rightarrow H \bar{S}(\bar{X}) - , \quad (\text{II-2.5})$$

which causes the fluid below I to be set into motion.

Immediately the length scale $\Delta = O(H^3)$ suggests itself. For, as P is typically $O(H)$ from (II-2.2a), then predominantly inviscid mechanics in the $O(H)$ thick layer III (occupying $0 < Y < HS(\bar{X})$) beneath I implies that U is $O(H^{1/2})$ there, corresponding to an ψ of $O(H^{3/2})$, due to the pressure response. So a comparison with the viscous condition (II-2.5) indicates that $\Delta = O(H^3)$ may represent a crucial stage in the flow development, as indeed the calculations of Part I suggest also. On a shorter scale $\Delta \ll H^3$ the entrainment ψ_E is negligible compared with a pressure-induced ψ of $O(H^{3/2})$ in layer III, so that such a flow in layer III, if nontrivial, must recirculate between I and the center line. This is not implausible, but it leads to no clear sign of eddy closure or anything of significance. For Bernoulli's law holding in layer III does not allow positive pressure \bar{P} , from the center line flow, therefore $\bar{S}(\bar{X}) > 1$ from (II-2.4) and that excludes the closure requirement $\bar{S} \rightarrow 0$. The same objection must be overcome for all inviscid analysis along the centerline.

In passing we note four asides. First, a reasoning similar to the above tends to rule out the Prandtl-Batchelor proposal of a strong mainly inviscid recirculating eddy of uniform vorticity, as follows. If such an eddy is thin, then it induces little pressure change, from (II-2.4), so that the bounding forward shear layer cannot be forced back at closure. On the other hand, if the eddy is thick, with Y of $O(1)$ [$0 < Y < s(\bar{X})$, say], then between it and $Y = 1$ the inviscid properties holding allow no significant vorticity $\partial^2\psi/\partial Y^2$ because of the uniform starting profile in (II-2.1d), and mass and momentum conservation then give the nonlinear counterpart of (II-2.4), $P = (s^2/2 - s)/(1 - s)^2$ since $s(0) = 0$ to leading order; however, constant vorticity $\partial^2\psi/\partial Y^2 = \Omega$ inside the eddy yields $\psi = \Omega Y(Y-s)/2$, $U = \Omega(Y - s/2)$, $P = -\Omega^2 s^2/8$ on integration; so the pressure match demands the final result $s(\bar{X}) = 0$. Both cases lead to failure, therefore. The above requires the length scale Δ to be small, incidentally, study of the $O(1)$ scale in X being deferred to Section II-3 below. Second, viscous forces in the lowest layer III remain secondary effects provided $|U\partial U/\partial X| = O(H\Delta^{-1})$ is larger than $|\partial^2 U/\partial Y^2| = O(H^{-3/2})$, i.e., for $\Delta \ll H^{5/2}$, given the proposed scalings of (II-2.2a) - (II-2.5). Consequently, inviscid mechanics can still apply in Part III at the suggested $X \sim H^3$ stage. Third, preliminary comparisons with the computed solutions of Part I for small H are indicated already. Thus, the $X \sim H^3$ scaling ties in well with the computations (Fig. 5), and the law (II-2.4) leads to $P = H + o(H)$ at eddy closure (where $\bar{S} \rightarrow 0$), in fair agreement again with the calculated results (see Fig. 5). There is also agreement concerning the initial pressure drop (see also (II-2.7) below) and the consequent rise initially in the velocity $U(X,1)$ at the upper symmetry line, from (II-2.3), as Figs. 4-5 show. Fourth, since reversed flow is present, combined non-uniqueness and nonlinearity locally require further caution. It is not known yet what the upstream influence of closure is on the short X scale under discussion. For instance, a strong backward jet of fluid near the center line could be produced by the closure downstream (see later comments) and its presence when X is $O(\Delta)$ would modify our earlier reasoning.

Nevertheless, the agreement just noted does give encouragement, albeit guarded, to a study of the description in (II-2.2a) - (II-2.5), which is self-consistent so far anyway, and we continue for now with the latter. That description emphasizes the stage $\Delta = H^3$ at which (II-2.5) first becomes significant, leaving the motion in sublayer III controlled by the inviscid system

$$\bar{U} = \frac{\partial \bar{\psi}}{\partial \bar{Y}}, \quad \bar{U} \frac{\partial \bar{U}}{\partial \bar{X}} - \frac{\partial \bar{\psi}}{\partial \bar{X}} \frac{\partial \bar{U}}{\partial \bar{Y}} = - \bar{P}'(\bar{X}) \quad (\text{II-2.6a})$$

$$\text{with } \begin{cases} \bar{\psi} = \frac{\partial \bar{U}}{\partial \bar{Y}} = 0 \text{ at } \bar{Y} = 0 \text{ [center line],} \\ \bar{\psi} = -\kappa \bar{X}^{1/2} \text{ at } \bar{Y} = \bar{S}(\bar{X}) \text{ [entrainment].} \end{cases} \quad (\text{II-2.6b})$$

Here $Y = H\bar{Y}$, and the expansion implied above,

$$(\psi, U) = (H^{3/2} \bar{\psi}, H^{1/2} \bar{U}) + (H^2 \psi_1, H\bar{U}_1) + \dots \quad (\text{II-2.6c})$$

has been used. Also, the full symmetry condition is imposed in (II-2.6b) at the center line. For in the reversed motion there viscous forces cannot act substantially and, in addition, vorticity conservation in layer III coupled with the initial zero profile (II-2.1d) requires zero vorticity $\partial \bar{U} / \partial \bar{Y}$ along the center line $\bar{\psi} = 0+$. Viscous action in layer III, which could destroy a nonzero vorticity $\partial \bar{U} / \partial \bar{Y}$, is negligible so far on this $X \sim H^3$ scale, being confined to the next order terms $\psi_1, \bar{U}_1, \bar{P}_1$ which satisfy $\bar{U}_1 = \partial \bar{\psi}_1 / \partial \bar{Y}$ and

$$\bar{U} \frac{\partial \bar{U}_1}{\partial \bar{X}} + \bar{U}_1 \frac{\partial \bar{U}}{\partial \bar{X}} - \frac{\partial \bar{\psi}}{\partial \bar{X}} \frac{\partial \bar{U}_1}{\partial \bar{Y}} - \frac{\partial \bar{\psi}_1}{\partial \bar{X}} \frac{\partial \bar{U}}{\partial \bar{Y}} = - \frac{d\bar{P}_1}{d\bar{X}} + \frac{\partial^2 \bar{U}}{\partial \bar{Y}^2} \quad (\text{II-2.6d})$$

where $H^{3/2} \bar{P}_1$ is the next order pressure term in (II-2.2a). The whole local flow is then dictated by the hyperbolic problem (II-2.6a, b), with (II-2.4), the characteristics being the lines $\bar{\psi} = \text{const.}$, $\bar{X} = \text{const.}$, and we might expect the condition

$$\bar{\psi}, \bar{P} \rightarrow 0 \text{ as } \bar{X} \rightarrow 0. \quad (\text{II-2.6e})$$

to hold, from (II-2.1d).

A point of strategy here is that

$$\bar{P}(\bar{X}) = - \frac{1}{2} \bar{U}^2(\bar{X}, 0) \leq 0 \quad (\text{II-2.7})$$

from (II-2.6a, b, e), so that $\bar{S}(\bar{X}) > 1$ from (II-2.4) and wake closure $\bar{S} \rightarrow 0$ is not attainable directly yet, as remarked before. The equivalent Bernouilli constraint (II-2.7) persists downstream in fact as long as the center line flow properties remain predominantly inviscid. So for wake closure ($S \rightarrow 0$) to be achieved it seems essential for viscosity to come back into play significantly before or during the closure process. Inviscid mechanics alone apparently fails to explain the eddy closure here.

The solution in layer III still requires a downstream condition to be set, however, and so several distinct possibilities arise. These possibilities are followed through in the subsequent sections.

II-3. THE LONG EDDY

The simplest flow solution of (II-2.6a, b, e) is

$$\bar{\psi} = -\kappa \bar{X}^{1/2} \frac{\bar{Y}}{\bar{S}(\bar{X})}, \quad \bar{U} = -\frac{\kappa \bar{X}^{1/2}}{\bar{S}(\bar{X})}, \quad P = -\frac{\frac{1}{2} \kappa^2 \bar{X}}{(\bar{S}(\bar{X}))^2} \quad (\text{II-3.1})$$

which yields locally uniform reversed streaming. This motion can continue for all positive \bar{X} , in principle, and corresponds to a downstream condition of negligible vorticity in layer III. Allied with (II-2.4), it gives the implicit equation

$$\bar{S}^3 - \bar{S}^2 = \frac{1}{2} \kappa^2 \bar{X}, \quad \text{with } \bar{S}(0) = 1, \quad (\text{II-3.2})$$

for $\bar{S}(\bar{X})$, the solution being shown in Fig. 7. The width $\bar{S}(\bar{X})$ of sublayer III grows monotonically with distance \bar{X} and as $\bar{X} \rightarrow \infty$

$$-\bar{P} \sim \bar{S}(\bar{X}) \sim (\kappa^2/2)^{1/3} \bar{X}^{-1/3}, \quad \bar{U} \sim - (2\kappa)^{1/3} \bar{X}^{-1/6}, \quad (\text{II-3.3})$$

so that the reversed flow becomes accentuated. An eddy closure at finite X , yielding a small X_{reatt} of $O(H^3)$, seems unlikely within such a structure. Instead (II-3.3) continues downstream until \bar{X} becomes $O(H^{-3})$, or $X \rightarrow O(1)$, at which stage the pressure $P \sim H\bar{P}$ increases to $O(1)$ and the outer motion in layer II becomes disturbed significantly, from (II-2.3).

The next (and final) stage, therefore, is relatively far downstream where ψ, U, P, X, Y are all of $O(1)$ and so there the full governing equations (II-2.1a-c) apply across the entire flow. To leading order the starting condition is now

$$U \rightarrow 1, \quad \psi \rightarrow Y \quad \text{as } X \rightarrow 0 \quad \text{for } 0 < Y \leq 1 \quad (\text{II-3.4a})$$

but with $P \sim -(\kappa^2/2)^{1/3} X^{1/3}$ then and

$$\left. \begin{aligned} \psi &\sim - (2\kappa)^{1/3} X^{1/6} Y \\ U &\sim - (2\kappa)^{1/3} X^{1/6} \end{aligned} \right\} \quad \text{for } 0 \leq Y < (\kappa^2/2)^{1/3} X^{1/3} \quad (\text{II-3.4b})$$

to match (II-3.3). The Chapman singularity is still present, but in an $O(X^{1/2})$ layer centered around $Y = (\kappa^2/2)^{1/3} X^{1/3}$ as $X \rightarrow 0$, and it requires $\psi \sim -\kappa X^{1/2}$ there. This is satisfied by (II-3.4b). Further terms in the small X expansion (II-3.4b) can be generated in principle.

The current stage shows up a surprising nonuniqueness in the boundary layer equations, in fact. For, with the constraints (II-3.4a) holding, one solution of (II-2.1a-c) is simply the uniform stream $U = 1$, $\psi = Y$ continuing for all X , Y . So the starting form (II-3.4b) represents a second (eigen) solution, branching from the incoming uniform stream. Again, the branching solution appears to be self-consistent for small X and it can be shown to satisfy the momentum integral equation

$$P(X) + \int_0^1 U^2 dY = 1 \quad (\text{II-3.5})$$

obtained from (II-2.1a), as well as the momentum integral of Part I.

There appears to be no theoretical objection to this account at first sight, nor any obvious reason why wake closure and subsequent flow recovery should not occur downstream, for $X > 0$, yielding self-consistency: Fig. 7. The objection raised earlier by (II-2.7) for instance is overcome here because viscosity reasserts its necessary influence when X is $O(1)$. Accordingly, it would be very interesting to see the results of a numerical study of the branching solution stemming from (II-3.4a, b). On the other hand, there is little evidence yet from the finite-spread calculations of Part I to support the prediction of an $O(1)$ eddy length as $H \rightarrow 0$. It could well be that the trend of a small eddy suggested by those calculations at smallish H values is misleading and that a switch to the current structure with a longer eddy will emerge for still smaller values of H , but that remains to be seen. Subsequently, we search for an account which yields a smaller eddy, alternative to that in (II-3.1)-(II-3.5), bearing in mind the need (satisfied by the above solution) for viscous action during the closure process but noting that simultaneously the pressure force is likely to become negligible* then because of the relation (II-2.4) with (II-2.2a). The latter property leads to the study in Section II-4 of alternative downstream forms for sublayer III and to the study in Section II-5 of viscous closure under zero pressure gradient. Section II-5 has quite general application since many eddies are slender in practice (e.g., in external flow: see later) and so cannot produce an extensive zone of significant pressure gradient.

*This is more in line with the calculations of Part I. In addition, both the pressure-displacement law (II-2.4) at closure ($\bar{S} \rightarrow 0$) and the momentum integral of Part I demand the same small pressure rise overall, namely $P = H + o(H)$, when H is small.

II-4. SHORTER EDDIES

Few other self-consistent downstream conditions seem immediately possible for the sublayer III of Section II-2, as described in (II-2.6a-e) at least, although they do all tend to suggest eddy lengths shorter than that just considered. Two categories (a) and (b) arise (see Fig. 8), as described below.

In the first, the sublayer III continues for all positive \bar{X} . In consequence, a description must be obtained for (II-2.6a, b, e) when $\bar{X} \rightarrow \infty$. Since $\bar{S} \geq 1$ from (II-2.4), (II-2.7), there are only two plausible trends (labelled (a1), (a2) below), then: either $\bar{S} \rightarrow \infty$ or $\bar{S}(\infty)$ is finite.

For subcategory (a1) if $\bar{S} \rightarrow \infty$ as $\bar{X} \rightarrow \infty$, one solution is the form with negligible vorticity, giving $\bar{S} \propto \bar{X}^{1/3}$, which was discussed in the previous section. Other candidates arise as follows (Fig. 8). Suppose

$$\bar{S} \sim s_o \bar{X}^{n_o} \text{ as } \bar{X} \rightarrow \infty, \tag{II-4.1}$$

with the unknown constants s_o, n_o both positive. Then $\bar{P} \sim -s_o \bar{X}^{n_o}$ from (II-2.4). Hence (II-2.7) implies that \bar{U} is $O(\bar{X}^{n_o/2})$ sufficiently near the wake center line, say for an extent $O(\bar{X}^{n_1})$ [$n_1 \leq n_o$] in the \bar{Y} direction, giving $\bar{\psi}$ of order $\bar{X}^{n_1+n_o/2}$ there for continuity, so that $\psi \sim \bar{X}^{n_1+n_o/2} f(\bar{\eta})$ with $\bar{\eta} \equiv \bar{Y}/\bar{X}^{n_1}$ of $O(1)$. Here $f(\bar{\eta})$ satisfies

$$n_o f'^2 - (n_o + 2n_1) ff'' = 2n_o s_o, f(0) = 0, f''(0) = 0 \tag{II-4.2a,b,c}$$

from (II-2.6a,b). We may take it that $f \neq \pm (2s_o)^{1/2} \bar{\eta}$, for otherwise we are led back to the earlier solution and to the result $n_o = n_1 (= 1/3)$. Again, if $n_o = n_1$ it can be shown that the earlier solution is the only permissible one. Therefore we consider $n_1 < n_o$ and $f \neq \pm (2s_o)^{1/2} \bar{\eta}$. Then, as $\bar{\eta} \rightarrow 0$ (II-4.2a) requires $f \propto \bar{\eta}$. So the derivative of (II-4.2a), $(n_o - 2n_1) f'f'' = (n_o + 2n_1)ff'''$, which gives the vorticity conservation result

$$f'' \propto |f|^M, \tag{II-43}$$

requires $f'' \propto \bar{\eta}^{-M}$ as $\bar{\eta} \rightarrow 0$, where $M = (n_o - 2n_1)/(n_o + 2n_1)$. In addition, further away from the center line, as $\bar{\eta} \rightarrow \infty$, $f \propto -\bar{\eta}^{1+n_o/2n_1}$ from (II-4.2a) and the restriction $n_1 > 0$ is necessary. So $\bar{\psi} \propto -\bar{Y}^{1+n_o/2n_1}$ there, and the entrainment condition (II-2.6b) leaves us with $n_o+n_o^2/2n_1 = 1/2$, since \bar{S} is $O(\bar{X}^{n_o})$ from (II-4.1). Hence $M = 1 - 4n_o$, giving $M < 1$. However, f must be regular as $\bar{\eta} \rightarrow 0$, to prevent an irremovable singularity in higher order terms in layer III (see (II-2.6d) above),

and that points to the value $M = 1$. Accordingly, no extra solution is forthcoming here except perhaps in the limit as $n_0 \rightarrow 0$, $n_1 = 0$ (n_0^2). It is tempting here to support the candidate $M = 0$ ($n_0 = 1/4$, $n_1 = 1/8$), incidentally, associated with the simple solution

$$\begin{aligned} \bar{\psi} &= (\sqrt{2\bar{S}-2} - \bar{\Omega}\bar{Y}/2) \bar{Y}, (1/2)\bar{\Omega}\bar{S}^2 - \bar{S}\sqrt{2\bar{S}-2} = \kappa\bar{X}^{-1/2}, \bar{P} = 1 - \bar{S} \\ \bar{U} &= \sqrt{2\bar{S}-2} - \bar{\Omega}\bar{Y}, \text{ with } \bar{S} \sim \left(\frac{2\kappa}{\bar{\Omega}}\right)^{1/2} \bar{X}^{1/4} \text{ as } \bar{X} \rightarrow \infty \end{aligned} \quad (\text{II-4.4})$$

and a constant vorticity level $\bar{\psi}_{\bar{Y}\bar{Y}} = -\bar{\Omega}$. This is an interesting solution which produces forward flow along the center line and reversed flow nearer the shear layer II, with a dividing streamline $\bar{\psi} = 0$, $\bar{Y} = 2\sqrt{2\bar{S}-2}/\bar{\Omega}$ returning in reversed flow towards the center line if $\bar{\Omega} > 0$. Nevertheless the requirement (II-2.6b) is not fully satisfied and, although the forward motion along the center line can allow viscosity to exert a smoothing effect there, the starting condition (II-2.6e) is still violated. As always in inviscid theory, the possibility of discontinuous solutions comes to mind, here and elsewhere, but their relevance does not appear especially likely at the present stage.

Still assuming that $\bar{S} \rightarrow \infty$ as $\bar{X} \rightarrow \infty$, and that the trial (II-4.1) points us in the right direction, we are left only with the question of the limit $n_0 \rightarrow 0$, then, with n_1 of order n_0^2 . This corresponds to a linear vorticity dependence

$$\bar{\psi}_{\bar{Y}\bar{Y}} = \lambda \bar{\psi} \quad (\text{II-4.5})$$

in fact, from (II-4.3), where λ is a constant. Thus with (II-4.5) holding another exact solution of (II-2.6a, b, e) is obtained,

$$\begin{aligned} \bar{\psi} &= -\bar{A}(\bar{X}) \sinh(\lambda^{1/2} \bar{Y}), \bar{U} = -\bar{A}(\bar{X}) \lambda^{1/2} \cosh(\lambda^{1/2} \bar{Y}) \\ \bar{P} &= -\frac{1}{2} \lambda \bar{A}^2(\bar{X}) \end{aligned} \quad (\text{II-4.6a,b,c})$$

(provided $\lambda > 0$) where $\bar{A}(\bar{X})$ is unknown but $\bar{A}(0) = 0$. Substituting (II-4.6a-c) into (II-2.4), (II-2.6b), we have then

$$\bar{S}(\bar{X}) = 1 + \frac{1}{2} \lambda \bar{A}^2(\bar{X}), \bar{A}(\bar{X}) \sinh(\lambda^{1/2} \bar{S}(\bar{X})) = \kappa \bar{X}^{-1/2}, \quad (\text{II-4.7a,b})$$

two equations determining $\bar{S}(\bar{X})$, $\bar{A}(\bar{X})$ for all \bar{X} , given the value of λ (see Fig. 8). The solution is regular for all \bar{X} and, as $\bar{X} \rightarrow \infty$, $\bar{S}(\bar{X})$ grows only logarithmically with

$$\bar{S}(\bar{X}) \sim -\bar{P}(\bar{X}) \sim \frac{\ln \bar{X}}{2 \lambda^{1/2}} + O[\ln(\ln \bar{X})]. \quad (\text{II-4.8a,b})$$

A link with (II-4.2a)-(II-4.3) for n_0 small, $n_1 \propto n_0^2$, is then achieved.

The solution (II-4.5)-(II-4.8b) appears to be self-consistent for all \bar{X} . The next issue is whether it preserves consistency on all longer scales further downstream. It is found that the next distinct stage downstream arises when X is of order $H^{5/2}(-\ln H)^{1/2}$. There, in a reversed sublayer where $Y = H\bar{Y}$ and \bar{Y} is again $O(1)$, $U = H^{1/2}(-\ln H)^{1/2} \tilde{U}$, $\psi = H^{3/2}(-\ln H)^{1/2} \tilde{\psi}$ from (II-4.6a)-(II-4.8b) and

$$P = [-(-\ln H)/(4\lambda^{1/2}) + \lambda_1 \ln(-\ln H) + \tilde{P}(\tilde{X})] H \quad (\text{II-4.9a})$$

with $X = H^{5/2}(-\ln H)^{1/2} \tilde{X}$ now, $\tilde{X} > 0$, and $\lambda_1 = 1/(4\lambda^{1/2})$ is a constant. The sublayer therefore achieves an inviscid-viscous balance but is pressure-free, its governing equations being

$$U \frac{\partial \tilde{U}}{\partial \tilde{X}} - \frac{\partial \tilde{\psi}}{\partial \tilde{X}} \frac{\partial \tilde{U}}{\partial \tilde{Y}} = 0 + \frac{\partial^2 \tilde{U}}{\partial \tilde{Y}^2}, \quad \tilde{U} = \frac{\partial \tilde{\psi}}{\partial \tilde{Y}}, \quad (\text{II-4.9b,c})$$

and symmetry requires

$$\tilde{\psi} = \frac{\partial \tilde{U}}{\partial \tilde{Y}} = 0 \text{ at } \tilde{Y} = 0, \quad (\text{II-4.9d})$$

from (II-2.1a,b). The outer condition required here is one of matching,

$$\psi \sim -2^{-3/2} \lambda^{-3/4} \exp[\lambda^{1/2}(\bar{Y} - \delta_2(\bar{X}))] \text{ as } \bar{Y} \rightarrow \infty \quad (\text{II-4.9e})$$

and needs further comment. The function $\delta_2(\bar{X})$ represents an unknown displacement effect on this length scale. The viscous detached shear layer, originally layer I in Section II-2, is now centered at $Y = H\{(-\ln H)/4\lambda^{1/2} - \lambda_1 \ln(-\ln H) + \delta_2(\bar{X})\}$ from (II-4.8a) and is of thickness $O\{H^{5/4}(-\ln H)^{1/4}\}$ from Section II-2, where the function $\delta_2(\bar{X})$ is unknown. Between the detached shear layer and the reversed center line viscous sublayer of (II-4.9b-d) the fluid mechanics is basically inviscid and pressure-free and so the ψ -profile there must be purely exponential in Y to merge with layer III upstream. Hence the form (II-4.9e) continues across the entire gap between the present two viscous layers; i.e., for $1 \ll \bar{Y} < (-\ln H)/4\lambda^{1/2} - \lambda_1 \ln(-\ln H) + \delta_2(\bar{X})$. At the upper limit here, i.e., the shear layer, under the assumption that the similarity result (II-2.5) still holds in effect, entrainment then demands that

$$\exp[\lambda^{1/2} (\tilde{\delta}_2(\tilde{X}) - \tilde{\delta}(\tilde{X}))] = 2^{3/2} \lambda^{3/4} \kappa \tilde{X}^{1/2}. \quad (\text{II-4.10a})$$

Finally, above the shear layer, linearized inviscid channel flow theory applies again, giving the relation

$$\tilde{P}(\tilde{X}) = -\tilde{\delta}_2(\tilde{X}). \quad (\text{II-4.10b})$$

The rationale here is that the viscous sublayer problem (II-4.9b-e) is the central one, determining $\tilde{\delta}_2$, hence (II-4.10a) determines $\tilde{\delta}_2$, then (II-4.10b) determines the pressure response P , and P then drives higher order corrections to the flowfield.

The rationale works for small positive \tilde{X} , where a match with the earlier properties for \tilde{X} finite is achieved. Thus the reversed sublayer (II-4.9b-e) becomes predominantly inviscid then, and is regular, with

$$\tilde{\psi} \sim F_0(\bar{Y}) + \tilde{X} F_1(\bar{Y}) + O(\tilde{X}^2) \quad (\text{II-4.10c})$$

where $F_0 = -2^{-1/2} \lambda^{-3/4} \sinh(\lambda^{1/2} \bar{Y})$ from (II-4.6a)-(II-4.8a). Here (II-4.9b-d) requires that

$$F_1(\bar{Y}) \propto \cosh(\lambda^{1/2} \bar{Y}) (\tan^{-1} [\exp(\lambda^{1/2} \bar{Y})] - \pi/4) \quad (\text{II-4.10d})$$

and so we have

$$|\tilde{\delta}| \propto \tilde{X} \text{ as } \tilde{X} \rightarrow 0+. \quad (\text{II-4.10e})$$

Further terms can be generated for small \tilde{X} .

The description apparently cannot continue for all positive \tilde{X} however. A similarity solution does suggest itself for $\tilde{X} \rightarrow \infty$, in the form

$$\tilde{\psi} \sim \tilde{X} \tilde{F}(\bar{Y}) + O(1) \quad (\text{II.4-11})$$

which yields for \tilde{F} the nonlinear differential equation

$$\tilde{F}''' + \tilde{F} \tilde{F}'' - \tilde{F}'^2 = 0 \text{ with } \tilde{F}(0) = \tilde{F}'(0) = 0 \quad (\text{II-4.12a-c})$$

from (II-4.9b-d). But an integral of (II-4.12a-c) is

$$\tilde{F}'' = \exp\left[-\int_0^{\bar{Y}} \tilde{F}(y_1) dy_1\right] \int_0^{\bar{Y}} \tilde{F}'^2(y_2) \exp\left[\int_0^{y_2} \tilde{F}(y_1) dy_1\right] dy_2 \quad (\text{II-4.13a})$$

so that $\tilde{F}'' > 0$ for $\bar{Y} > 0$. Hence the required asymptote,

$$\tilde{F} \sim -2^{-3/2} \lambda^{-3/4} \exp[\lambda^{1/2} (\bar{Y} - \text{const.})] \text{ as } \bar{Y} \rightarrow \infty \quad (\text{II-4.13b})$$

from (II-4.9e), is unobtainable since (II-4.13b) requires $\tilde{F}'' < 0$. Instead (II-4.12a)-(II-4.13a) can be shown to give

$$\tilde{F} \sim a_1 \exp(\lambda^{1/2} \bar{Y}), \bar{Y} \rightarrow \infty, a_1 > 0. \quad (\text{II-4.13c})$$

In a sense it is a pity that (II-4.13b) cannot be satisfied with (II-4.12a-c). For (II-4.13b), with (II-4.11), implies that $\tilde{\delta} \sim -\lambda^{-1/2} \ln \tilde{X}$ as $\tilde{X} \rightarrow \infty$; so (II-4.10a,b) give $-\tilde{P} = \tilde{\delta}_2 \sim (1/2 \lambda^{1/2}) \ln \tilde{X} \rightarrow -\infty$ and the detached shear layer approaches the center line at last; the shear layer and the reversed center line sublayer then merge (anticipating closure) downstream when X is $O(H^2)$; the boundary layer equations apply there without pressure gradient; and self-consistency could be achieved. The nonexistence of a solution to (II-4.12a-c) with (II-4.13b) rules out such an account, of course, but it does raise again the question of wake closure occurring without significant pressure forces: see Section II-5 below.

For the reversed sublayer of (II-4.9b-e) the solution most likely terminates in a singularity at a finite positive value \tilde{X}_0 of \tilde{X} . The singularity as $\tilde{X} \rightarrow \tilde{X}_0^-$ is given by (II-4.11) again, effectively, with \tilde{X} replaced by $(\tilde{X} - \tilde{X}_0)$ and self-consistency is maintained now with (II-4.13c) yielding

$$\tilde{\delta}(\tilde{X}) \sim -\lambda^{-1/2} \ln(\tilde{X}_0 - \tilde{X}) \text{ as } \tilde{X} \rightarrow \tilde{X}_0^-. \quad (\text{II-4.14})$$

Hence, $\tilde{\delta}$ and $\tilde{\delta}_2 \rightarrow +\infty$ then, the detached shear layer departs further from the center line and the pressure response $\tilde{P} \rightarrow -\infty$, from (II-4.10a,b). The further pressure fall due to this departure from the center line eventually affects the flow in the reversed sublayer first, within a more local scale around $\tilde{X} = \tilde{X}_0$, and so then the relations (II-4.9e), (II-4.10a) become altered. No clear means of closure of the eddy in these circumstances has emerged yet, but the pressure response could cause the detached shear layer to reverse its trend abruptly and turn back towards the center line within the localized scale. For no solution of the sublayer (II-4.9b-e) exists just downstream of the singular point $\tilde{X} = \tilde{X}_0$, and so a change of structure is necessary locally. If that causes wake closure the prediction $X_{\text{reatt}} = O[H^{5/2}(-\ln H)^{1/2}]$ follows.

So far, therefore, only two accounts have avoided obvious failure, the one of Section II-3 and the one just described in (II-4.5)-(II-4.14).

A third candidate emerges, subcategory (a2), when $\bar{S}(\infty)$ is assumed to be finite. This yields the property

$$\bar{\psi} \rightarrow \bar{\psi}_\infty(\bar{Y}), \bar{U} \rightarrow \bar{U}_\infty(\bar{Y}), \bar{P} \rightarrow 1 - \bar{S}(\infty) \text{ as } \bar{X} \rightarrow \infty \quad (\text{II-4.15a})$$

in layer III of Section II-2. Here the profiles $\bar{\psi}_\infty(\bar{Y}), \bar{U}_\infty(\bar{Y}) \equiv \bar{\psi}_\infty'(\bar{Y})$ are arbitrary except that $\bar{\psi}_\infty(0) = \bar{\psi}_\infty''(0) = 0$ for symmetry, we might expect $\bar{U}_\infty(0) < 0$ and, because of the increasing entrainment (II-2.6b), $\bar{\psi}_\infty(\bar{Y}) \rightarrow -\infty$ as $\bar{Y} \rightarrow \bar{S}(\infty)$. So the reversed velocity in III becomes accentuated just below the shear layer I.

The nature of the reversed acceleration here controls what happens further downstream on longer length scales. Suppose that

$$\bar{\psi}_\infty(\bar{Y}) \sim -b_1 (\bar{S}(\infty) - \bar{Y})^{-\gamma} \text{ as } \bar{Y} \rightarrow \bar{S}(\infty) - \quad (\text{II-4.15b})$$

where b_1, γ are positive constants. Then, as $\bar{X} \rightarrow \infty$

$$1 - \bar{S} = \bar{P} \sim 1 - \bar{S}(\infty) + b_2 \bar{X}^{-1/2\gamma}, \bar{\psi} \sim \bar{\psi}_\infty(\bar{Y}) + \bar{X}^{-1/2\gamma} \bar{\psi}_A(\bar{Y}) \quad (\text{II-4.15c})$$

and, from (II-2.6a,b,e),

$$\bar{\psi}_A(\bar{Y}) = -b_2 \bar{U}_\infty(\bar{Y}) \int_0^{\bar{Y}} \frac{d\bar{Y}}{\bar{U}_\infty^2(\bar{Y})} \quad (\text{II-4.15d})$$

with the constant b_2 remaining unknown. Hence $\bar{\psi}_A$ induces an increasing displacement effect as $\bar{Y} \rightarrow \bar{S}(\infty)$. As a result (Fig. 8), in a thinner layer just below $\bar{Y} = \bar{S}(\infty)$, the solution is

$$\bar{\psi} \sim -b_1 \bar{X}^{1/2} [b_2 I_A - \bar{\eta}]^{-\gamma} \quad (\text{II-4.15e})$$

for $\bar{\eta} = (\bar{Y} - \bar{S}(\infty)) \bar{X}^{1/2\gamma}$ now of the order unity. Here the constant $I_A \equiv \int_0^{\bar{S}(\infty)} \bar{U}_\infty^{-2}(\bar{Y}) d\bar{Y}$ is finite and positive, while (II-4.15e) merges with (II-4.15c,d) as $\bar{\eta} \rightarrow -\infty$ and enforces the entrainment condition

$$b_1 (1 + I_A)^{-\gamma} = b_2^\gamma \kappa \quad (\text{II-4.15f})$$

from (II-2.6b), since the shear layer is at $\bar{\eta} = -b_2$. Equation (II-4.15f) fixes the value of b_2 in terms of the final profile $\bar{\psi}_\infty(\bar{Y})$, since the latter determines b_1 and I_A . Further contributions can be generated, in inverse powers of \bar{X} , and forms other than (II-4.15b) are also possible, but the main point is that again a self-consistent description of layer III emerges.

Can this third account also remain consistent further downstream, producing wake closure? The next distinct stage arises when, in layer III, the maximum (reversed) velocity rises to $O(1)$ because then the forward shear layer I must be affected significantly by the motion underneath it. This maximum occurs where (II-4.15e) holds, giving \bar{U} of order $\bar{X}^{(\gamma+1)/2\gamma}$, i.e., U of order $H^{1/2} \bar{X}^{(\gamma+1)/2\gamma}$ from (II-2.6c), when $\bar{X} \gg 1$. Consequently, since $X = H^3 \bar{X}$, the stage $X = O[H^{(2\gamma+3)/(\gamma+1)}]$, greater than H^3 but less than H^2 , is the next crucial one downstream. Note that the thin layer where (II-4.15e) holds is of thickness $O[H \bar{X}^{-1/2\gamma}]$, i.e., $O[H^{1+3/2\gamma} X^{-1/2\gamma}]$; hence at the stage just mentioned the thickness decreases to $O[H^{(2\gamma+3)/(2\gamma+2)}]$, exactly the viscous thickness of $O(X^{1/2})$ associated with the Chapman solution. The latter solution can apply no longer then and the whole viscous shear layer must change in character. This prospect is studied further in Section II-8 below.

The second category, category b, has the sublayer III terminating after a finite distance, at $\bar{X} = \bar{X}_0$ - say, suggesting $X_{\text{reatt}} = O(H^3)$. Terminal forms can be written down which provide a self-consistent description of layer III as $\bar{X} \rightarrow \bar{X}_0^-$. The mechanism for completing eddy closure in such cases remains elusive, however, mainly because of the objection (to inviscid theory) arising from (II-2.7). Viscous forces must exert a strong influence before closure can take place; yet a termination at $\bar{X} = \bar{X}_0$ provides no clear sign of increased viscous action there. In contrast, the arguments supporting the earlier possibilities of Section II-3 and (a1), (a2) above all bring viscosity back into play before closure. A number of alternatives arise here including: the different forms of viscous shear layers (Section II-8); higher order terms in III, e.g., as in (II-2.6d), may reinstate viscous effects near the center line as $\bar{X} \rightarrow \bar{X}_0$ if \bar{P} , $\bar{U} \rightarrow 0$ there; layer III may have a discontinuous inviscid solution; multiple eddies may occur, e.g., if λ in (II-4.5) is negative; a backward jet may be present along the center line. None of these has been found to produce a complete self-consistent argument for a finite \bar{X} termination yet, although Section II-8 below, concerning nonentraining shear layers, does revitalize the possibility.

II-5. ON PRESSURE-FREE VISCOUS WAKES

Viscosity has to come back into the reckoning, for wake closure to take place, but if in addition the length scales governing the closure are relatively small (unlike Section II-3) then the induced pressure is small, in view of (II-2.4). Negligible downstream pressure is an attribute of the new inviscid solutions of Section II-4, for instance. Since the shear layer velocities are of $O(1)$ by contrast, the properties of pressure-free viscous closure must be addressed.

Our reasoning here hinges on the flow features near the centerline, given the pressure-free equations (for $x_1 > 0$)

$$U = \frac{\partial \psi}{\partial y_1}, \quad \frac{U \partial U}{\partial x_1} - \frac{\partial \psi}{\partial x_1} \frac{\partial U}{\partial y_1} = 0 + \frac{\partial^2 U}{\partial y_1^2} \quad (\text{II-5.1a})$$

holding on some short length scales $X = \Delta_1 x_1$, $y = \Delta_1^{1/2} y_1$, with $U = O(1)$. Here $\Delta_1 \ll 1$ is unknown as yet, but $\Delta_1 \gg \Delta$ and the constraints are

$$\begin{aligned} \psi = \frac{\partial U}{\partial y_1} = 0, \quad y_1 = 0 \quad (\text{symmetry}), \quad \text{and } U \rightarrow 1 \\ \text{as } y_1 \rightarrow \infty \quad (\text{freestream}). \end{aligned} \quad (\text{II-5.1b,c})$$

The constraints stem from (II-2.6b) and (II-2.3), respectively, for the wide-spread cascade, but the application intended is broader since many other wake flows with closure seem too slender to provoke a substantial pressure force.

If the starting profile at $x_1 = 0^+$ has only forward velocities then (II-5.1a-c) can be integrated forward in x_1 , giving a standard wake problem. If closure has still to occur, however, the starting profile must contain some reversed velocities. We consider whether such reversed flow can be present near the center line (to set up a downstream condition for a layer such as III above) and be initially small (to avoid sending a strong reversed jet back into the earlier, shorter length scale, motions). That indicates a local similarity solution holding as $x_1 \rightarrow 0^+$, of the form $\psi = x_1^{K/(K+1)} G(\xi)$ where $\xi = y_1/x_1^{1/(K+1)}$. Here K is an unknown constant but $|K| > 1$ so that $U = x_1^{(K-1)/(K+1)} G'(\xi)$ is small. If $K > 1$ this viscous region is contracting as $x_1 \rightarrow 0^+$, whereas it is expanding if $K < -1$. The function G satisfies

$$\left\{ \begin{aligned} (K+1) G''' + K G G'' - (K-1) G'^2 &= 0 & (\text{II-5.2a}) \\ G(0) = G''(0) &= 0 & (\text{II-5.2b}) \end{aligned} \right.$$

from (II-5.1a,b). An integral of (II-5.2a,b)

$$G'' = \frac{K-1}{K+1} \exp \left\{ \frac{-K}{K+1} \int_0^\xi G(\xi_1) d\xi_1 \right\} \int_0^\xi G'^2(\xi_2) \exp \left\{ \frac{K}{K+1} \int_0^{\xi_2} G(\xi_1) d\xi_1 \right\} d\xi_2 \quad (\text{II-5.3a})$$

then shows that the vorticity is positive,

$$G'' > 0 \text{ for } \xi > 0, \quad (\text{II-5.3b})$$

since $|K| > 1$. Therefore the velocity $G'(\xi)$ increases, with ξ , from the unknown center line value $G'(0)$. As ξ continues to increase only two ultimate trends can be observed: see Fig. 9. For $K < -1$ a singularity is encountered at a finite position $\xi = \xi_0 > 0$, with

$$G \sim + C_1 (\xi_0 - \xi)^{-|K|} + O(\xi_0 - \xi)^{-1} \text{ as } \xi \rightarrow \xi_0^-; \quad (\text{II-5.4a})$$

whereas for $K > 1$ the solution continues for all ξ , giving (apart from an origin shift)

$$G \sim + C_2 \xi^K + O(\xi^{-1}) \text{ as } \xi \rightarrow \infty. \quad (\text{II-5.4b})$$

Here C_1 and C_2 are unknown constants but both are positive because of (II-5.3b), so that the ultimate trends produce forward flow, $G' \rightarrow +\infty$. It is interesting that the forms (II-5.4a,b) are inevitable for any starting value $G'(0)$, whether positive or negative (the case $G'(0) = 0$ gives the trivial result $G = 0$ and is of no concern). This implies the surprising result that, for instance, the near-wake solution of Goldstein (Ref. 11) corresponding to $K = 2$ above is not unique (see Ref. 17): if reversed center line flow $G'(0) < 0$ is allowed then a second solution exists which, like Goldstein's, still gives $G''(\infty)$ finite and positive.

Suppose first that $K < -1$, the expanding case, implying the property (II-5.4a). A slimmer region of thickness $O(1)$ in y_1 is induced (see Fig. 9) near $\xi = \xi_0$ to smooth out the growth of (II-5.4a). The solution there has faster flow with U , ψ of $O(1)$, say

$$\psi \rightarrow \psi^{(0)}(\bar{y}) \text{ as } x_1 \rightarrow 0^+ \quad (\text{II-5.5a})$$

where $y_1 = \xi_0 x_1^{-1/(|K|-1)} + \bar{y}$ is large. The governing equations (II-5.1a) are satisfied, and the profile $\psi^{(0)}(\bar{y})$ remains arbitrary apart from the requirement

$$\psi^{(0)}(\bar{y}) \sim C_1 |\bar{y}|^{-|K|} \text{ as } \bar{y} \rightarrow -\infty \quad (\text{II-5.5b})$$

of matching with (II-5.4a), at one extreme, and, at the other, a matching condition required as $\bar{y} \rightarrow \infty$. The latter depends on how multi-structured the local wake is. The simplest condition is

$$\psi^{(0)'}(\infty) = 1 \quad (\text{II-5.5c})$$

which satisfies (II-5.1c) directly and gives, for the wake displacement $\delta(x_1)$ defined by $\psi \sim y_1 - \delta(x_1)$ in (II-5.1a-c), the growth

$$\delta(x_1) \sim \xi_0 x_1^{-1/(|K|-1)} (\rightarrow \infty) \text{ as } x_1 \rightarrow 0^+. \quad (\text{II-5.5d})$$

This growth upstream appears physically sensible with regard to both the wake closure anticipated further downstream and to the detached flow properties (Sections II-2,4) holding on shorter scales. So the question arises of whether those shorter scale flows can be joined to the present viscous structure for small x_1 , or not, given that in particular the $O(1)$ thick region of fast flow in which (II-5.5a) holds must exhibit the algebraic decay (II-5.5b) with $|K| > 1$. Again, realistic conditions other than (II-5.5c) are possible for $\bar{y} \rightarrow \infty$. For instance, a decay like that in (II-5.5b) can be achieved for $\bar{y} \rightarrow \infty$ with

$$\psi^{(0)}(\bar{y}) \sim C_3 + C_4 \bar{y}^{-\bar{\nu}} \quad (\text{II-5.5e})$$

where $\bar{\nu} (> 0)$, C_4 and C_3 (a mass flux) are constants. If (II-5.5e) holds then a further thicker viscous region arises above the fast flow region with thickness $\bar{y} = O(x_1^{-1/(\bar{\nu}-1)})$ and $\psi - C_3 = O(x_1^{\bar{\nu}/(\bar{\nu}-1)})$ is small provided $\bar{\nu} > 1$. In effect, the governing equation then is (II-5.2a) again, with K replaced by $-\bar{\nu}$ and (II-5.2b) is replaced by

$$G \sim C_4 (\xi - \xi_0)^{-\bar{\nu}} \text{ as } \xi \rightarrow \xi_0^+, \quad (\text{II-5.5f})$$

from (II-5.5e). As ξ increases further the solution tends to one of two forms, both yielding slower motion (see Ref. 17, however),

$$G \sim 6 \xi^{-1} \text{ or const.}, \text{ as } \xi \rightarrow \infty, \quad (\text{II-5.5g})$$

consistent with (II-5.2a); or a singularity like (II-5.4a) is repeated. Conversely, if $\bar{v} < 1$ then no such outer region arises. This enables the present form to be joined directly to a further incoming shear layer more removed from the center line if the mass flux ψ approaches the value C_3 in the lower reaches of the shear layer. There is a strong connection between these properties, involving algebraic decay at the onset of wake closure, and those of Section II-4(a2), where algebraic decay was found to be permissible nearer the start of the motion, and Section II-8 below pursues that theme.

If $K > 1$, on the other hand, the relevance to any shorter scale detached flow appears less, in view of the feature (II-5.4b) where $C_2 > 0$ gives forward motion. Thus the majority of the wake is initially forward on the present scale and major adjustments of the earlier detached motion would need to have taken place already, on a shorter scale. In particular, a join from the center line $y_1 = 0$ to an incoming detached shear layer is unlikely with $K > 1$ unless the lower part of the shear layer has acquired substantial forward motion beforehand.

Other issues arising here are as follows. First, the limit as $K \rightarrow \infty$ above recovers the finding of Section II-4(a1), in (II-4.11)-(II-4.13c), where the equation is related to that of the asymptotic suction profile. Second, simple power solutions for $G(\xi)$ in (II-5.2a) exist only for $K = 1, 2$. For $K = 1$, $G(\xi) = \pm \text{const.}$ ξ satisfies all of (II-5.2a,b) but this corresponds to $U = \pm \text{const.}$, producing a centerline flow which is not coming to rest, in contradiction to the shorter scale features. For $K = 2$, $G(\xi) = \pm d_1 \xi^2$ satisfies (II-5.2a) but not (II-5.2b); instead, it satisfies a no slip condition, a matter taken up in Section II-6. Third, although (in consequence) a study of the limit $K \rightarrow 1+$ suggests itself, further analysis shows that still, with virtually no pressure gradient present, a pronounced interval of reversed flow remains impossible, in line with (II-5.4b). If a significant pressure gradient is acting then more possibilities open up but really that forces us straight back to the self-consistent solution of Section II-3 and its scalings, in contrast with the smaller scale phenomena being sought here. Fourth, quite different self-consistent accounts for the start of the viscous wake (II-5.1a-c) are obtainable, with the centerline motion reversed as required, if U, ψ are taken to have finite nonzero profiles for y_1 of $O(1)$, say $\psi \rightarrow \psi^{(1)}(y_1)$, as $x_1 \rightarrow 0^+$. This is similar to (II-5.5a). The structure on a shorter length scale, however, then has to contend with a strong backward jet at the centerline, and that is a major task: see Sections II-7, II-8 below.

Next, an integral of (II-5.1a-c) requires the momentum deficit integral to be conserved,

$$\int_0^{\infty} U(1 - U) dy_1 = I_0 \quad (\text{II-5.6a})$$

where I_0 is a constant, deducible from the starting form of the motion. Far downstream if wake recovery occurs, then the left hand side of (II-5.6a) tends to $\delta(\infty)$, so that $\delta(\infty) = I_0$. But the linearized relation (II-2.4) still applies in effect here, i.e., $P = H - \Delta_1^{1/2} \delta(x_1)$ for all x_1 since the present length scales are short. Hence

$$P \rightarrow H - \Delta_1^{1/2} I_0 \text{ as } x_1 \rightarrow \infty. \quad (\text{II-5.6b})$$

The corresponding integral of the entire problem (II-2.1a-d) requires

$$P \rightarrow H + H^2 + H^3 + \dots \quad (\text{II-5.6c})$$

far downstream, however. Therefore two cases emerge. Either $\Delta_1 \geq 0(H^2)$ (yielding $X_{\text{reatt}} \geq 0(H^2)$), in which case the starting solution for (II-5.1a-c) must satisfy $I_0 = 0$, which is a severe constraint. Or $\Delta_1 \ll H^2$, $X_{\text{reatt}} \ll H^2$, in which case I_0 can be nonzero if $\Delta_1 = H^4$ but otherwise must be zero again. Notice that I_0 cannot be positive, from (II-5.6b,c). This singles out the scaling $\Delta_1 = H^4$, $X_{\text{reatt}} = H^4$ if the integrated momentum deficit I_0 is initially nonzero and negative. Moreover, if $I_0 < 0$ then initially there must be substantial regions of strong reversed flow ($U < 0$) or of velocity overshoot ($U > 1$), because of (II-5.6a). In any region where $|U|$ is small the integral in (II-5.6a) contributes only the jump in ψ across the region and this is negligible from the starting forms of (II-5.2a-c). Some care is necessary over these conclusions when $\delta(o+)$ is not finite, as in (II-5.5d), of course, since (II-5.6b) becomes questionable and the connection back to the earlier shorter scale properties then is not yet clear; nevertheless, the results (II-5.6b,c) must always be reconciled.

The sixth and final issue here concerns the integral form

$$\frac{\partial U}{\partial y_1} = \exp \left\{ \int_0^{y_1} v_1 dy_1 \right\} \int_0^{y_1} U \frac{\partial U}{\partial x_1} \exp \left\{ - \int_0^{y_1} v_1 dy_1 \right\} dy_1 \quad (\text{II-5.7a})$$

obtained from (II-5.1a-c), where $V_1 = -\partial\psi/\partial x_1$: c.f., (II-5.3a). If the centerline flow is coming to rest at $x_1 \rightarrow 0+$, $U(x_1, 0) \rightarrow 0$, as supposed prior to (II-5.2a), then (II-5.7a) yields $\partial U/\partial y_1 > 0$ for small $y_1 > 0$. So the velocity U has a local minimum at the centerline.

II-6. ON MASSIVE EDDY CLOSURE AND REATTACHMENT
ONTO A SOLID SURFACE

This section, a by-product of Section II-5, hinges on the feature that the exact solution of (II-5.2a) with reversed flow for $K = 1$ is $G = -d_1 \xi^2$, giving

$$U = -2d_1 y_1, \quad \psi = -d_1 y_1^2; \quad (\text{II-6.1a})$$

the constant d_1 is assumed positive here. The local solution (II-6.1a) for small x_1 satisfies the following conditions: (1) no slip holds at $y_1 = 0$; (2) the Chapman entrainment $\psi = -\kappa x_1^{1/2}$ is supplied at the position

$$y_1 = (\kappa/d_1)^{1/2} x_1^{1/4} + \dots, \quad (\text{II-6.1b})$$

around which the thinner $O(x_1^{1/2})$ Chapman form applies; (3) the reversed velocities U induced between the centerline $y_1 = 0$ and the shear layer at (II-6.1b) are small, of order $x_1^{1/4}$ as $x_1 \rightarrow 0$, in keeping with an assumption of slower flow beneath the shear layer on shorter length scales; (4) the pressure response required remains negligible (see comments on previous section).

Hence the initial form (II-6.1a, b) of the boundary layer (II-5.1a, c) can describe the start of viscous, pressure-free, reattachment onto a solid surface, in principle, with (II-5.1b) replaced by $\psi = U = 0, y_1 = 0$. See Fig. 10, also Ref. 17. Further terms in the small- x_1 expansion stemming from (II-6.1a, b) can be generated at will, including exponentials (see Section II-7 and Appendix D below), integral properties like those of Section II-5 can be derived, and it would be interesting to follow the subsequent downstream development of (II-5.1a, c) with no slip at $y_1 = 0$, which necessarily poses a challenging numerical task. Meanwhile, we consider below the repercussions of (II-6.1a, b), and its features (1)-(4) above, for the shorter scale motion. The applications in mind here include the gross separation and subsequent reattachment in flow past ramps, past bluff bodies with trailing splitter plates, and in wind-tunnels, all of which are of wide concern.

The first distinct stage encountered as the length scale is shortened (say $x_1 \rightarrow O(\Delta_2)$, small) appears where the induced pressure, while still small, first affects the centerline motion, since the latter is relatively slow and decelerating, from (II-6.1a, b). There the boundary layer equations still hold, with induced pressure included, in a thin sublayer where y_1 is $O(\Delta_2^{1/3})$ and U, ψ, P become $O(\Delta_2^{1/3}, \Delta_2^{2/3}, \Delta_2^{2/3})$ in turn. So, in effect, Eqs. (II-2.1a) apply again but now,

$$U = \psi = 0 \quad \text{at } Y = 0 \text{ (no slip)} \quad (\text{II-6.2a})$$

$$\psi \sim -d_1 Y^2 \quad \text{as } Y \rightarrow \infty \text{ (outer match)} \quad (\text{II-6.2b})$$

$$\psi \sim -d_1 \xi^2 X^{2/3} \quad \text{as } X \rightarrow +\infty \text{ (downstream match)} \quad (\text{II-6.2c})$$

where $\xi \equiv Y/X^{1/3}$, and the induced pressure is

$$P(X) = -(\kappa/d_1)^{1/2} X^{1/4}. \quad (\text{II-6.2d})$$

Here (see Fig. 10) the pressure is provoked by a combination of the interaction law $P = -S$ (due to the current small-scale effect on the outer flow, as in (II-2.4)), and the entrainment law $\psi \rightarrow -\kappa X^{1/2}$ as $Y \rightarrow S^-$, from (II-2.5), giving $d_1 S^2 = \kappa X^{1/2}$ because of (II-6.2b). This combination is analogous to that in Section II-4 (a1) and is taken only as an example, relating to the cascade with a splitter plate present along $y = 0$. The other applications mentioned above yield pressure forms different from (II-6.2d), although equally simple in certain cases.

The boundary layer problem (II-6.2a-d) with (II-2.1a) looks unusual at first sight, in having its starting condition at downstream infinity, in the uniform shear flow (II-6.2c), but that is because the motion is reversed. The flow solution can develop satisfactorily there in the form

$$\psi \sim -d_1 \xi^2 X^{2/3} + X^{1/4} g_1(\xi) + \dots, \quad X \rightarrow \infty. \quad (\text{II-6.3a})$$

Here g_1 satisfies $g_1'''' - d_1 (2\xi^2 g_1'''/3 - \xi g_1''/2 + g_1'/2) = -(\kappa/16d_1)^{1/2}$ with $g_1(0) = g_1'(0) = g_1''(\infty) = 0$, from (II-2.1a), (II-6.2a, b, d). Hence

$$g_1'' = (27\kappa)^{1/2} \int_0^\infty \exp(-rd_1 \xi^3) (2+9r)^{-3/4} r^{-7/12} dr / [12(-1/3)! d_1^{5/6}] \quad (\text{II-6.3b})$$

and $g_1''(0) > 0$. The incident reversed flow downstream is therefore decelerated further by the pressure field as X decreases. Further terms, including an origin shift in X , can be generated in the expression (II-6.3a).

Since the local problem (II-6.2a-d), (II-2.1a) has a prescribed pressure gradient which is adverse in the minus X direction, however, the flow solution cannot continue for all X and come to rest at $X = 0+$ as the body scale properties demand. Instead, either the classical Goldstein (Ref. 12) separation singularity is produced at a finite positive value of X , say $X \rightarrow X_3+$, or, due to an origin

shift if allowed, the flow reaches $X = 0 +$ with nonzero velocity. We expect the former option in general. Fortunately, Goldstein's singularity is not necessarily a disastrous occurrence here, if around $X = X_3$ local interaction brings in the pressure-displacement law (2.4) which yields regular separation, from Ref. 5. Therefore secondary separation probably can be accommodated either directly or interactively, depending on the particular local interaction near $X = X_3$, and self-consistency seems not unlikely. Moreover, in some applications the pressure form replacing (II-6.2d) turns out to have favorable gradient, thus preventing secondary separation, an aspect worth following through.

The overall trend of the flow structure produced above as a result of (II-6.1a, b) is encouraging, then, as a strong back flow is prevented by means of viscous action but little pressure force. There seems good reason to pursue the matter further, relating to the specific applications mentioned before, but that must be regarded as future work. We return now to the original wake closure problem.

II-7. CONNECTION FROM WIDESPREAD CASCADE TO EXTERNAL FLOW;
AND HOW FAR CAN THE KIRCHHOFF PARABOLA LAST?

Before considering the relation between the widespread cascade and external flow, we discuss certain features of the external flow problem itself.

In external flow past a bluff body, Kirchhoff's inviscid separated flow solution produces a parabolic growth (Fig. 11)

$$S(x) \sim bx^{1/2} \quad \text{as } x \rightarrow \infty \quad (\text{II-7.1})$$

for the eddy height $y = S(x)$ downstream, as mentioned in Part I. The viscous shear layer near the eddy boundary, specifically where $y = S(x) + \text{Re}^{-1/2} \hat{y}$ with \hat{y} of $O(1)$, also grows parabolically as $x \rightarrow \infty$ if the Chapman form (II-2.2d) holds then, with $\eta = \hat{y}/x^{1/2}$, $u \sim f_c'(\eta)$, $\psi \sim \text{Re}^{-1/2} x^{1/2} f_c(\eta)$, $f_c'(\infty) = 1$, $f_c'(-\infty) = 0$, $f_c(-\infty) = -\kappa$. Also, Ref. 1 shows that the mild uniform reversed streaming

$$u \rightarrow -\text{Re}^{-1/2} \frac{\kappa}{b}, \quad \psi \sim -\text{Re}^{-1/2} \frac{\kappa y}{b}, \quad \text{as } x \rightarrow \infty, \quad 0 \leq y < bx^{1/2}, \quad (\text{II-7.2})$$

then satisfies the inviscid, but slower flow, properties of the eddy as well as the entrainment ($\psi \rightarrow -\kappa \text{Re}^{-1/2} x^{1/2}$, $y \rightarrow bx^{1/2}$) and symmetry ($y \rightarrow 0$) conditions, downstream.

Viewed separately, each of the three parts of the downstream flow here, (1) the uniform stream $u = 1$ above the shear layer, (2) the Chapman form within, and (3) the mild reversed stream (II-7.2) underneath, constitutes an acceptable downstream limit for the Navier-Stokes equations, and so produces no call for wake closure to occur at all. Yet, viewed together, (1)-(3) do not satisfy the Navier-Stokes equations in a far-wake sense, for there (II-5.2a,b) apply with $K = 1$, so that (II-5.3a) then requires zero vorticity G'' and only the limit $u = 1$ remains acceptable. Therefore wake closure has to occur, and the (open wake) description involving (1)-(3), stemming from (II-7.1), must break down on some long length scale downstream. It cannot persist indefinitely.

This brings us to the question posed above: what is that length scale? Also, what forces the breakdown to occur? The former question is important when the relation between the widespread cascade and external flows is considered, while the latter question leads to some perhaps unexpected aspects of separated motions. The reasoning involved must be tentative again, because recirculatory motion is present, but consistency overall is the eventual aim.

The matter centers on certain exponentially small terms. Take the body scale flow first (see Fig. 11). In the eddy (E), an acceptable solution is $(\psi, u, p) = (\text{Re}^{-1/2} \bar{\psi}, \text{Re}^{-1/2} \bar{u}, \text{Re}^{-1} \bar{p} + \text{const.})$ to leading order, with x, y of $O(1)$, so that $\bar{\psi}, \bar{u}, \bar{p}$ are governed by the Euler equations. Vorticity conservation gives $\nabla^2 \bar{\psi} = \bar{f}(\bar{\psi})$ and if (II-7.2) applies then $\bar{f} \equiv 0$. Also,

$$\bar{\psi} = -\bar{\kappa}(x) \quad \text{at } y = S(x)-, \quad \bar{\psi} = \frac{\partial \bar{u}}{\partial y} = 0 \quad \text{at } y = 0 \quad (\text{II-7.3a})$$

from entrainment and symmetry respectively (see also Section II-2). Here $\bar{\kappa}(x) = -\hat{\psi}(x, -\infty)$ is the reduced mass flux required by the shear layer (SL), in which $\psi = \text{Re}^{-1/2} \hat{\psi}(x, \hat{y})$, and $d\bar{\kappa}/dx > 0$ to avoid exponential growth as $\hat{y} \rightarrow -\infty$ in SL, which is governed by the pressure-free boundary layer equations

$$u = \partial \hat{\psi} / \partial \hat{y}, \quad u \frac{\partial u}{\partial x} - \frac{\partial \hat{\psi}}{\partial x} \frac{\partial u}{\partial \hat{y}} = 0 + \frac{\partial^2 u}{\partial \hat{y}^2} \quad (\text{II-7.3b})$$

with

$$u(x, \infty) = 1, \quad u(x, -\infty) = 0, \quad \bar{\kappa}(x_{\text{sep}}) = 0. \quad (\text{II-7.3c,d,e})$$

Separation occurs at $x = x_{\text{sep}}$. The exponential dependence mentioned arises from the behavior

$$\hat{\psi} \sim -\bar{\kappa}(x) + \hat{A}(x, \hat{y}) \exp(\bar{\kappa}'(x) \hat{y}), \quad \hat{y} \rightarrow -\infty \quad (\text{II-7.3f})$$

of the SL solution, where the amplitude \hat{A} is algebraic in \hat{y} . As a result the eddy E, $0 < y < S(x)$, has the development

$$\psi = \text{Re}^{-1/2} \bar{\psi}(x, y) + \dots + \bar{A}(x, y) \exp[\text{Re}^{1/2} \bar{g}(x, y)] + \dots \quad (\text{II-7.4a})$$

where

$$\text{Real}(\bar{g}) < 0 \quad (\text{II-7.4b})$$

is required, but \bar{g}, \bar{A} are functions to be found, and the condition

$$\bar{g} \rightarrow 0- \quad \text{as } y \rightarrow S(x)- \quad (\text{II-7.4c})$$

applies, to match with (II-7.3f). Substituting (II-7.4a) into the Navier-Stokes equations we find the governing equation

$$\left(\bar{u} \frac{\partial}{\partial x} - \frac{\partial \bar{\psi}}{\partial x} \frac{\partial}{\partial y}\right) \bar{g} = \left(\frac{\partial \bar{g}}{\partial y}\right)^2 + \left(\frac{\partial \bar{g}}{\partial x}\right)^2 \quad (\text{II-7.5a})$$

for the exponent function \bar{g} , the right hand side being a viscous contribution, whereas \bar{u} , $\bar{\psi}$ satisfy Euler's inviscid equations

$$\bar{u} = \frac{\partial \bar{\psi}}{\partial y}, \quad \bar{u} \frac{\partial \bar{u}}{\partial x} - \frac{\partial \bar{\psi}}{\partial x} \frac{\partial \bar{u}}{\partial y} = - \frac{\partial \bar{p}}{\partial x}, \quad - \frac{\bar{u} \partial^2 \bar{\psi}}{\partial x^2} + \frac{\partial \bar{\psi}}{\partial x} \frac{\partial^2 \bar{\psi}}{\partial x \partial y} = - \frac{\partial \bar{p}}{\partial y}, \quad (\text{II-7.5b})$$

or $\nabla^2 \bar{\psi} = \bar{f}(\bar{\psi})$. In addition, near the centerline a thin viscous extra region VE is found necessary for the exponential terms (but not for any algebraic terms). In VE, $y = \text{Re}^{-1/2} y^*$ with y^* of $O(1)$,

$$\psi = \text{Re}^{-1} y^* u_0(x) + \dots + A^*(x, y^*) \exp[\text{Re}^{1/2} g_0(x)] + \dots, \quad (\text{II-7.6a})$$

$g_0(x) \equiv \bar{g}(x, 0^+)$, $\text{Real}(g_0) < 0$ and $u_0(x) \equiv \bar{u}(x, 0)$ is the reduced centerline velocity. In VE the Navier-Stokes equations reduce to the form

$$u_0(x) g_0'(x) \frac{\partial A^*}{\partial y^*} = - g_0'(x) p_0(x) + \frac{\partial^3 A^*}{\partial y^{*3}} \quad (\text{II-7.6b})$$

for A^* , where $p_0(x)$ is a local pressure force. Hence the solution satisfying the symmetry condition $A^* = \partial^2 A^* / \partial y^{*2} = 0$ at $y^* = 0$ is nontrivial in VE,

$$A^* = a_1^*(x) \sinh(\gamma^*(x) y^*) - \frac{p_0(x)}{u_0(x)} y^*, \quad \gamma^* \equiv (u_0 g_0')^{1/2} \quad (\text{II-7.6c})$$

the function $a_1^*(x)$ being fixed in principle by matching with E as $y^* \rightarrow \infty$.

The behavior of SL, E, VE as $x \rightarrow \infty$ downstream is as follows. In SL a momentum integral of (II-7.3b-d) gives, for all $x > x_{\text{sep}}$

$$\bar{\kappa}(x) = \int_{-\infty}^{\infty} u(u-1) dy + I_{\text{sep}} \quad (\text{II-7.7})$$

where I_{sep} is the integrated momentum deficit at separation, from (II-7.3e), and so is negative usually. That suggests that as $x \rightarrow \infty$ the Chapman form (f_c) is attained with a surprisingly high relative error of order $x^{-1/2}$, such that

$$\hat{\psi} \sim x^{1/2} f_c(\eta) + f_1(\eta) + \dots \quad (x \rightarrow \infty). \quad (II-7.8a)$$

From (II-7.3b-d), f_1 satisfies $f_1''' + (f_c f_1'' + f_c' f_1')/2 = 0$ and $f_1'(\pm\infty) = 0$. Hence

$$f_1(\eta) = D_1 f_c'(\eta) + E_1 \quad (II-7.8b)$$

where D_1, E_1 are constants dependent upon starting conditions and an origin shift in \hat{y} . Consistency with (II-7.7) then yields the asymptote

$$\bar{\kappa}(x) \sim \kappa x^{1/2} + I_{sep} \quad \text{as } x \rightarrow \infty, \quad (II-7.8c)$$

and $E_1 = I_{sep}$. The relative error in Kirchhoff's parabola (II-7.1) is also generally of the same high order, $x^{-1/2}$, in that

$$S(x) \sim b x^{1/2} + s_0 \quad \text{as } x \rightarrow \infty \quad (II-7.9)$$

with $s_0 \neq 0$. This can be established either by analysis of the farfield in Kirchhoff's free streamline solution or by reference to the exact solution for a broadside-on flat plate for instance: see page 499 of Ref. 18.

The small corrections in (II-7.8c), (II-7.9) control the downstream flow. Thus in E, as $x \rightarrow \infty$ with $\sigma = y/x^{1/2}$ fixed, $\bar{\psi} \sim -\kappa x^{1/2} \sigma/b + c_1 \sigma + O(1)$ from (II-7.5b), (II-7.3a), with $c_1 = (\kappa s_0^2/b - I_{sep}/b)$ positive. So (II-7.5a) requires the underlying form

$$\bar{g} \sim \bar{g}_0(\sigma) + x^{-1/2} \bar{g}_1(\sigma) + \dots + x^{-1} \bar{g}_2(\sigma) + \dots \quad (II-7.10a)$$

for \bar{g} , where

$$\bar{g}_0 = \kappa(\sigma^2 - b^2)/4b, \quad \bar{g}_1 = B_1\sigma,$$

$$\bar{g}_2 = \frac{bB_1^2}{\kappa} + \frac{bc_1B_1}{\kappa}\sigma + B_2\sigma^2 + \frac{c_2}{2}\sigma^2 \ln\sigma - \frac{\kappa}{16b}\sigma^4 \quad (\text{II-7.10b})$$

which satisfies (II-7.4b, c), provided $B_1 = -\kappa s_0/2b$. Hence the centerline value $g_0(x) \equiv \bar{g}(x, 0)$, required for VE, has the development

$$g_0(x) \sim -\kappa b/4 + bB_1^2/\kappa x + \dots \text{ as } x \rightarrow \infty. \quad (\text{II-7.10c})$$

That leaves the exponent function γ^* defined in (II-7.6c) having the behavior $\gamma^* \sim B_1 x^{-1}$ as $x \rightarrow \infty$, so that essentially

$$A^* \propto \sinh(B_1 y^*/x) \quad (\text{II-7.10d})$$

there. Further terms can be investigated for large positive x , including the nature of E when y remains finite and the equations controlling the amplitude \bar{A} in (II-7.4a). Also, as a check we notice that the exponential dependence in (II-7.4a) becomes $\exp[\kappa \text{Re}^{1/2} (y-b x^{1/2})/2 x^{1/2}]$ from (II-7.10a, b) as $y \rightarrow b x^{1/2}$ in E , which reproduces the Chapman decay in SL; see (II-7.3f) when (II-7.8c) holds. The principal concern, however, is that VE expands linearly $\propto \text{Re}^{-1/2} x$ downstream (Fig. 11), from (II-7.10d), due to the factor B_1 , i.e., to s_0 , i.e., to the correction term in (II-7.9). Significant viscous effects therefore spread out faster than the $x^{1/2}$, $\text{Re}^{-1/2} x^{1/2}$ expansion rates of Kirchhoff's parabola and Chapman's SL and are bound to affect the latter to some extent on a longer scale downstream. That scale is $x = 0$ (Re), from comparison of the growth rates $\text{Re}^{-1/2} x$ and $x^{1/2}$.

At least one adjustment of the solution does occur first on a scale $x = 0$ ($\text{Re}^{1/2}$), we note, where $\hat{X} = \text{Re}^{-1/2} x$ is finite. There, in summary, VE expands to $O(1)$ thickness in y and its solution has the development

$$\psi = -\kappa y \text{Re}^{-1/2}/b + \dots + A_1(\hat{X}, y) \exp[-\text{Re}^{1/2} \kappa b/4] + \dots \quad (\text{II-7.11a})$$

implied by (II-7.10c). The Navier-Stokes equations yield the backward heat equation $-\kappa \partial^2 A_1/\partial \hat{X} \partial y = b \partial^3 A_1/\partial y^3$ for the amplitude $\partial A_1/\partial y$. The solution satisfying symmetry at the centerline and the join with both E and VE as $\hat{X} \rightarrow 0+$ and with E as $y \rightarrow \infty$ is again nontrivial,

$$A_1 = \frac{\hat{a}_2}{\hat{X}^{1/2}} \exp\left(\frac{b\hat{c}_2^2}{\kappa\hat{X}}\right) \int_0^y \cosh\left(\frac{\hat{c}_2 y}{\hat{X}}\right) \exp\left(\frac{\kappa y^2}{4b\hat{X}}\right) dy . \quad (\text{II-7.11b})$$

Here \hat{a}_2, \hat{c}_2 are constants. Therefore downstream, as $\hat{X} \rightarrow \infty$, A_1 remains $O(1)$ if y is restricted to $O(\hat{X}^{1/2})$ or less, but A_1 increases exponentially for y of order \hat{X} and the linear growth of VE noted earlier is maintained then. So the length scaling $x \sim Re$ is implied still.

It can be established next that Kirchhoff's parabola (II-7.1) with simple entraining motion underneath in E becomes unacceptable on the $x = O(Re)$ scale. For suppose (II-7.1) does continue to hold, with the motion in E then having

$$\psi = \psi_2(X^*, Y_2) + \dots + A_2(X^*, Y_2) \exp[Re^{1/2} g_2(X^*, Y_2)] + \dots, \quad (\text{II-7.12a})$$

dominated by the $O(1)$ entrainment necessary for SL when $x = ReX^*$ with X^* finite. Here $y = Re^{1/2} Y_2$, and $0 < Y_2 < bX^{*1/2}$ in E. From the Navier-Stokes equations we obtain the governing equations

$$\left(u_2 \frac{\partial}{\partial X^*} - \frac{\partial \psi_2}{\partial X^*} \frac{\partial}{\partial Y_2}\right) g_2 = \left(\frac{\partial g_2}{\partial Y_2}\right)^2, \quad (\text{II-7.12b})$$

$$\left(u_2 \frac{\partial}{\partial X^*} - \frac{\partial \psi_2}{\partial X^*} \frac{\partial}{\partial Y_2}\right) A_2 \frac{\partial g_2}{\partial Y_2} + u_2 \frac{\partial g_2}{\partial X^*} \frac{\partial A_2}{\partial Y_2} + \frac{\partial u_2}{\partial X^*} \frac{\partial g_2}{\partial Y_2} A_2 \quad (\text{II-7.12c})$$

$$- \frac{\partial \psi_2}{\partial X^*} \frac{\partial g_2}{\partial Y_2} \frac{\partial A_2}{\partial Y_2} - \frac{\partial u_2}{\partial Y_2} \frac{\partial g_2}{\partial X^*} A_2 = 3 \left[\left(\frac{\partial g_2}{\partial Y_2}\right)^2 \frac{\partial A_2}{\partial Y_2} + \frac{\partial g_2}{\partial Y_2} \cdot \frac{\partial^2 g_2}{\partial Y_2^2} A_2 \right]$$

for g_2, A_2 , omitting certain unimportant contributions, where $u_2 = \partial \psi_2 / \partial Y_2$. So if the simple entraining solution holds for all X^* ,

$$\psi_2 = -\kappa Y_2 / b, \quad u_2 = -\kappa / b, \quad (\text{II-7.13})$$

continuing the trend (II-7.2), then (II-7.12b) gives $g_2 = \kappa (\sigma^2 - b^2)/4b$ to merge with (II-7.10a, b), where $\sigma \equiv Y_2 X^{*-1/2}$, and (II-7.12c) reduces to

$$2Y_2 \frac{\partial A_2}{\partial Y_2} + 2 X^* \frac{\partial A_2}{\partial X^*} + A_2 = 0. \quad (\text{II-7.14a})$$

The general solution for A_2 is

$$A_2 = X^{*-1/2} f_2(Y_2/X^*), \quad (\text{II-7.14b})$$

where the function f_2 is to be found. Matching with VE, however, as VE spreads out into E (Fig. 11), demands that

$$f_2(\xi) \propto \sinh(\hat{c}_2 \xi) \quad (\text{II-7.15a})$$

from (II-7.11b). In contrast the match with SL requires

$$f_2(\xi) = \beta_0 b^2 \exp(-\kappa \xi d_2 / 2b) / \xi^2, \quad (\text{II-7.15b})$$

from (II-7.3f) where $\hat{A} \sim \beta_0 x^{1/2}$ for large x , and the constant d_2 represents an origin shift. The two forms (II-7.15a, b) for finite ξ cannot be reconciled and so the description assumed breaks down.

This breakdown on the $O(\text{Re})$ length scale may be taken as evidence that Kirchhoff's parabola must be adjusted then, although other interpretations exist. Further, since an ellipse $y = \text{Re}^{1/2} b X^{*1/2} (1 - X^*/L)^{1/2}$ is the only other eddy shape consistent with the initial parabola and maintaining enough uniform pressure, the conclusion of an $O(\text{Re})$ closure length $L\text{Re}$ follows as in Refs. 1, 2, 14. These references appeal instead to an overall momentum balance (as in Section II-5) to suggest the closure length, whereas the breakdown above provides a perhaps firmer local cause for the closure.

The elliptical shape is found to remove the contradiction of (II-7.15a, b). But in turn it emphasizes another difficult feature. It points (at first sight - see Section II-8 below) to the inviscid closure problem

$$\nabla^2 \psi = F(\psi) \quad (\text{II-7.16})$$

within $O(1)$ distances of $x = LRe$. Here the vorticity $F(\psi)$ is nonzero, because of the incident, $O(1)$ thick, Chapman profile in SL. So (II-7.16) provokes the well-known difficulty concerning a strong $O(1)$ thick jet being forced upstream, out of the closure process, thus violating the slower flow assumption made for the majority of the eddy upstream: see Fig. 11. The backward jet is unavoidable, to preserve vorticity along the centerline, in the above account unless viscosity or some other subtle mechanism comes into action. Similar difficulties were discussed in previous sections for the widespread cascade. Proposals on this wake closure difficulty for external flow are given in Section 8 below. Meanwhile, we turn to the relation between widespread cascade flows and external flow, given the importance of the $O(Re)$ length scale in the latter.

In the relation between the widespread cascade and external flow it is noted first that while the cascade spread $H \equiv H_W/H_C$ is finite, as in Part I, the body scale flow and its exponential corrections are effectively as in (II-7.3a) - (II-7.6c). The difference is that now $S(\infty) = H_W$ is finite (Part I), instead of (II-7.1) holding. Properties of the exponential terms then are summarized in Ref. 17 and Appendix D (a novel aspect there is that the exponent function \bar{g} becomes complex, inducing oscillatory behavior). As the cascade spread becomes wide, for a fixed body size ($H \rightarrow 0$), however, the parabola (II-7.1) emerges as a first downstream asymptote, encountered for $1 \ll x \ll H_C$, before the bound $S \rightarrow S(\infty)$ reasserts itself as x becomes $O(H_C)$. Also $H_W = O(H_C^{1/2})$ because of (II-7.1). The solution for the eddy shape S during this adjustment is found to be

$$S = \frac{2H_W}{\pi} \cos^{-1} \left\{ e^{-\pi b^2 x / 8H_W^2} \right\} \quad (\text{II-7.17})$$

for large $x \sim H_W^2 \sim H_C$, matching with (II-7.1) for small x/H_W^2 but giving $S \rightarrow H_W$ for large x/H_W^2 . Here $0 < \cos^{-1} < \pi/2$, while the constant b is $O(1)$ generally, equal to 0.50 for the circular cylinder. Let us write $H_W = b_1 H_C^{1/2}$ for large H_C , where b_1 is of $O(1)$ in general. Then $H = b_1 H_C^{-1/2} \rightarrow 0$, and so the widespread cascade first upsets the Kirchhoff parabola (II-7.1) downstream only when x is increased to $O(H^{-2})$, from (II-7.17).

Comparison with the $x \sim Re$ external closure scale indicated above therefore re-emphasizes the stage $H \sim Re^{-1/2}$ or $H_C \sim Re$ as in Part I. On the other hand, the viscous closure for the cascade wake always yields the scaled closure length X_{reatt} , i.e., the unscaled closure length from Part I is $x_{\text{reatt}} = Re H_C^2 X_{\text{reatt}} = Re b_1^4 H^{-4} X_{\text{reatt}}$. So if $X_{\text{reatt}} \sim H^n$, say, for the widespread cascade ($H \rightarrow 0$) studied in Sections II-2-5, then $x_{\text{reatt}} \sim b_1^4 Re H^{n-4}$. Three subcases arise, therefore, which can be summarized as follows. First, if $n = 4$, x_{reatt} stays at $O(Re)$ when $H \rightarrow 0$, i.e., as (in a more physical interpretation) the cascade spacing H_C is increased for fixed Re ; and when H then falls through the stage $O(Re^{-1/2})$ there is a continuous adjustment from (II-7.17) to the elliptical shape above as in Refs. 1, 14. Second, if $n < 4$, x_{reatt} increases beyond $O(Re)$ when H falls, at least until the stage $H \sim Re^{-1/2}$ when the closure first affects matters and

reduces x_{reatt} back to $O(Re)$. Third, if $n > 4$, x_{reatt} becomes shorter than $O(Re)$ as H is decreased, and indeed x_{reatt} enters the adjustment zone of (II-7.17) when H falls to $O(Re^{-1/(n-2)})$ or H_c is increased to $Re^{2/(n-2)}$.

So, whatever the value of n , the above arguments imply that Kirchhoff's solution for external flow does emerge from the widespread cascade solution.

II-8. NON-ENTRAINING SHEAR LAYERS

Encouraged by the final remark of Section II-7, we seek an alternative account for wake closure consistent with Kirchhoff's (body scale) flow but avoiding the central difficulty of backward jets noted after (II-7.16). Again, previous comments suggest that viscous forces must play a key role, if the objection (II-7.16)ff is to be placated, and that algebraic behavior and nonuniqueness within the shear layer can occur. We pursue these themes below.

Section II-4 (A2) anticipated that algebraic behavior can be achieved in the lower reaches of a detached shear layer near the start of a separated wake, while Section II-5 showed the same can occur at the other extreme, just before wake closure. This raises the issue of whether such algebraic dependence can persist in-between, for virtually all the shear layer's length, in the widespread cascade or the external flow in particular although the application is quite wider. In whatever context the shear layer is governed by (II-2.2b-d) or (II-7.3b-d), involving essentially the same pressure-free viscous boundary layer equations as in the wake closure of Section II-5. Algebraic velocity decay for any x does turn out to be possible, as (say) $\hat{y} \rightarrow -\infty$ in (II-7.3b-d), in the form $\hat{\psi} \sim -b_1 |\hat{y}|^{-\gamma}$, $u \sim -b_1 \gamma |\hat{y}|^{-\gamma-1}$ with $\gamma+1$ positive for decay. The governing equation (II-7.3b) then requires the expansion

$$\hat{\psi} \sim -b_1 |\hat{y}|^{-\gamma} + \dots + E(x) |\hat{y}|^{-1} + \dots, \quad \hat{y} \rightarrow -\infty, \quad (\text{II-8.1a})$$

however, with b_1 being constant and

$$E = -(\gamma+1)(\gamma+2)(x-l)/\gamma \quad (\text{II-8.1b})$$

where l is an arbitrary constant. So the restriction $-1 < \gamma < 1$ applies to (II-8.1a) as well as $\gamma \neq 0$ to suppress any constant of addition to $\hat{\psi}$. Otherwise, if $\gamma \geq 1$ is assumed, (II-8.1a) is replaced by

$$\hat{\psi} \sim -6(x-l) |\hat{y}|^{-1} + \dots, \quad \hat{y} \rightarrow -\infty. \quad (\text{II-8.1c})$$

The leading term in (II-8.1c) gives an exact solution of the boundary layer equations, incidentally, while (II-8.1a) verifies that for the widespread cascade the downstream form (II-4.15b-f) in III merges satisfactorily into the shear layer I on a longer length scale. The two allowable forms, (II-8.1a) (with

$0 < |\gamma| < 1$) and (II-8.1c), present an alternative to the classical exponential decay (see (II-7.3f)) usually taken by shear layers but, unlike the latter, (II-8.1a) do not require any direct entrainment of fluid from below the shear layer. This is another encouraging point, for classical entrainment tends to ruin most previous models (Refs. 1,2,13-15) of grossly separated motion.

The non-entraining shear layer can also start satisfactorily (Fig. 12), for example by taking over from an incoming, entraining, Chapman form holding as $x \rightarrow 0 +$ (as required in (II-2.2d) for example), in the following manner. The relatively thin $O(x^{1/2})$ Chapman form requires the entrainment $\hat{\psi} = -\kappa x^{1/2}$, say at $\hat{y} = 0 -$. Beneath this, therefore, a thicker subzone is induced where $|\hat{y}|$ is $O(d_1(x))$ say, $d_1 \gg x^{1/2}$ is unknown and the solution has the displaced form of a power law

$$\hat{\psi} = -\kappa (-\kappa_1 \hat{y} + d_1(x))^{-\Gamma} + \dots \quad (\text{II-8.2a})$$

where $\Gamma, \kappa_1 (>0)$ are constants, $d_1(x) > 0$, and $\hat{y} < 0$. Here the inviscid form (II-8.2a) is consistent with the pressure-free equations as $x \rightarrow 0 +$ provided $d_1 \ll x^{-1/(\Gamma-1)}$, or $(\Gamma+1)/\Gamma(\Gamma-1) > 0$. But entrainment at $\hat{y} = 0 -$ requires $-\kappa d_1^{-\Gamma} = -\kappa x^{1/2}$, so that

$$d_1(x) = x^{-1/2\Gamma} \quad (\text{II-8.2b})$$

Hence (II-8.2a, b) apply for $\Gamma > 1$. Consequently yet another subzone is provoked, as viscous forces enter play where \hat{y} falls to -0 ($x^{-1/(\Gamma-1)}$) and $\hat{\psi} \rightarrow O(x^{\Gamma/(\Gamma-1)})$ from (II-8.2a), say

$$\hat{\psi} = x^{\Gamma/(\Gamma-1)} G(\xi) + \dots, \text{ with } \xi = \hat{y}/x^{-1/(\Gamma-1)} \quad (\text{II-8.2c})$$

and ξ is finite and negative. Then G satisfies the viscous Falkner-Skan type equation (II-5.2a) with $K = -\Gamma < -1$ now, and

$$G \sim -\kappa \kappa_1^{-\Gamma} (-\xi)^{-\Gamma} \text{ as } \xi \rightarrow 0 - \quad (\text{II-8.2d})$$

to join with (II-8.2a). The required solution of (II-5.2a), (II-8.2d) has the property (Ref. 17)

$$G \sim -6 (-\xi)^{-1} \text{ as } \xi \rightarrow -\infty \quad (\text{II-8.2e})$$

consistent with (II-5.2a), while (II-5.3a) still hold provided the middle integration range there runs from positive ξ_1 to ξ rather than 0 to ξ , leaving negative vorticity

$$G'' < 0 \quad \text{for all } \xi < 0, \quad (\text{II-8.2f})$$

in line with (II-8.2d,e), since $\Gamma > 1$. We note that, since d_1 is large and \hat{y} negative, $\hat{\psi}$ is small in (II-8.2a), as it is in (II-8.2c), meaning that all the motion in the algebraic subzones below the Chapman layer comes to rest as $x \rightarrow 0^+$ as required. Moreover, for small positive x reversed flow is forced to occur, from (II-8.2a-e), so that the algebraic shear layer immediately becomes subject to the influence of the conditions further downstream. This seems a desirable feature in the flow. The emergent behavior (II-8.2e) for small x is the analogue of, and continues into, the case (II-8.1c) for finite positive x , provided the origin ℓ in (II-8.1c) is zero.

The above indicates that the solution of the characteristic shear layer problem posed in (II-2.2b-d) is not unique, then. The further aspects below reinforce that conclusion.

First, another successful start at $x = 0^+$ is possible for the non-entraining shear layer when the decay condition (II-8.1a) holds instead of (II-8.1c), or when ℓ in (II-8.1c) is nonzero. In these cases (II-8.2a-f), beneath the incident Chapman form, are replaced by a simpler consistent description in which

$$\hat{\psi} \rightarrow \hat{\psi}_0 [\hat{y} - d_2(x)/\kappa_2] \quad \text{as } x \rightarrow 0^+ . \quad (\text{II-8.3a})$$

Here $\hat{\psi}_0$ is an arbitrary profile, except that $\hat{\psi}_0(\hat{y}) \sim -\kappa (-\kappa_2 \hat{y})^\lambda$ as $\hat{y} \rightarrow 0^-$, with constants $\kappa_2, \lambda > 0$, and the displacement effect $d_2(x)$ is small such that

$$d_2(x) = x^{1/2\lambda} , \quad (\text{II-8.3b})$$

for the entrainment condition. Also, the behavior

$$\hat{\psi}_0(\hat{y}) \sim b_1 (-\hat{y})^{-\gamma} \quad \text{as } \hat{y} \rightarrow -\infty \quad (\text{II-8.3c})$$

must hold with $\gamma \leq 1$ and b_1 then identifies either with the coefficient b_1 in (II-8.1a) at finite positive x , for $\gamma < 1$, or with ℓ in (II-8.1c) for $\gamma = 1$.

The restriction $\gamma \leq 1$ avoids the setting up of a thicker zone where (II-8.2c) would apply and would lead instead to (II-8.2e).

Thus both the algebraic decay forms (II-8.1a, c) can be initiated self-consistently (with ℓ zero or nonzero in (II-8.1c)), branching away from the incoming, exponentially decaying, Chapman form at $x = 0+$. The algebraic start can be from rest - see (II-8.2a-e) - if (II-8.1c) holds with ℓ zero, but otherwise a nonzero initial profile (II-8.3a) is required (Fig. 12), below the Chapman layer. Both the starts (II-8.2a-e), (II-8.3a-c), however, are consistent with the earlier scaled inviscid properties of Section II-4 (a2) depending on the value of γ there. Again, all the shear layer analysis is subject to an unknown origin shift in \hat{y} , due to Prandtl's transformation, which adds arbitrariness to the solution, while reversed flow in the non-entraining shear layer can readily be present depending inter-alia on the signs of the unknown constants b_1, ℓ ; e.g., it occurs simply if $x > \ell$ in (II-8.1c), since $u \sim -6(x-\ell)\hat{y}^{-2}$ then.

Second, the non-entraining shear layer can terminate in a physically sensible fashion after a finite distance $x = x_2$; it cannot continue for all positive x , we believe. The termination can involve a singularity as $x \rightarrow x_2 -$ in which the shear layer splits into two main zones, 1, 3, each of $O(1)$ thickness in \hat{y} and with $O(1)$ velocities u , separated by a thickening viscous zone 2 of width $O(x_2-x)^{-m}$ in \hat{y} where the shear layer fluid is coming to rest (see Fig. 12). Here $m > 0$ and zone 2 has

$$\hat{\psi} \sim \text{const.} + (x_2-x)^{m+1} G(\xi), \quad \xi \equiv \hat{y}/(x_2-x)^{-m}. \quad (\text{II-8.4a})$$

So G satisfies (II-5.2a) again, but with $\kappa = -(m+1)/m < -1$ and $-G'''$ replaces G''' . The range of ξ is finite here, however, with minus the growth (II-5.4a) being achieved as $\xi \rightarrow \xi_0 -$, a similar growth occurring as $\xi \rightarrow -\xi_0 +$, all subject again to an origin shift, and the symmetry condition (II-5.2b) can effectively hold in-between. So (II-5.3a) now shows that

$$G'' < 0 \text{ for } 0 < \xi < \xi_0, \quad G'' > 0 \text{ for } -\xi_0 < \xi < 0. \quad (\text{II-8.4b})$$

Centered around $\xi = +\xi_0$ zone 1 occurs with an arbitrary shifted profile

$$\hat{\psi} \rightarrow \hat{\psi}_{11} [\hat{y} - \xi_0(x_2-x)^{-m}], \quad x \rightarrow x_2-, \quad (\text{II-8.4c})$$

consistent with the governing equations and satisfying

$$\hat{\psi}_{11}(\hat{y}) \sim \text{const.} - C_1 (-\hat{y})^{-\frac{m+1}{m}} \quad \text{as } \hat{y} \rightarrow -\infty \quad (\text{II-8.4d})$$

$$\hat{\psi}'_{11}(\infty) = 1, \quad (\text{II-8.4e})$$

to match minus the growth (II-5.4a) from zone 2 and to comply with the outer uniform stream. Likewise, centered around $\xi = -\xi_0$ is zone 3 in which

$$\hat{\psi} \rightarrow \hat{\psi}_{12} [\hat{y} + \xi_0 (x_2 - x)^{-m}], \quad x \rightarrow x_2^-, \quad (\text{II-8.4f})$$

and the profile $\hat{\psi}_{12}$ is arbitrary apart from the two matching constraints

$$\hat{\psi}_{12}(\hat{y}) \sim \text{const.} + C_1 \hat{y}^{\frac{m+1}{m}} \quad \text{as } \hat{y} \rightarrow \infty, \quad (\text{II-8.4g})$$

$$\hat{\psi}_{12}(\hat{y}) \sim b_1 (-\hat{y})^{-\gamma} \quad \text{as } \hat{y} \rightarrow -\infty. \quad (\text{II-8.4h})$$

The latter follows from (II-8.1a) for $0 < |\gamma| < 1$ but from (II-8.1c) with b_1 denoting $6(\ell - x_2)$ for $\gamma=1$ and $x_2 \neq \ell$.

Alternatively the shear layer can finish in a regular form as $x \rightarrow x_2^-$ [the conditions (II-8.4e,h) are then satisfied by a single arbitrary profile] or, if $x_2 = \ell$, a multi-structure akin to that of (II-8.2a-e) can be set up. The precise form taken as $x \rightarrow x_2^-$ depends on the subsequent wake closure properties and on the flow beneath the shear layer.

Underneath the shear layer a broader zone of slower motion is produced whose character is controlled by whichever of (II-8.1a, c) applies. In either case however the small pressure force almost certainly reasserts its influence, yielding governing equations of the form

$$\bar{u} = \frac{\partial \bar{\psi}}{\partial \bar{y}}, \quad \frac{\bar{u} \partial \bar{u}}{\partial \bar{x}} - \frac{\partial \bar{\psi}}{\partial \bar{x}} \frac{\partial \bar{u}}{\partial \bar{y}} = -\bar{p}'(\bar{x}) + \lambda_1 \frac{\partial^2 \bar{u}}{\partial \bar{y}^2} \quad (\text{II-8.5a})$$

and the matching condition, from (II-8.1a, c),

$$\bar{\psi} \sim -\lambda_2 (\bar{\delta} - \bar{y})^{-\gamma} \quad \text{as } \bar{y} \rightarrow \bar{\delta}(x) \text{ --.} \quad (\text{II-8.5b})$$

Here, for (II-8.1a), $\lambda_1 \equiv 0$ (inviscid properties, $\lambda_2 \equiv b_1$ (constant) and $0 < |\gamma| < 1$), whereas for (II-8.1c) $\lambda_1 \equiv 1$ (viscous properties, $\lambda_2 = 6(x-l)$ and $\gamma = 1$). Also, $\bar{y} = \bar{\delta}(x)$ gives the reduced position of the non-entraining shear layer. At the initial station $x = 0 +$, or at the terminal one $x = x_2 -$, the solution of (II-8.5a, b) can start either from an arbitrary velocity profile \bar{u} (this is appropriate to Section II-4 (a2) for the widespread cascade for instance, where \bar{u} , \bar{y} , \hat{y} above stand for \bar{U} , \bar{Y} , Y_0 respectively, and the X-scaling is $X \rightarrow H(2^{1/\gamma+3})/(\gamma+1)x$) or from a similarity form. For the latter, if $\lambda_1 = 1$ and $x \rightarrow x_2 -$ say, we have $\bar{\psi} \sim (x_2 - x)^{1-M} G(\xi)$, $\xi = \bar{y}/(x_2 - x)^M$, so that (II-5.2a) holds but with $K = (1-M)/M$ and $-G'''$ replacing G''' . Here $|K| < 1$ and the ξ -range is finite, $0 \leq \xi < \xi_2$, implying that $\bar{\delta}(x) \sim \xi_2 (x_2 - x)^M$ if, as we assume here, the symmetry condition is achieved directly in this broader zone, i.e. (II-5.2b) also applies. We would expect $M > 0$, for the onset of closure ($\bar{\delta} \rightarrow 0$), and $M > 1/2$, for the scaled velocity \bar{u} to increase then. Hence $-1 < K < 1$. Solutions of (II-5.2a, b) then exist (Ref. 17) and yield the required property

$$G \sim -6 (\xi_2 - \xi)^{-1} \quad \text{as } \xi \rightarrow \xi_2 \text{ --.} \quad (\text{II-8.5c})$$

which satisfies (II-8.5b). Solutions are also possible if the pressure \bar{p} remains influential as $x \rightarrow x_2 -$; see Ref. 17 and Appendix E.

In summary, it seems clear that the motion within and beneath the non-entraining shear layer can remain self-consistent, from its start to its terminal form. So the main difficulty remaining is to account self-consistently for the wake closure, near or beyond $x = x_2$. The correct account there is not so clear yet.

It is tempting to appeal first to (II-7.16), or its counterpart $\partial^2 \psi / \partial y^2 = F(\psi)$ for thin layers, and conclude that a finite fraction (where $\hat{\psi} < 0$) of the shear layer should be reversed and turned upstream during closure (Fig. 12), due to local inviscid and pressure action. Certainly the splitting in (II-8.4a-h) seems to herald this and the strong backward jet so produced would continue to entrain no fluid, which is encouraging. Each of the conditions (II-8.1b, c), however, requires a linear decrease of the velocity contribution $O(\hat{y}^{-2})$ whose continuity around the eddy therefore cannot be reconciled readily with smooth inviscid turning near closure at one end and with the slower flow or smooth turning necessary back towards the body scale flow at the other end.

It is tempting, secondly, to imagine the lower part (II-8.4f-h) of the terminating shear layer proceeding smoothly through $x = x_2$ with no significant velocity or pressure change and coming out as a starting profile for the viscous

closure studied in Section II-5. There, relatively near the centerline, the requirement $|K| > 1$ leads to (II-5.4a), demanding in effect that (II-8.1c) holds and $\ell = x_2$ is the closure length. That is all consistent so far, but back at $x = 0 +$, the initial shear layer then has the form (II-8.3a-c), with $b_1 = 6 \ell$, $\gamma = 1$, and requires an $O(1)$ velocity profile below the incident Chapman form. The origins of such a lower $O(1)$ profile are hard to explain.

A third temptation is to postulate that a strong backward centerline jet with edge decay different from the terminal shear layer's emerges from the unified viscous closure of Section II-5 as $x_1 \rightarrow 0 +$ there. Yet the difference in decay rates then requires a similarity solution, i.e. (II-5.2a), to hold between the jet and shear layer for small x_1 . This forces (II-5.4a) with $|K| > 1$ which in turn implies that $x_2 = \ell$ for both the shear layer and the jet. So again continuity of the velocity profile around the circuit of the eddy appears likely.

Thus the x -dependence in (II-8.1b, c) poses certain global difficulties, just as entrainment does in classical shear layers. However, a novel description of the closure near and beyond $x = x_2$ is possible now. Suppose that the viscous splitting (II-8.4a-h) is followed by the inviscid process of (II-7.16) locally again, but all the streamlines turned back there remain part of the lower incident layer (II-8.4f-h). This can happen in principle because of the small velocities and reversed flow attainable at the edges of the lower layer, in (II-8.4g, h): it cannot happen with classical shear layers because the latter have at least one nonzero edge velocity with forward flow. (Consider (II-7.16) and Bernoulli's law). So the non-entraining shear layer can "feed itself", in a sense, via the closure process; see Fig. 12. Further downstream the viscous closure of Section II-5 can then emerge also. There is no clear objection to this description and it appears self-consistent globally. The dominant velocities, and the eddy center, of the recirculating flow are confined within the shear layer itself, which is a strange feature perhaps but which we feel can be defended simply by emphasizing that previous searches (Refs. 1,2,13-15) for straightforward accounts have all failed.

II-9. FURTHER COMMENTS

1. The first clear sign to come out of the widespread cascade analysis of Part II is that viscous forces must play a significant role in massive wake closure. Inviscid theory fails (Section II-2), because of the Bernouilli relation between pressure and centerline velocity.

That means broadly that straightforward estimates (Refs. 1,2,13-15) of eddy closure properties also fail since they point to predominantly inviscid theory. Hence the explanation of massive wake closure must contain some initially unexpected but realistic feature(s).

The allied proposals of Section II-5,8 concerning non-entraining shear layers and viscous closure with algebraic decay seem to fall in line with the above two paragraphs, as does the long eddy result of Section II-3.

2. That non-entraining shear layers can exist in principle, providing a switch at any stage from exponential entraining to algebraic behavior, seems fairly definite (Section II-8). Two aspects need further examination nonetheless.

First, at what stage, on what length scale, is the switch made (if at all)? For external flow, Section II-7(a) suggests the $x \sim Re$ scale, in keeping with most experimental and computational evidence. For the wide-spread cascade there is less certainty. Sections II-3 and 4 (a2) tend to emphasize lengths greater than $O(H^3)$ in X but in retrospect there appears no obvious reason to really discount shorter scalings, despite the earlier estimates. Indeed, Section II-5 points to the scalings H^4 and H^2 (see near (II-5.6a-c)), Sections II-2, 4 imply that the flow solution can no longer remain simple once X reaches $O(H^3)$, while the computations of Part I seem to give the H^3 scaling. Against that, Section II-3 shows that the switch above may even be unnecessary for the cascade motion, in which case the non-entraining shear layer can become relevant only later in external bluff body motion, as described by Section II-7, or in other grossly separated flows.

This introduces the second aspect, namely that wake closure following a non-entraining shear layer still seems to demand a substantial localized pressure response (Section II-8). In external motion such a response is readily produced by the blunt shape of the end of the eddy (Refs. 1,13 and Section II-7). By contrast the widespread cascade tends to suppress the pressure response according to both analysis (see Sections II-2, 4, 5) and calculation (Part I). The objections may well be ill-founded, however, for the alternative account of Section II-3 also induces a substantial pressure, while the upper portion of the splitting in Section II-8, Eqs. (II-8.4c-e), could be responsible for the required pressure rise locally.

3. Further accurate numerical study, of the nonlinear problems posed by (1) the Section II-3 proposal for a long eddy and branching solutions, (2) the viscous wake closure of Section II-5, (3) the viscous reattachment onto a solid surface (Section II-6), (4) the Section II-8 non-entraining shear layers of finite length, and (5) the full cascade problem in Part I for smaller values of H , is desirable and would add undoubted help to the arguments followed above for massive stall. Otherwise, such arguments always stay very tentative due to the presence of nonuniqueness, nonlinearity and recirculating motion. All of (1)-(5) set not inconsiderable tasks but it is felt that the prospects and insight into massive stall properties provided by the widespread cascade problem are also not inconsiderable.

4. The connection (Section II-7) from the widespread cascade to external bluff-body motion, although hindered by our not knowing for certain the power governing the behavior $X_{\text{reatt}} \propto H^n$ as $H \rightarrow 0$ (see point 2 above), is fairly definite on one important feature. The Kirchhoff solution with its parabolic growth downstream does take control of the body scale flow when the cascade spread H^{-1} is large.

This holds whatever the value of n . The precise value of n then merely dictates what happens on longer length scales downstream of Kirchhoff's parabola. Given that, it would be very surprising if Kirchhoff's solution for the body scale were affected at all significantly by further increase of the cascade spread as external flow properties take over still more.

The sole hesitation we feel in stating the above is slight and concerns the possibility that the whole description of wake closure for the finite-spread cascade in Part I breaks down at a finite value of H , allowing no limit form as $H \rightarrow 0$. That would alter the scene completely. The possibility seems remote but it serves to stress the need for more computational study of the sensitive flow properties arising at smaller values of H in Part I.

5. This work has concentrated mostly on symmetric wake closure with centerline flow. A proposal on massive eddy closure, or reattachment, onto a solid surface has also emerged (Section II-6), however, which is believed to merit further attention. It suggests secondary separation as a possible consequence and finds application in (e.g.) the separating flow past ramps, past bodies with trailing splitter plates, and through wind tunnels, all of which have attracted much theoretical and experimental interest in recent times. See also Ref. 17. Again, nonsymmetric wake closure is of much practical and theoretical concern.

REFERENCES

1. Smith, F. T.: J. Fluid Mech., 92, 171, 1979, and 113, 407, 1981.
2. Messiter, A. F.: AGARD Conf. on Flow Separation, 1975.
3. Sychev, V. V.: Izv. Akad. Nauk. Mekh., Zh.i. Gaza 3, 47, 1972.
4. Smith, F. T., Eagles, P. M.: J. Eng. Mathematics, 14, 219, 1980.
5. Smith, F. T., Daniels, P. G.: J. Fluid Mechanics, 110, 1, 1981.
6. Smith, F. T.: J. Fluid Mechanics, 90, 725, 1979.
7. Carter, J. E.: AIAA paper, 74-583, AIAA paper 79-1450.
8. Smith, F. T.: J. Inst. Maths and its Applics., 13, 127, 1974.
9. Woods, L. C.: The Theory of Subsonic Plane Flow. Cambridge Univ. Press, 1961.
10. Smith, F. T.: UTRC Rept. UTRC82-13; also to appear in J. Fluid Mech., 1983.
11. Goldstein, S.: Proc. Camb. Phil. Soc., 26, 1, 1930.
12. Goldstein, S.: Quart. J. Mech. Appl. Math., 1, 43, 1948.
13. Burggraf, O. R.: AGARD paper 168 on flow separation, Göttingen, 1975.
14. Sychev, V. V.: Rept. to 8th Symp. Recent Problems in Mech. Liquids & Gases, Tarda, Poland, 1967.
15. Messiter, A. F., Hough, G. R., Feo, A.: J. Fluid Mech., 60, 605, 1973.
16. Reyhner, T. A., Flügge-Lotz, I.: Int. J. Nonlinear Mechs. 3, 173, 1968
17. Smith, F. T.: UTRC Rept., 1983, in preparation, and paper submitted to Proc. Roy. Soc. A, London.
18. Batchelor, G. K.: An Introduction to Fluid Dynamics. Cambridge Univ. Press, 1967.

APPENDIX A

A MECHANISM FOR UPSTREAM INFLUENCE

Consider an oncoming shear layer with virtually zero flow underneath, which seems not unreasonable on the verge of reattachment. In terms of an $O(1)$ shear layer thickness for convenience, the oncoming motion satisfies

$$\left. \begin{aligned} \psi &= \psi_0(y) \sim -\bar{k} + \sigma^{-1} e^{\sigma y} \text{ as } y \rightarrow -\infty \\ U &= U_0(y) \left\{ \begin{aligned} &\sim e^{\sigma y} \text{ as } y \rightarrow -\infty \\ &\rightarrow 1 \text{ as } y \rightarrow +\infty \end{aligned} \right. \end{aligned} \right\} \quad (\text{A-1})$$

where the constants \bar{k} , $\sigma > 0$ due to entrainment upstream. Then upstream influence can occur on a relatively short length scale $\Delta (\ll 1)$ in X , with a two- or three-tiered structure. In the first tier where y is $O(1)$, the oncoming form (A-1) suffers merely a displacement effect, giving

$$\psi = \psi_0(y + \bar{A}(\bar{X})), \quad U = U_0(y + \bar{A}(\bar{X})) \quad (\text{A-2})$$

from the controlling boundary layer Eqs. (I-2.6a), where $-\bar{A}(\bar{X})$ is the displacement locally, $\bar{A}(-\infty) = 0$ and $X = \Delta \bar{X}$. Because of the properties (A-1) the solution (A-2) sets up a second lower tier, at a logarithmically large distance below the first tier, in which

$$(\psi, U, P(X)) = [-\bar{k} + \Delta \bar{\psi}, \Delta \bar{U}, \Delta^2 \bar{P}(\bar{X})] + \dots \quad (\text{A-3a})$$

and $y = \sigma^{-1} \ln \Delta + \bar{y}$, where \bar{y} is $O(1)$. Substituting again into the boundary layer equations, we have now the full nonlinear viscous governing equations holding,

$$\bar{U} = \frac{\partial \bar{\psi}}{\partial \bar{y}}, \quad \bar{U} \frac{\partial \bar{U}}{\partial \bar{X}} - \frac{\partial \bar{\psi}}{\partial \bar{X}} \frac{\partial \bar{U}}{\partial \bar{y}} = -\frac{d\bar{P}}{d\bar{X}} + \frac{\partial^2 \bar{U}}{\partial \bar{y}^2} \quad (\text{A-3b})$$

with the matching conditions [from (A-1), (A-2)]:

$$\bar{U} \sim e^{\sigma(\bar{y} + \bar{A}(\bar{X}))} \text{ as } \bar{y} \rightarrow +\infty \quad (\text{A-3c})$$

$$\bar{U} \rightarrow \bar{U}_B(\bar{X}) \text{ as } \bar{y} \rightarrow -\infty \quad (\text{A-3d})$$

$$\left. \begin{aligned} \bar{U}(-\infty, \bar{y}) &= e^{\sigma \bar{y}}, \quad \bar{P}(-\infty) = 0 \\ \partial \bar{\psi} / \partial \bar{X}(-\infty, \bar{y}) &= -\sigma, \quad \bar{P}(\bar{X}) = -\frac{1}{2} \bar{U}_B^2(\bar{X}) \end{aligned} \right\} \quad (A-3e)$$

where $\bar{U}_B(\bar{X})$ is the slip velocity induced beneath this second tier. A third tier may also arise, above the first tier, to connect the unknown pressure \bar{P} inviscidly with the displacement $-\bar{A}$, but that is secondary to the basic feature which is the behavior of the second tier dictated by Eqs. (A-3b-e). For this admits upstream influence, as $\bar{X} \rightarrow -\infty$, in the form

$$\begin{aligned} \bar{\psi} &= -\sigma \bar{X} + \sigma^{-1} e^{\sigma \bar{y}} + e^{\theta \bar{X}} \bar{f}(\bar{y}) + O(e^{2\theta \bar{X}}) \\ \bar{P} &= O(e^{2\theta \bar{X}}) \end{aligned} \quad (A-4a)$$

where θ is an unknown positive constant. From Eqs. (A-3b) with Eq. (A-4a), the unknown function $\bar{f}(\bar{y})$ satisfies the linear ordinary differential equation

$$\bar{f}'''' - \sigma \bar{f}'' - \theta e^{\sigma \bar{y}} (\bar{f}' - \sigma \bar{f}) = 0; \quad (A-4b)$$

or, setting $Z \equiv 2 \theta^{1/2} \sigma^{-1} \exp(1/2 \sigma \bar{y})$, $F \equiv \bar{f}' - \sigma \bar{f}$, we obtain the Bessel equation

$$Z^2 \frac{d^2 F}{dZ^2} + Z \frac{dF}{dZ} - Z^2 F = 0 \quad (A-4c)$$

for $F(Z)$. Hence,

$$F(Z) = C_1 I_0(Z) + C_2 K_0(Z) \quad (A-4d)$$

where C_1, C_2 are constants and I_0, K_0 are Bessel functions. However, I_0 grows too fast $\propto Z^{-1/2} \exp(Z)$ as $Z \rightarrow \infty$ ($\bar{y} \rightarrow \infty$) to allow the match (A-3c) to be achieved. So $C_1 = 0$. In addition we require \bar{A} to be 0 ($e^{2\theta \bar{X}}$): this is either from the linearity of the inviscid pressure-displacement law or from the requirement of negligible displacement, $\bar{A} \equiv 0$, which often holds on short length scales like the present. So $|\bar{f}| \ll e^{\sigma \bar{y}}$ as $\bar{y} \rightarrow +\infty$, and from Eq. (A-4d) we have the solution

$$\bar{f}(\bar{y}) = C_2 e^{\sigma \bar{y}} \int_{\infty}^{\bar{y}} K_0(Z) e^{-\sigma \bar{y}} d\bar{y} \quad (A-4e)$$

Finally, as $\bar{y} \rightarrow -\infty$, $Z \rightarrow 0$, and $K_0(Z) \sim -\ln Z$, so that $\bar{f}'(-\infty) = \frac{1}{2} C_2$. Hence,

$$U_B(X) \sim \frac{1}{2} C_2 e^{\theta \bar{X}}, \quad P(X) \sim -\frac{1}{8} C_2^2 e^{2\theta \bar{X}} \quad (\text{A-4f})$$

where C_2 remains arbitrary.

APPENDIX B

FURTHER UPSTREAM INFLUENCE

Appendix A described upstream influence arising in a forward-moving shear layer with zero flow underneath, but such shear layers can also set up a small reversed motion underneath because of their entrainment. This Appendix considers the extra effects of that small reversed motion. The main effect found below is the production of transverse waves. These stem from the local velocity and stream-function profiles of the form

$$\left. \begin{aligned} u &= \text{Re}^{-1/2} (e^{\gamma y} - k_1) \\ \psi &= -\kappa + \text{Re}^{-1/2} \left(\frac{1}{\gamma} e^{\gamma y} - k_1 y \right) - \text{Re}^{-1} \gamma x \end{aligned} \right\} \text{for } -\infty < y < \infty \quad (\text{B-1})$$

with k_1 a positive constant, κ being the positive entrainment constant and γ being the corresponding positive index for exponential decay in the shear layer, thus giving exponential growth in the subregion where (B-1) holds, below the shear layer. The Re scaling in (B-1) indicates the smallness of the velocities involved, although similar analysis in the cascade problem shows that (B-1) occurs for small X instead there without an Re scaling.

The local form (B-1) is an exact solution of the Navier-Stokes or the boundary layer equations, interestingly enough, related to the asymptotic suction solution. A nonlinear disturbance to (B-1) then takes place if $(\psi, u, p) = (-\kappa + \text{Re}^{-1/2} \hat{\psi}, \text{Re}^{-1/2} \hat{u}, \text{Re}^{-1} \hat{p})$ within the $x = \text{Re}^{1/2} \hat{x}$ scale where y is $O(1)$, so that $\hat{\psi}, \hat{u}, \hat{p}$ are controlled by the boundary layer equations. Matching requires $\hat{u} \sim \exp(\gamma y)$ as $y \rightarrow \infty$ and $\hat{u} \rightarrow -k_1$ as $y \rightarrow -\infty$, where $k_1 k_1' = -\hat{p}'$ for k_1 nonuniform.

It would be interesting to tackle the nonlinear version above since it admits upstream influence, as does that in Appendix A. In the present case the upstream influence starts from a small deviation $\alpha \exp(\beta \hat{x})$ about the exact solution (B-1). This yields the linearized equation

$$\bar{f}''' - \gamma \bar{f}'' - (e^{\gamma y} - k_1) \beta \bar{f}' + \gamma e^{\gamma y} \beta \bar{f} = \hat{a} \quad (\text{B-2})$$

for the stream function perturbation, with \hat{a} being a pressure constant. Notice that the normal velocity $v \propto -\partial \hat{\psi} / \partial \hat{x}$ plays a part here, contributing the term in \bar{f}'' as in Appendix A: (B-2) is an extension of (A-4b) in fact incorporating the flow reversal due to k_1 in (B-1). The solution of (B-2) may be found from the substitutions $\hat{h} = Q^{-1} (\bar{f}'' - \gamma \bar{f}')$, $Q = 2 \gamma^{-1} \beta^{1/2} \exp(\gamma y/2)$, which reduce (B-2) to the Bessel equation

$$Q^2 \frac{d^2 \hat{h}}{dQ^2} + Q \frac{d\hat{h}}{dQ} + \left[\left(\frac{4\beta}{\gamma^2} - 1 \right) - Q^2 \right] \hat{h} = 0 \quad (\text{B-3})$$

for $\hat{h}(Q)$ in $0 < Q < \infty$, where we have normalized k_1 to be unity.

The solutions of (B-3) are the Bessel functions $I_\nu(Q)$, $K_\nu(Q)$ where $\nu^2 = 1 - 4\beta/\gamma^2$. Assuming first that $\nu^2 \geq 0$ we may discount the I_ν function as in Appendix A and construct the form of $\hat{f}(y)$ by integration much like that in (A-4e). The solution decays exponentially as $y \rightarrow -\infty$ ($Q \rightarrow 0+$), as required, and so upstream influence is admissible, with $\beta \leq \gamma^2/4$. In contrast, if $\nu^2 < 0$, so that $\nu = i\hat{\nu}$ with $\hat{\nu}$ real and $\beta > \gamma^2/4$, then although I_ν is ruled out again by the behavior as $y \rightarrow \infty$ the solution for $\hat{h}(Q)$ is oscillatory $\propto \cos[\hat{\nu} \ln Q]$ as $Q \rightarrow 0+$. Hence we obtain waves $\propto \cos(\hat{\nu}\gamma y/2)$ as $y \rightarrow -\infty$. Upstream influence is still admissible with these transverse waves provided the now significant motion set up beneath this subregion can accommodate the waves. Appendix C below suggests that accommodation is possible.

APPENDIX C

SIGNIFICANT VISCOUS INFLUENCE IN LARGE-SCALE REVERSED FLOW

Throughout Part 2 the necessity of viscous action during wake closure is emphasized (e.g., see Section 2 of Part 2), even though for the wide-spread cascade viscous forces seem largely negligible at first sight: again see Section 2. So the question arises of how viscous action may come into play in a predominantly inviscid motion containing significant reversed flow. Effectively this amounts to considering the boundary layer equations for a large-scale flow, in the form

$$u = \frac{\partial \psi}{\partial y}, \quad u \frac{\partial u}{\partial x} - \frac{\partial \psi}{\partial x} \frac{\partial u}{\partial y} = - \frac{dp}{dx} + \frac{1}{Re} \frac{\partial^2 u}{\partial y^2} \quad (C-1)$$

where $Re \gg 1$ but x, y, ψ, u, p are generally $O(1)$ rather than scaled in the typical boundary layer fashion.

At first sight the viscous contribution in (C-1) should be disregarded, therefore, but that then points to the backward jet inconsistency referred to in Section 7 of Part 2 if wake closure is to be described. However, in view of the short-scale oscillatory responses from viscous effects found in Appendices B and D, there is an alternative account in which viscosity matters more, as follows. Suppose the solution throughout depends on both the general $O(1)$ scale in y and on the traditional shorter scale $Y \propto Re^{1/2} y$ locally. Then a multiple-scales treatment is called for, with

$$\frac{\partial}{\partial y} \rightarrow Re^{1/2} g'(y) \frac{\partial}{\partial Y} + \frac{\partial}{\partial y} \quad (C-2)$$

where $g(y)$ is generally of $O(1)$. The emphasized role of the viscous derivative $\partial/\partial Y$ here allows a viscous perturbation of small amplitude in ψ to produce a sizeable response in u and a large response in the vorticity $\partial u/\partial y$. Thus if a basic ψ -profile is disturbed linearly in the form

$$\psi = \psi_B(y) + Re^{-1/2} \psi_o(x, y, Y) + \dots \quad (C-3)$$

then (C-2) gives, with $u_B \equiv \psi_B'$,

$$u = [u_B(y) + g'(y) \frac{\partial \psi_o}{\partial Y}] + Re^{-1/2} \frac{\partial \psi_o}{\partial y} + \dots \quad (C-4)$$

and the disturbance in u is nonlinear. Further, $\partial u / \partial y$ is dominated by $Re^{1/2} (g'(y))^2 \partial^2 \bar{\psi}_0 / \partial Y^2$. So if we set $u_B + g' \partial \bar{\psi}_0 / \partial Y \equiv g'^2 \partial \bar{\psi}_0 / \partial Y$ then (C-1) yields the full boundary layer equation for $\bar{\psi}_0$, in terms of x, Y ,

$$\frac{\partial \bar{\psi}_0}{\partial Y} - \frac{\partial^2 \bar{\psi}_0}{\partial x \partial Y} - \frac{\partial \bar{\psi}_0}{\partial x} - \frac{\partial^2 \bar{\psi}_0}{\partial Y^2} = \frac{\partial^3 \bar{\psi}_0}{\partial Y^3} \quad (C-5)$$

with y -dependence remaining passive, and the range of interest is $-\infty < Y < \infty$ because of the short scale involved. The pressure gradient has no effect here.

Upstream where viscous effects decay $\bar{\psi}_0 \rightarrow 0$ and so we require $g'^2 = \pm u_B$, from the y -dependence in $\bar{\psi}_0$, and $\bar{\psi}_0 \rightarrow \pm Y$. Hence the upstream profile for $\bar{\psi}_0(x, y, Y)$ is simply a uniform stream. The stream is forward if $u_B > 0$, since then $g' = u_B^{1/2}$, but is reversed where $u_B < 0$ giving $g' = (-u_B)^{1/2}$. In consequence, wherever reversed flow ($u_B < 0$) is present upstream wave-like viscous behavior occurs transversely with

$$\bar{\psi}_0 \sim -Y + a_0 e^{\sigma x} \sin(\sigma^{1/2} Y + b_0), \quad (C-6)$$

from (C-5) as $x \rightarrow -\infty$, where $\sigma > 0$, a_0, b_0 are constants. The waves span the entire reversed flow zone $u_B < 0$. They become a nonlinear influence as x becomes finite and offer an alternative to the earlier inviscid description. Again, wherever there is forward flow upstream, $u_B > 0$, the transverse viscous response is exponential with

$$\bar{\psi}_0 \sim Y + c_0 e^{\sigma x} e^{-\sigma^{1/2} Y} \quad (C-7)$$

if $Y > 0$, where c_0 is a constant.

Thus viscous effects can exert a significant influence even in a large-scale separated flow, and despite the largeness of Re in (C-1) the flow properties need not be mainly inviscid. A backward jet can then be avoided, in particular, if wake closure takes place. Higher order terms overall still require study but the sustained waves in (C-6) tie in with those of Appendices B and D, while the transition between (C-6) and (C-7) is achieved by means of internal layers near where $u_B = 0$. A continued study of the multiple scales effects here should be interesting.

APPENDIX D

EXPONENTIAL BEHAVIOR IN REVERSED MOTIONS

Here, for definiteness, the reversed flow occurring far downstream on the body scale (Part 2 - Section 7), i.e., near the start of the viscous closure process (Part 2 - Sections 2-4), is considered for the cascade of finite spread H . Non-uniqueness corresponding to the influence of conditions further downstream has been noted already in Part 1 for algebraically higher order terms, but the situation is aggravated by the more sensitive exponentially small corrections present as follows.

The simplest starting form holding below the Chapman layer, for small X , has the reversed flow given by the inviscid solution $\psi \approx -\kappa X^{1/2} Y H^{-1} (1-H)^{-1/2}$ for $0 < Y < H$, from (2.12a) of Part 2. Exponential viscous dependence then enters the reckoning through the decay in the lower reaches of the Chapman layer, which requires the underlying expression

$$\psi = \frac{-\kappa X^{1/2} Y}{H(1-H)^{1/2}} + \dots + \hat{A}(Y) \exp\left(\frac{g(Y)}{X^m}\right) + \dots \quad (D-1)$$

for $0 < Y < H$. Here, the functions $\hat{A}(Y)$, $g(Y)$, and constant $m > 0$ are unknown, but real $(g) < c$ for decay as $X \rightarrow 0+$. The boundary layer equations then give $m = 1/2$ and require g to satisfy the nonlinear form

$$g + Y g' = g^2, \quad (D-2)$$

where we omit certain finite multiplying factors from the equation, for convenience, and need $g(1) = 0$ to match with the Chapman layer. In standard form the solution of the differential equation (D-2) can be written parametrically

$$g = \phi^2 - Y\phi \text{ where } 3Y = 2\phi + \phi^{-1/2} \quad (D-3)$$

for $Y < 1$ now. This keeps g real and negative but only for $1 > Y > 2^{-1/3}$. As $Y \rightarrow 2^{-1/3} = Y_0$ from above, an irregularity arises since there $g(Y_0) = -2^{-8/3}$, $g'(0) = 2^{-4/3} Y_0$ are finite, but $g'' \propto (Y - Y_0)^{-1/2}$ from (D-3). Hence g becomes complex in $Y < Y_0$. The smoothing out for the $3/2$ irregularity in g at $Y = Y_0 \pm$, plus the removal of the irregularity found to occur in $\hat{A}(Y)$ there, can be shown to be achieved by Airy functions in a subzone of width $X^{1/3}$ near $Y = Y_0$. These

introduce a degree of arbitrariness into the solution for g in $Y < Y_0$ but $\text{Real}(g)$ remains negative as required. This is seen perhaps most readily from the cubic equation for $g(Y)$, obtainable fortunately in this case, from (D-3),

$$16 g^3 - 24 Y^2 g^2 + (9Y^4 - 12Y) g + (Y^3 - 1) = 0. \quad (\text{D-4})$$

For (D-4) can be used to show that g cannot become pure imaginary in $0 < Y < 1$, so that $\text{Real}(g)$ must remain negative. Also, at the centerline ($Y \rightarrow 0+$) g acquires one of the complex roots of $g^3 = 1/16$ and so again keeps $\text{Real}(g) < 0$.

As a result, exponential-oscillatory behavior is present in the reversed motion near the start of the wake closure process, the oscillations being of small amplitude but very high frequency transversely. Similar oscillations are found to be induced with the other starting forms of Section 2 in Part 1, with the start of the long eddy in Section 3, Part 2 and with the downstream form of Section 7 to which (D-1)-(D-4) are equivalent. Ref. 17 covers the application of Section 6, Part 2.

APPENDIX E

VISCOUS WAKE CLOSURE WITH PRESSURE FORCING

An analytical example occurs if the non-entraining shear layer of Section 8, Part 2 approaches closure linearly, $\bar{\delta} \sim \xi_2(x_2 - x)$ as $x \rightarrow x_2 -$ with the constant ξ_2 positive. The eddy flow beneath acquires a similarity form then, corresponding to $K = 0$ in Section 5, Part 2, so that the eddy velocity \bar{u} is $O(x_2 - x)^{-1}$ and increasing. The local similarity equation is

$$G''' - G'^2 = \pi_0 \quad (\text{E-1})$$

from (5.2a), including a sign change, since x is increasing here, and a pressure gradient $\propto \pi_0$. The range of concern is $0 \leq \xi < \xi_2$. If there is no reversed center-line jet (5.2b) apply, although symmetry conditions can also be supported within $0 < \xi < \xi_2$ if a jet is present. We take (5.2b) here. Integration of (E-1) then gives the implicit solution

$$\int_{h_0}^h \frac{dh}{(h-h_0)^{1/2} (h^2 + h_0 h + h_0^2 + 3\pi_0)^{1/2}} = \left(\frac{2}{3}\right)^{1/2} \xi \quad (\text{E-2})$$

for $h(\xi) \equiv G'(\xi)$, where $h_0 = h(0)$ is unknown. Equation (E-2) satisfies the symmetry condition (5.2b) but also yields $h \rightarrow \infty$ as $\xi \rightarrow \xi_2 -$, where

$$\left(\frac{2}{3}\right)^{1/2} \xi_2 = \int_{h_0}^{\infty} \frac{dh}{(h-h_0)^{1/2} (h^2 + h_0 h + h_0^2 + 3\pi_0)^{1/2}} \quad (\text{E-3})$$

and $h \sim 6 (\xi_2 - \xi)^{-2}$ as $\xi \rightarrow \xi_2 -$. This reproduces the required behavior (8.5c), on integration for $G(\xi)$, verifying that (8.5c) is attainable with or without a pressure gradient acting. Further examples are noted in Ref. 17.

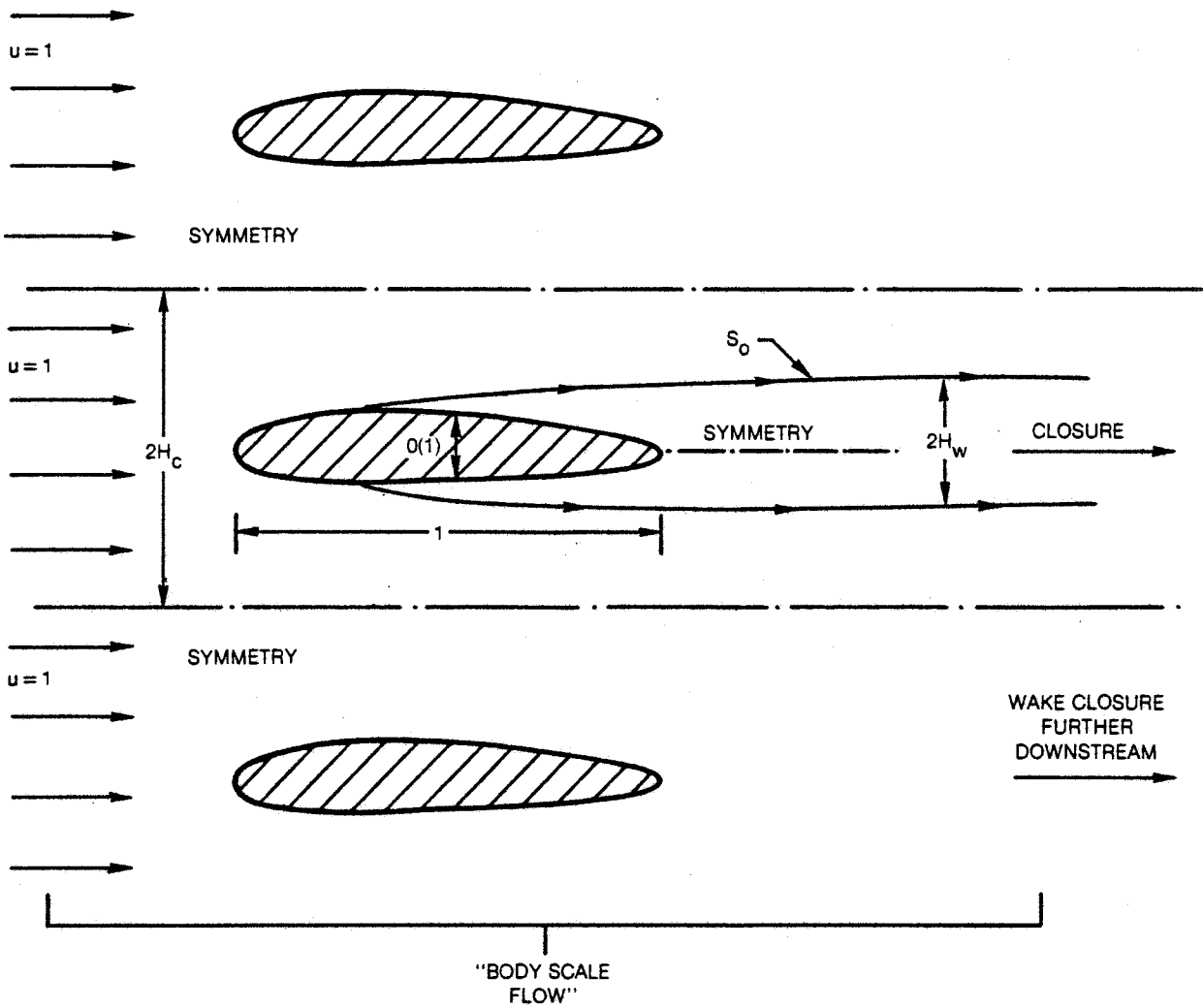


Figure 1 The Overall Cascade Flow Structure

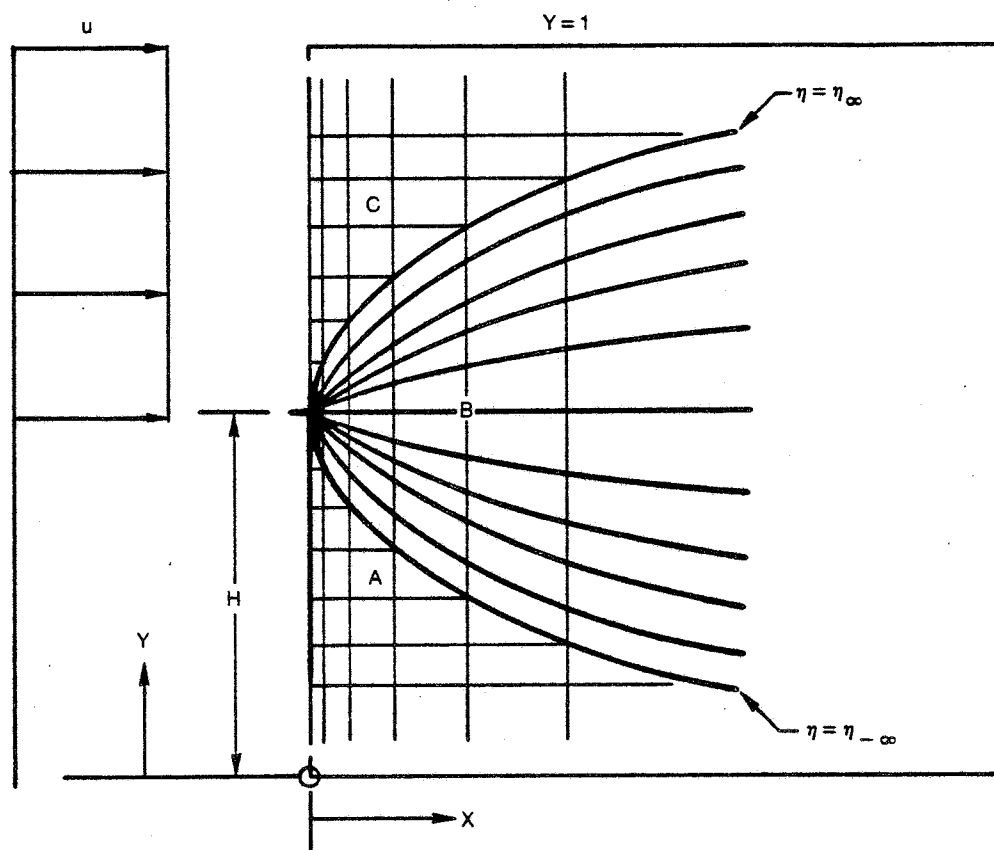


Figure 2 Computational Grid for 3-Region Flow Representation

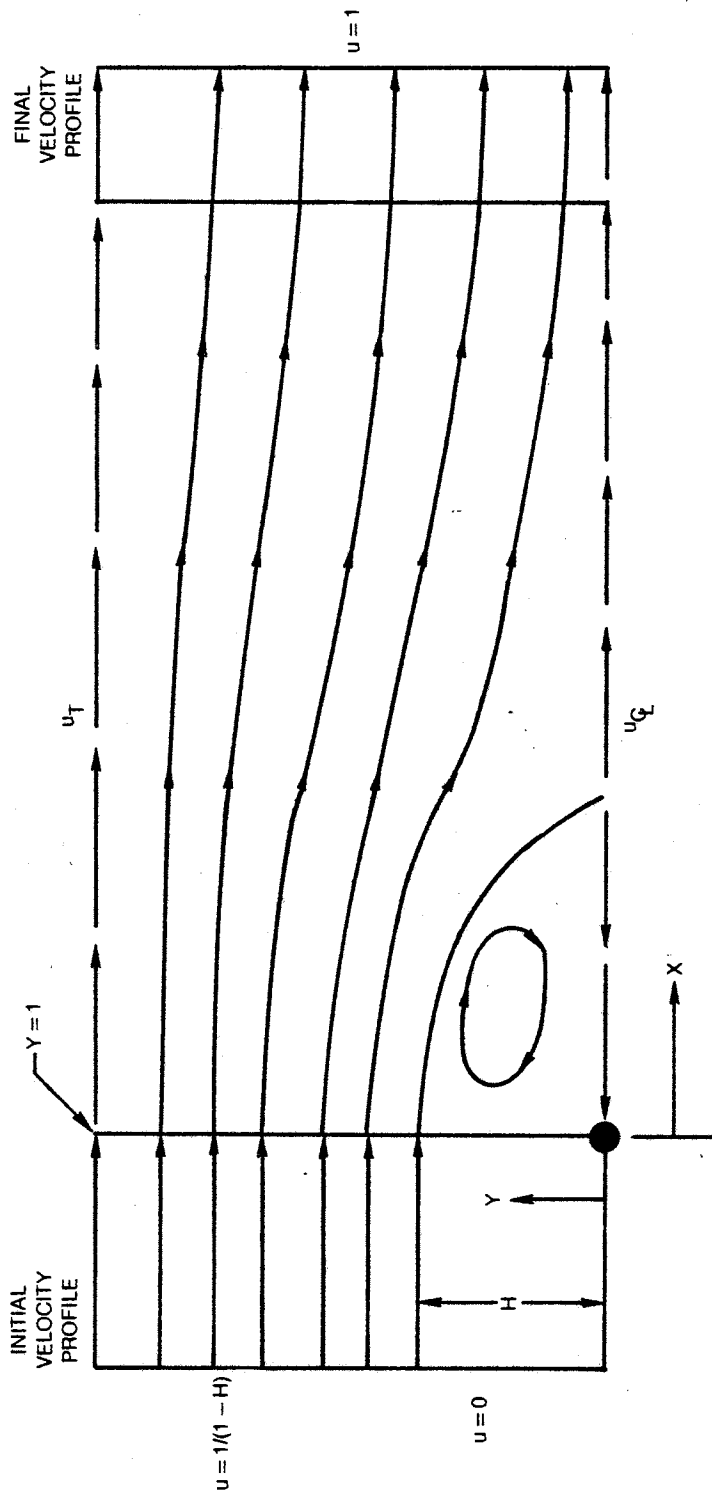
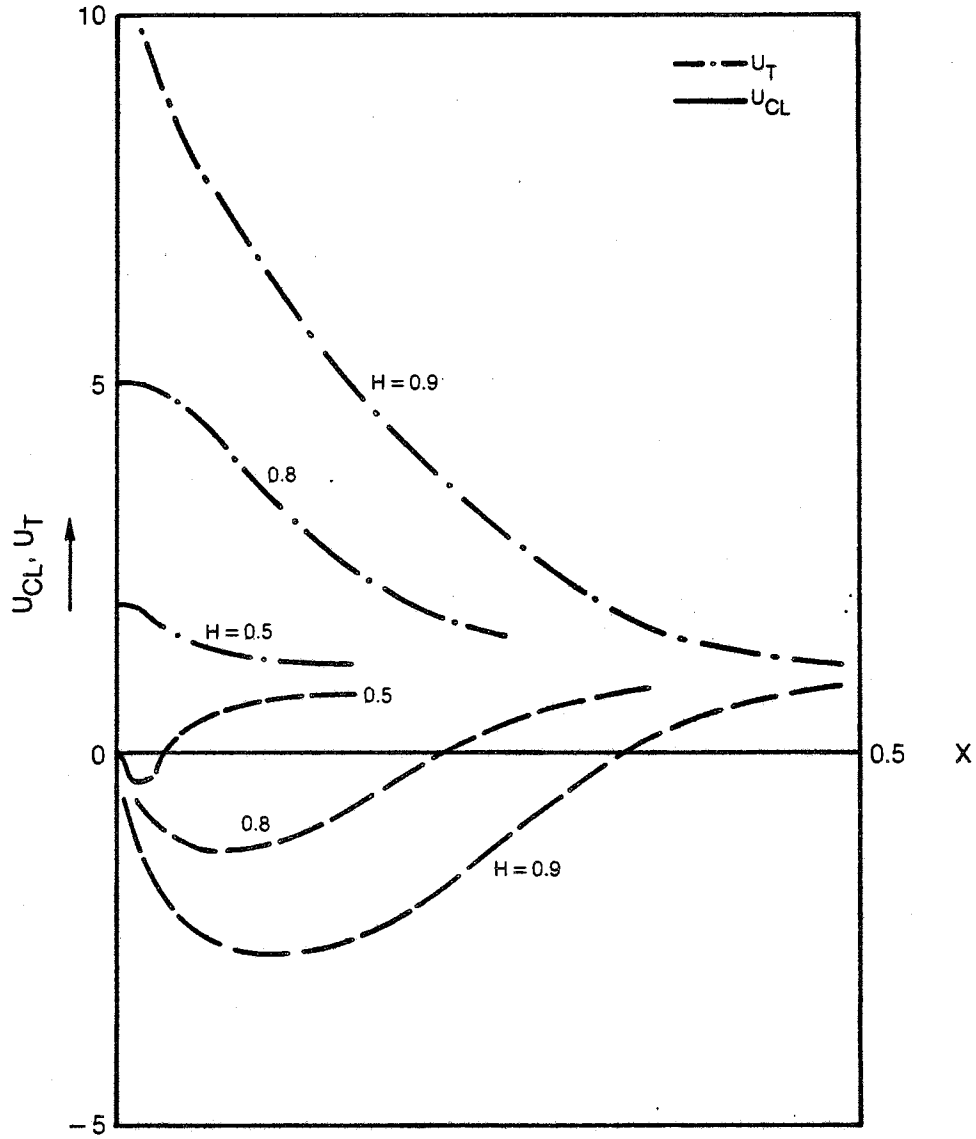


Figure 3 Wake, Edge and Centerline Velocities
(a) Nomenclature



**Figure 3 Wake, Edge and Centerline Velocities
(b) $H = 0.5, 0.8, 0.9$**

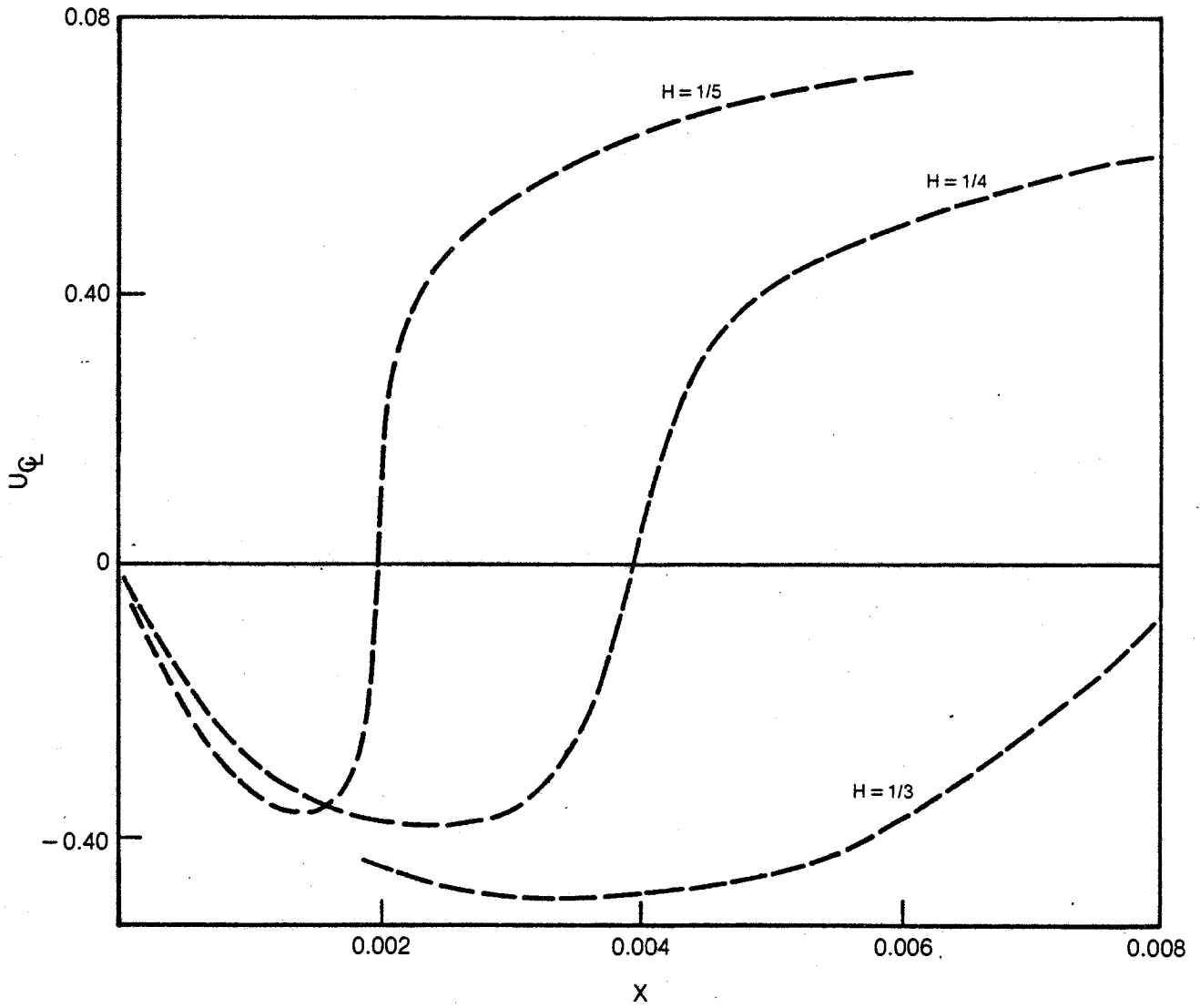


Figure 3 Wake, Edge and Centerline Velocities
(c) H = 1/3, 1/4, 1/5

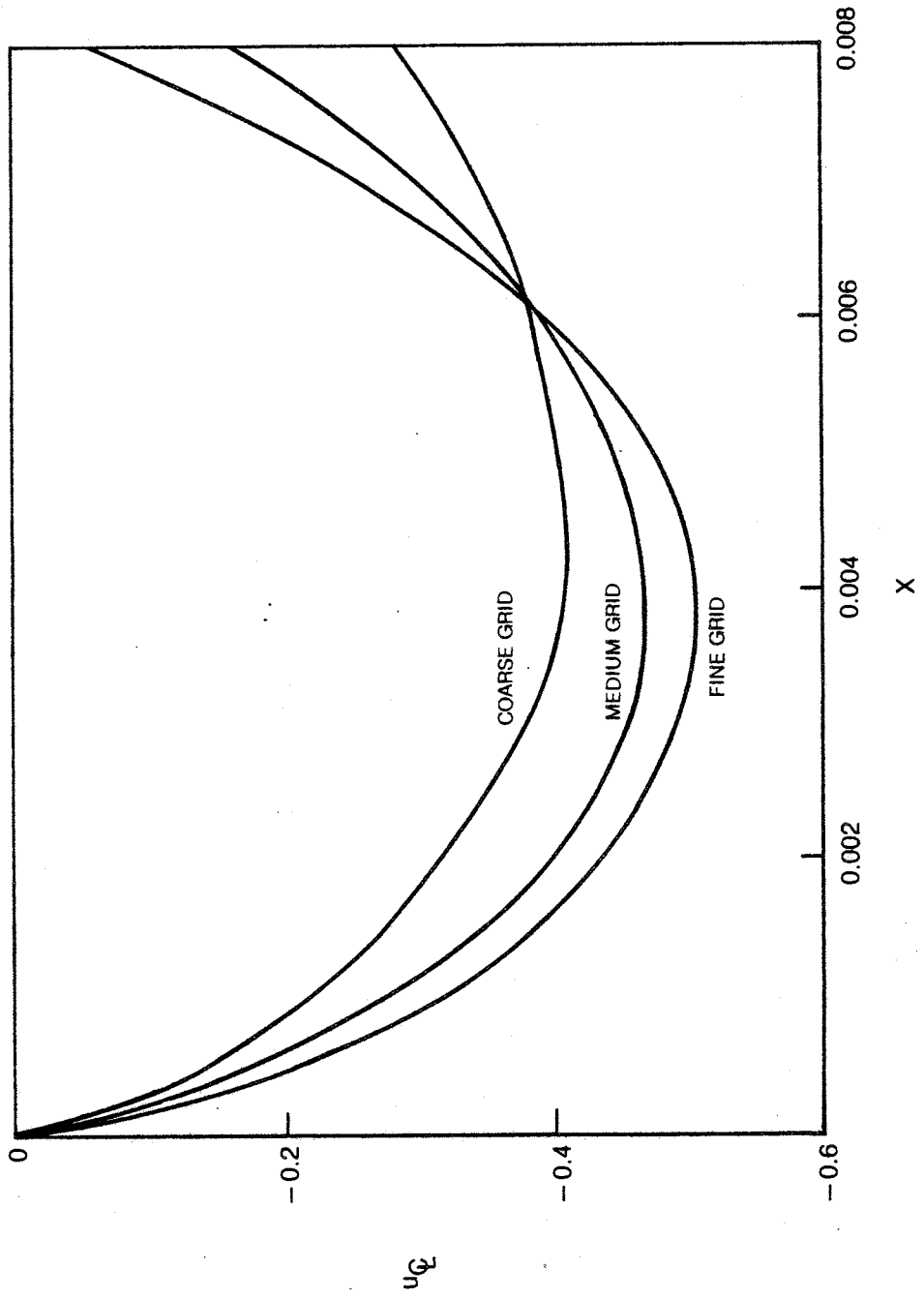


Figure 3 Wake, Edge and Centerline Velocities
(d) Mesh Size Influence for $H = 1/3$

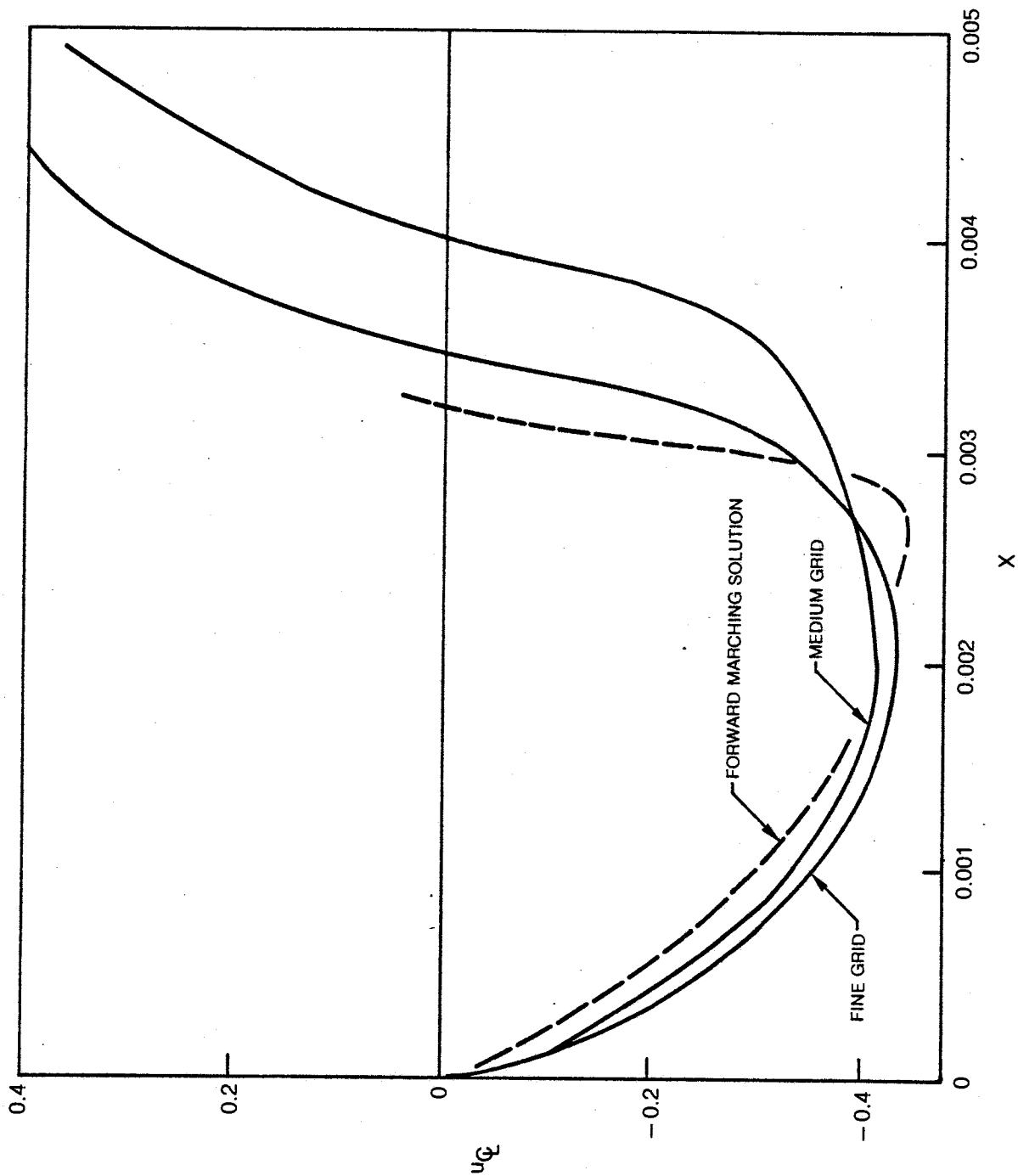
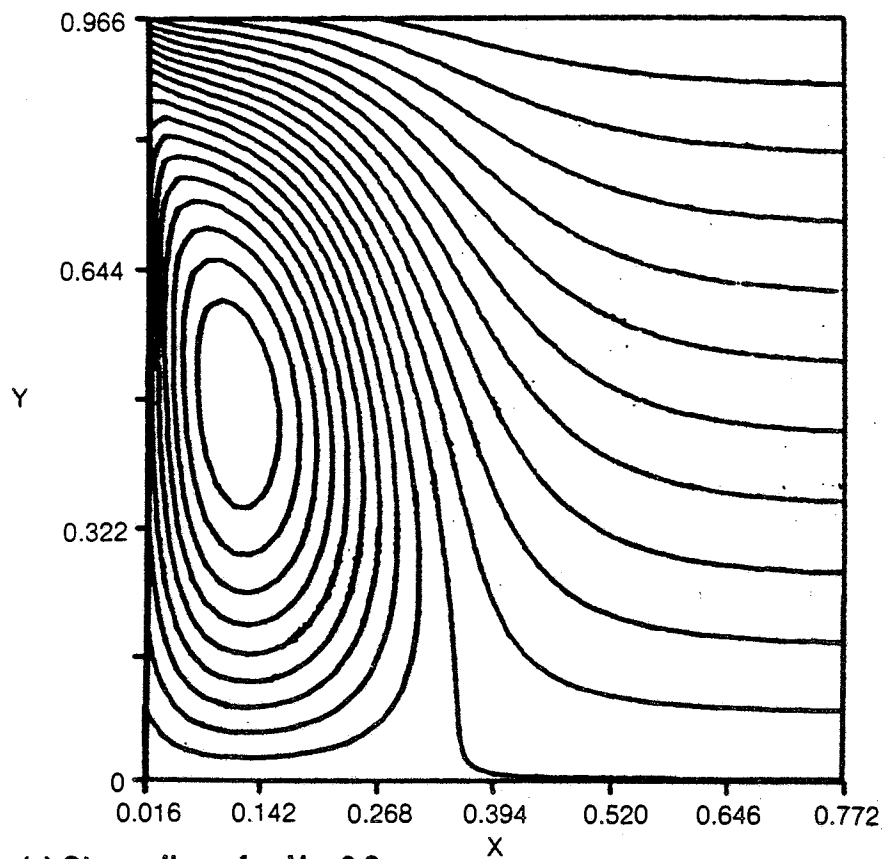
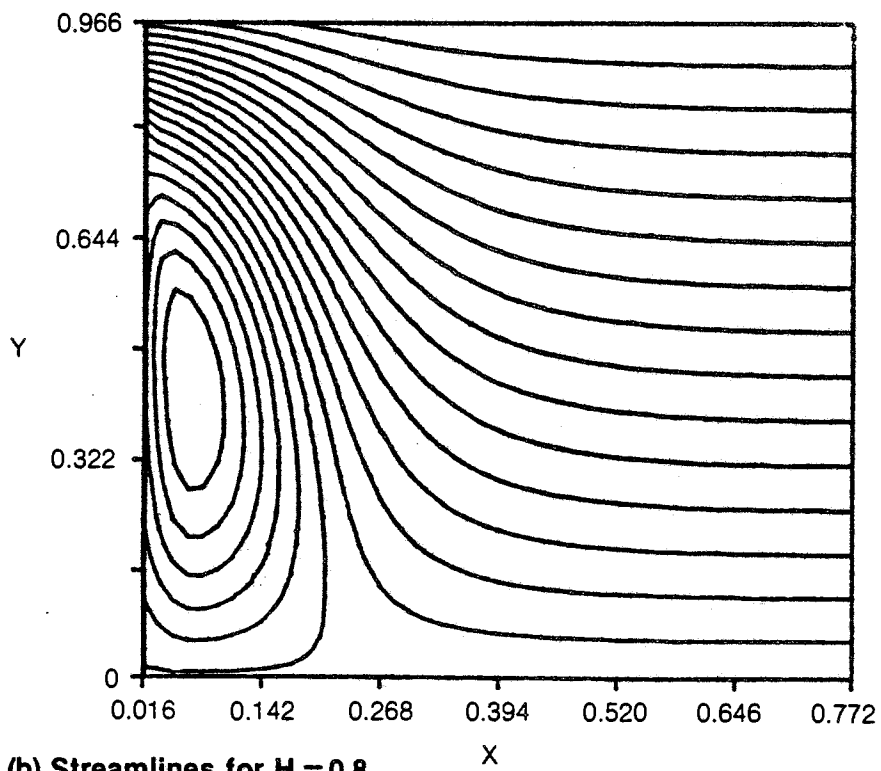


Figure 3 Wake, Edge and Centerline Velocities
(e) Reverse Flow Region for $H = 1/4$



(a) Streamlines for $H = 0.9$



(b) Streamlines for $H = 0.8$

Figure 4 Streamline and Velocity Profiles

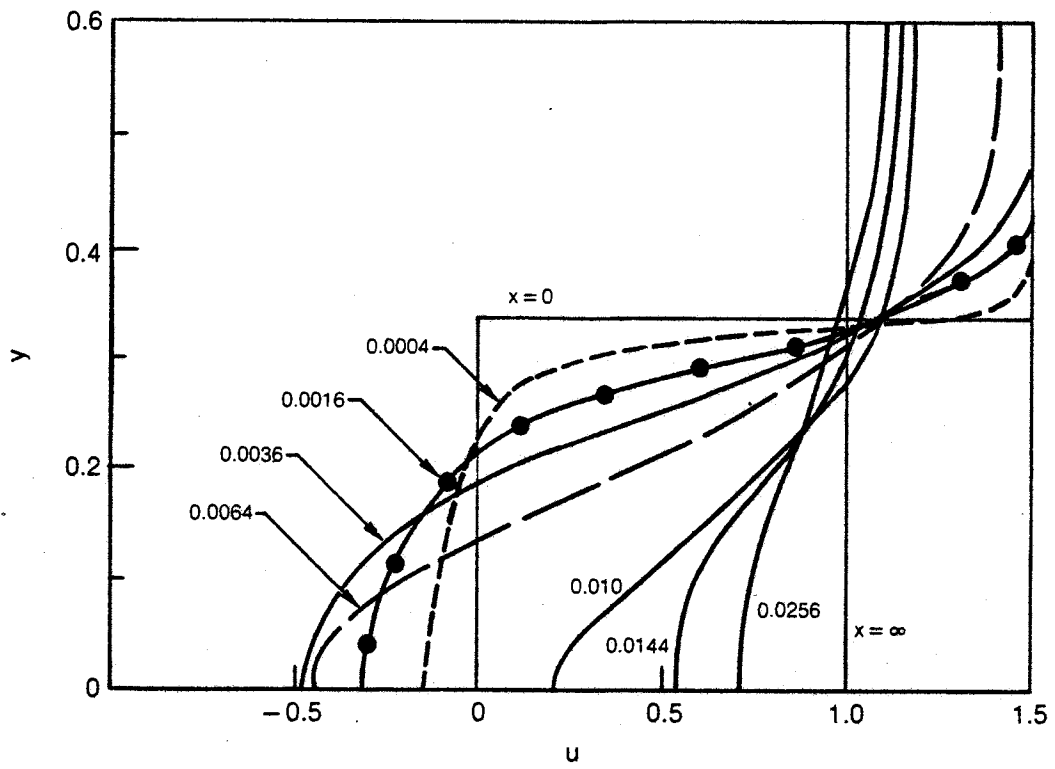


Figure 4 (c) Velocity Profiles, $H = 1/3$

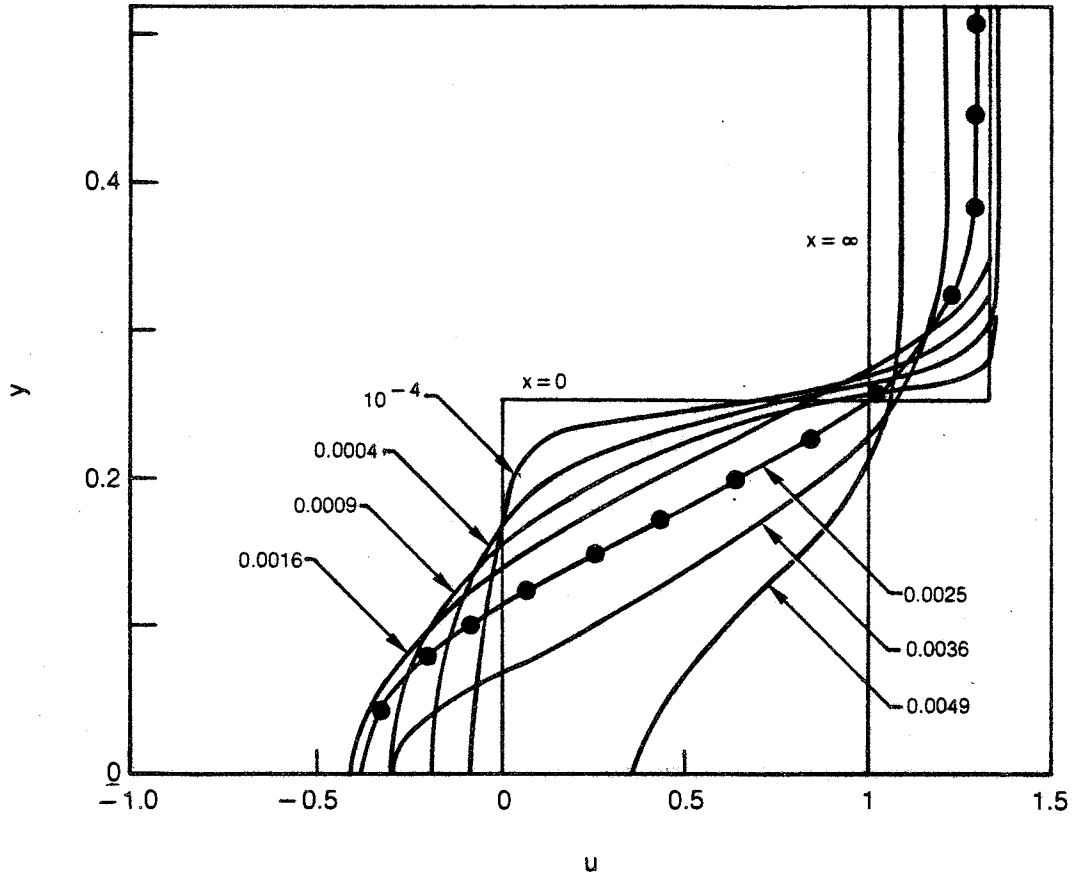


Figure 4 (d) Velocity Profiles, $H = 1/4$

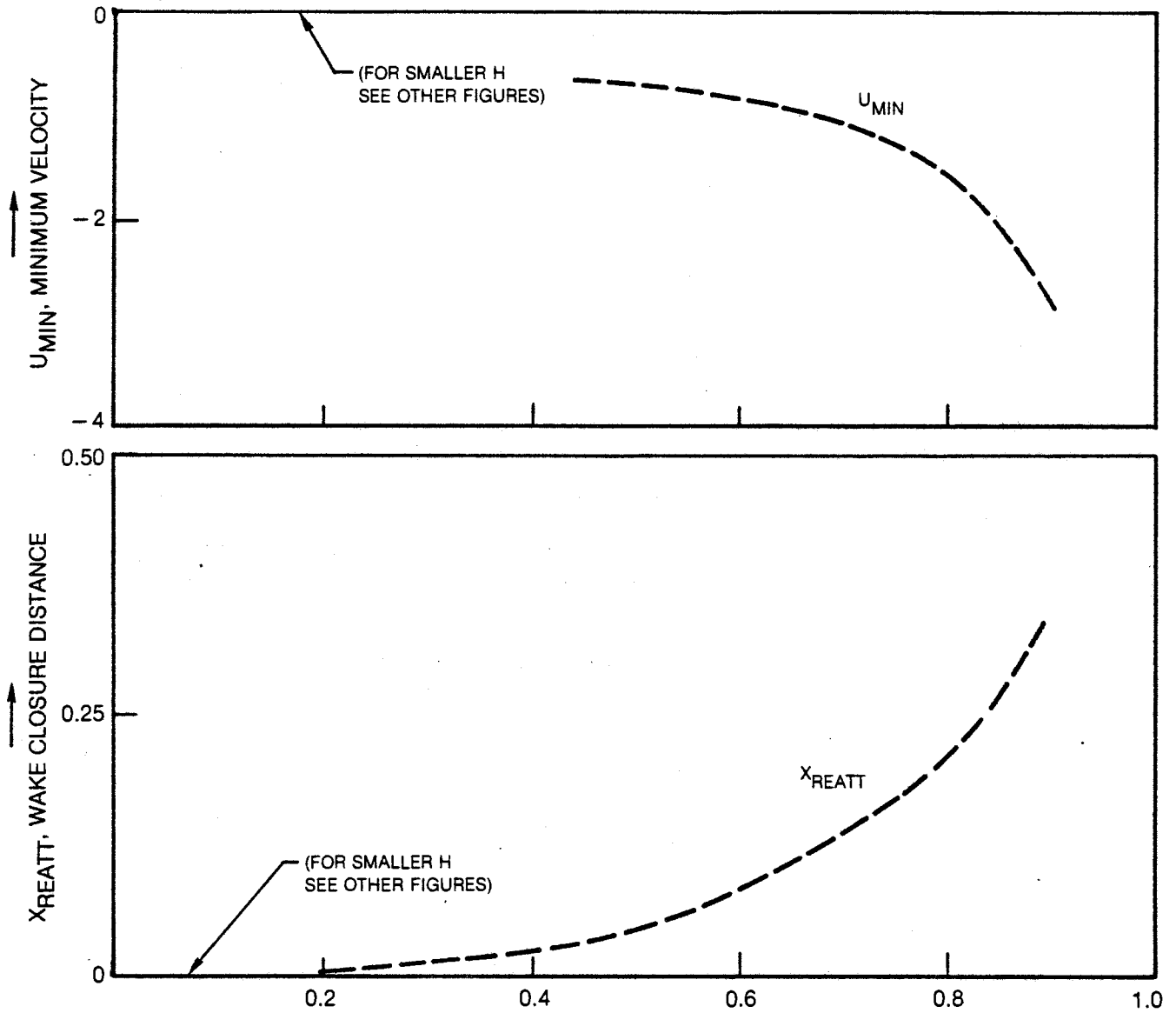
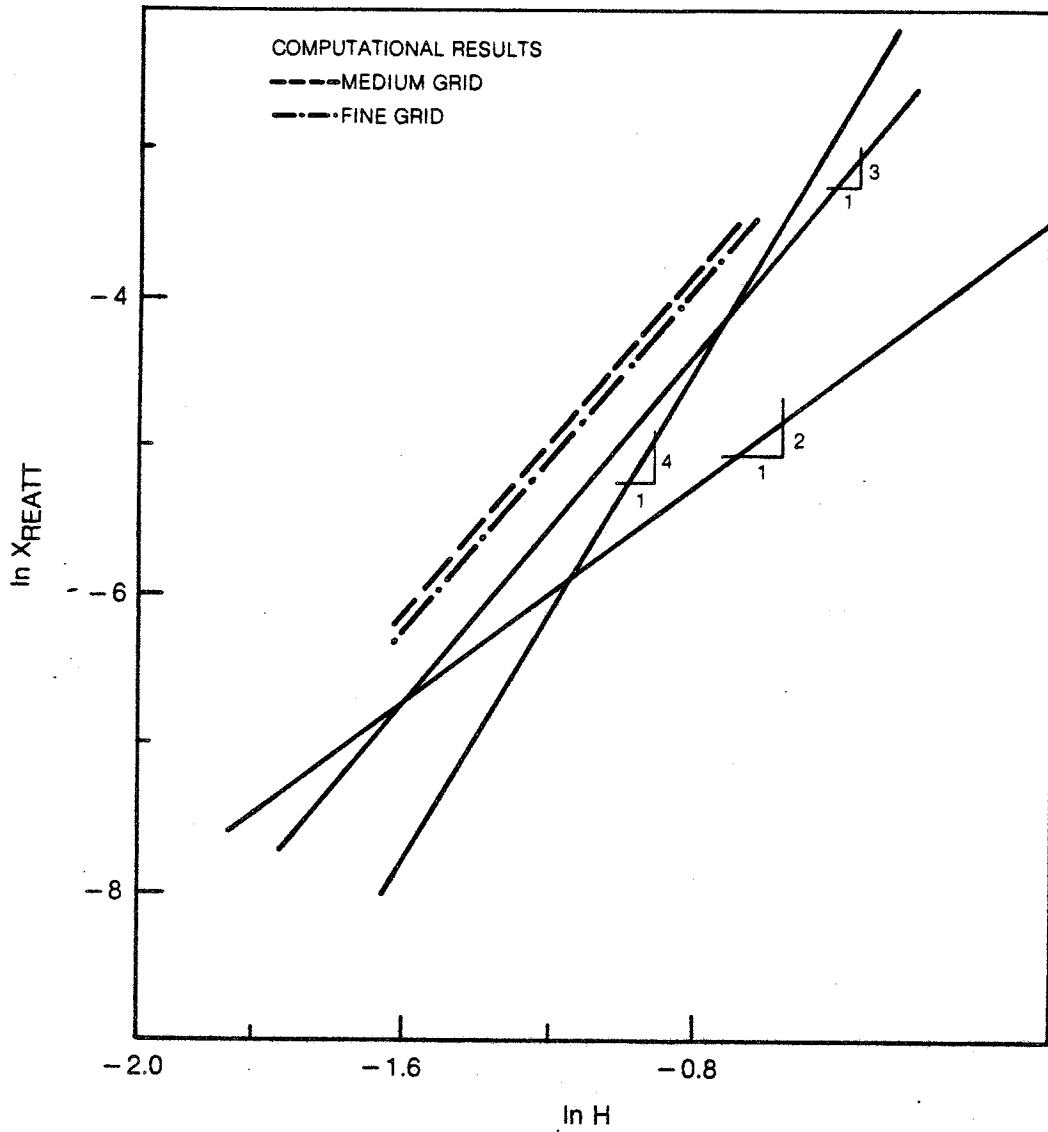
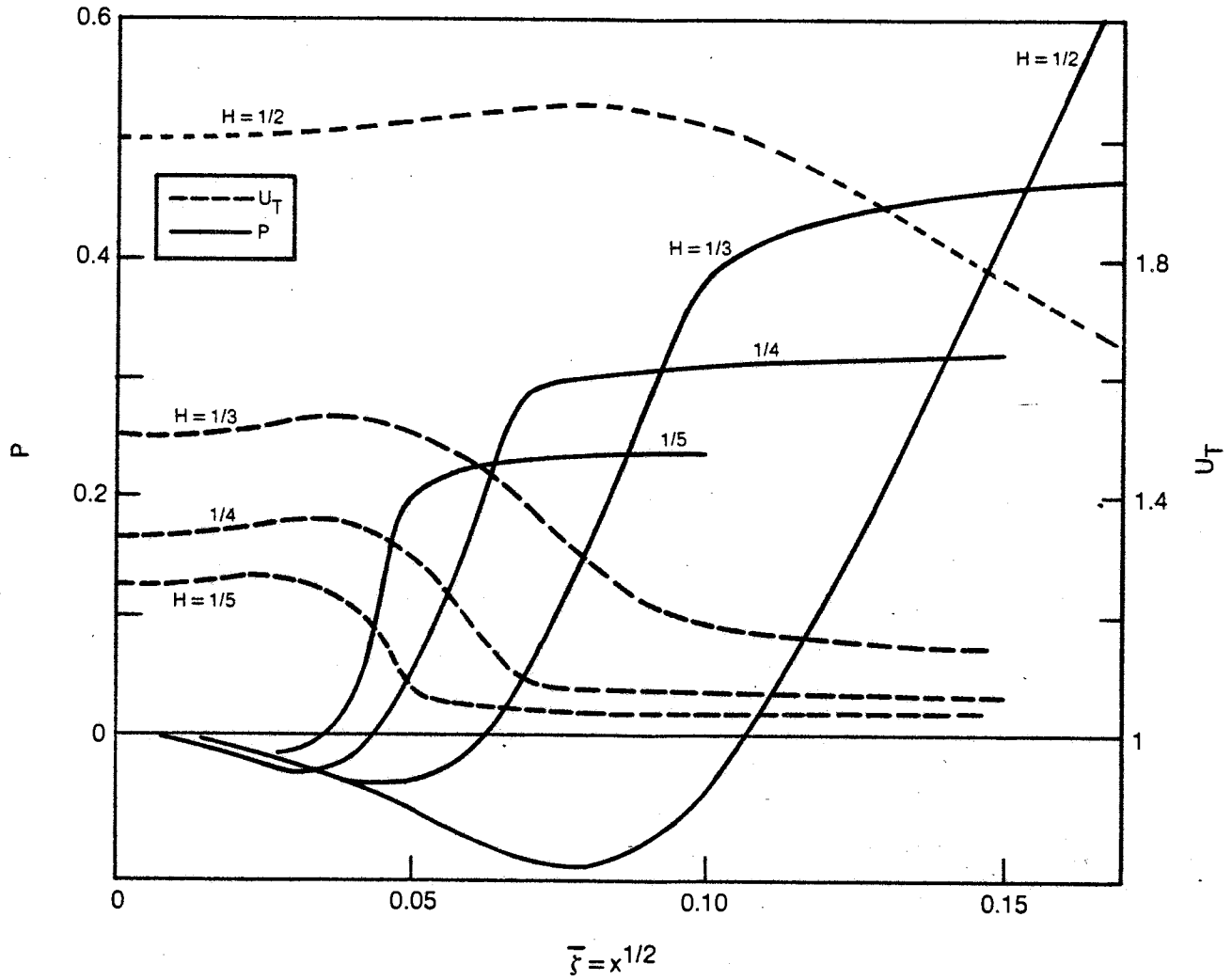


Figure 5 Wide Spacing Flow Structure
(a) X_{reatt} and U_{min} versus H



**Figure 5 Wide Spacing Flow Structure
(b) Reattachment Length Asymptotic Behavior**



**Figure 5 Wide Spacing Flow Structure
(c) Pressure and Edge Velocity**

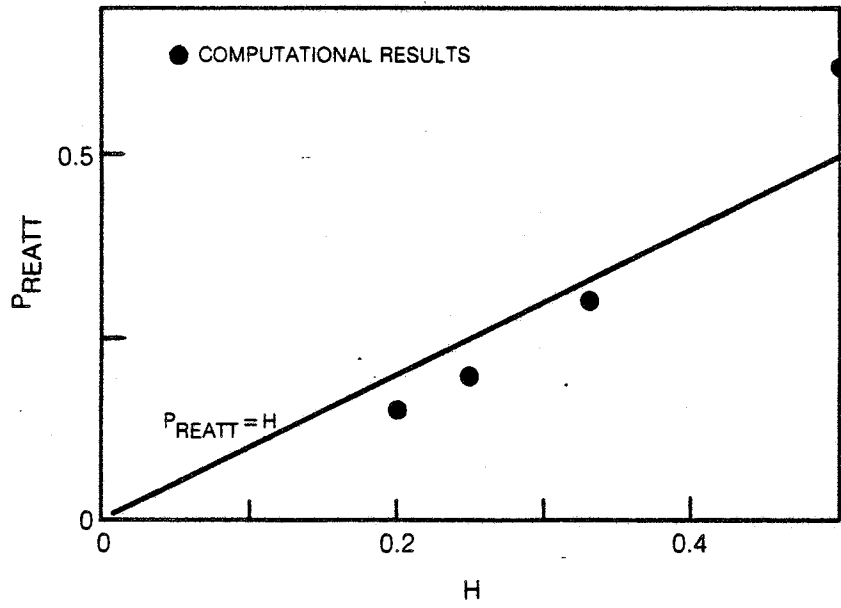


**Figure 5 Wide Spacing Flow Structure
(d) Reattachment Pressure Level**

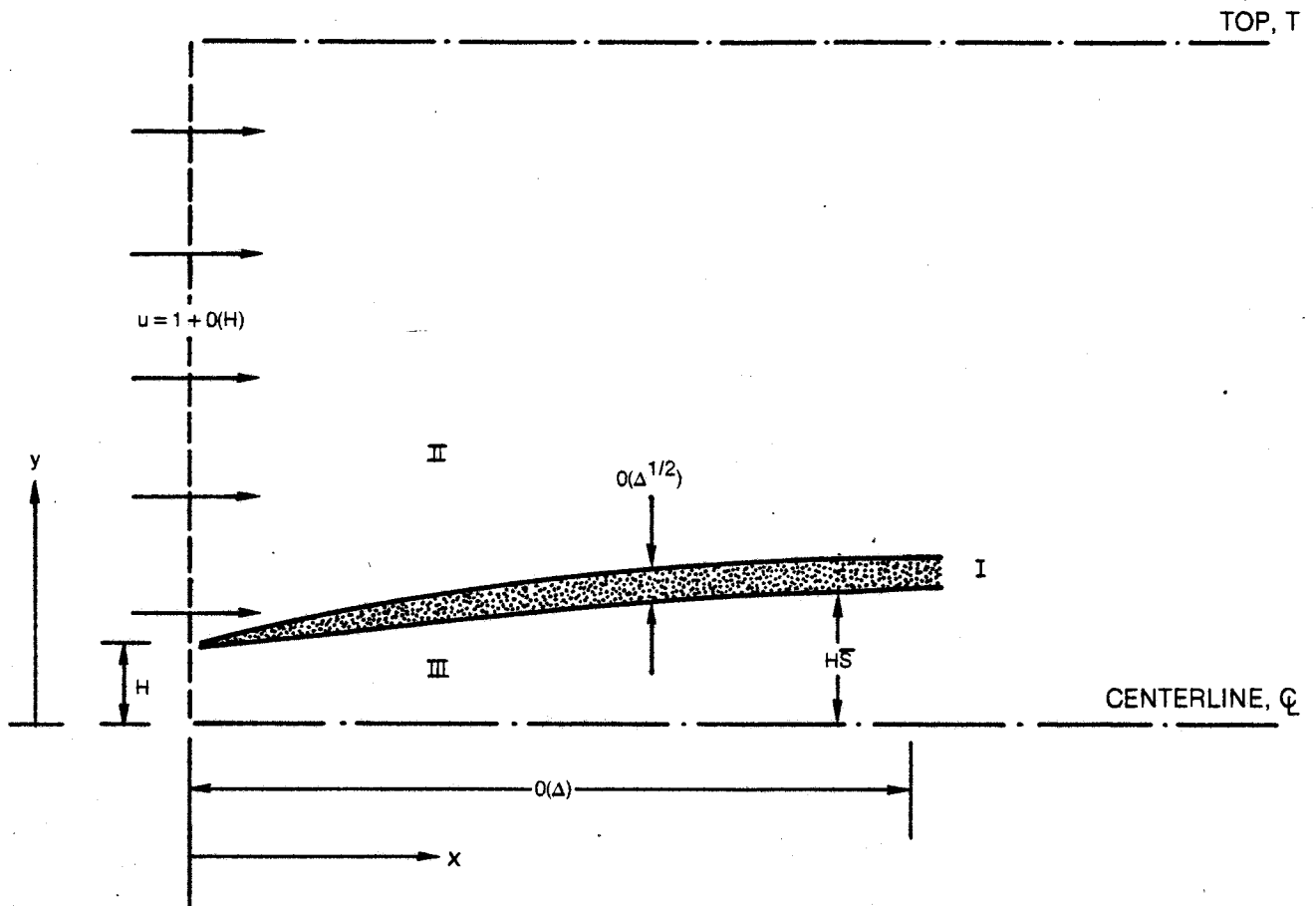
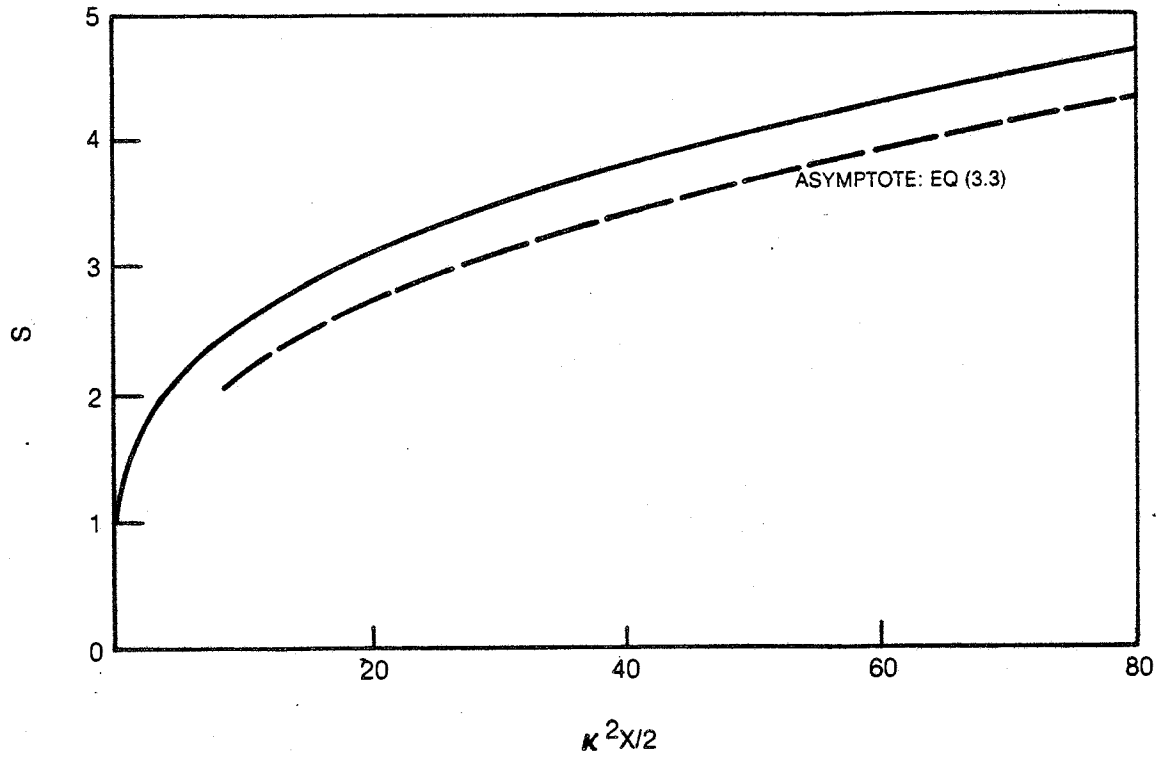


Figure 6 Wide Spacing Scalings



**Figure 7 Nonuniqueness in Cascade Flow
(a) Edge Shape**

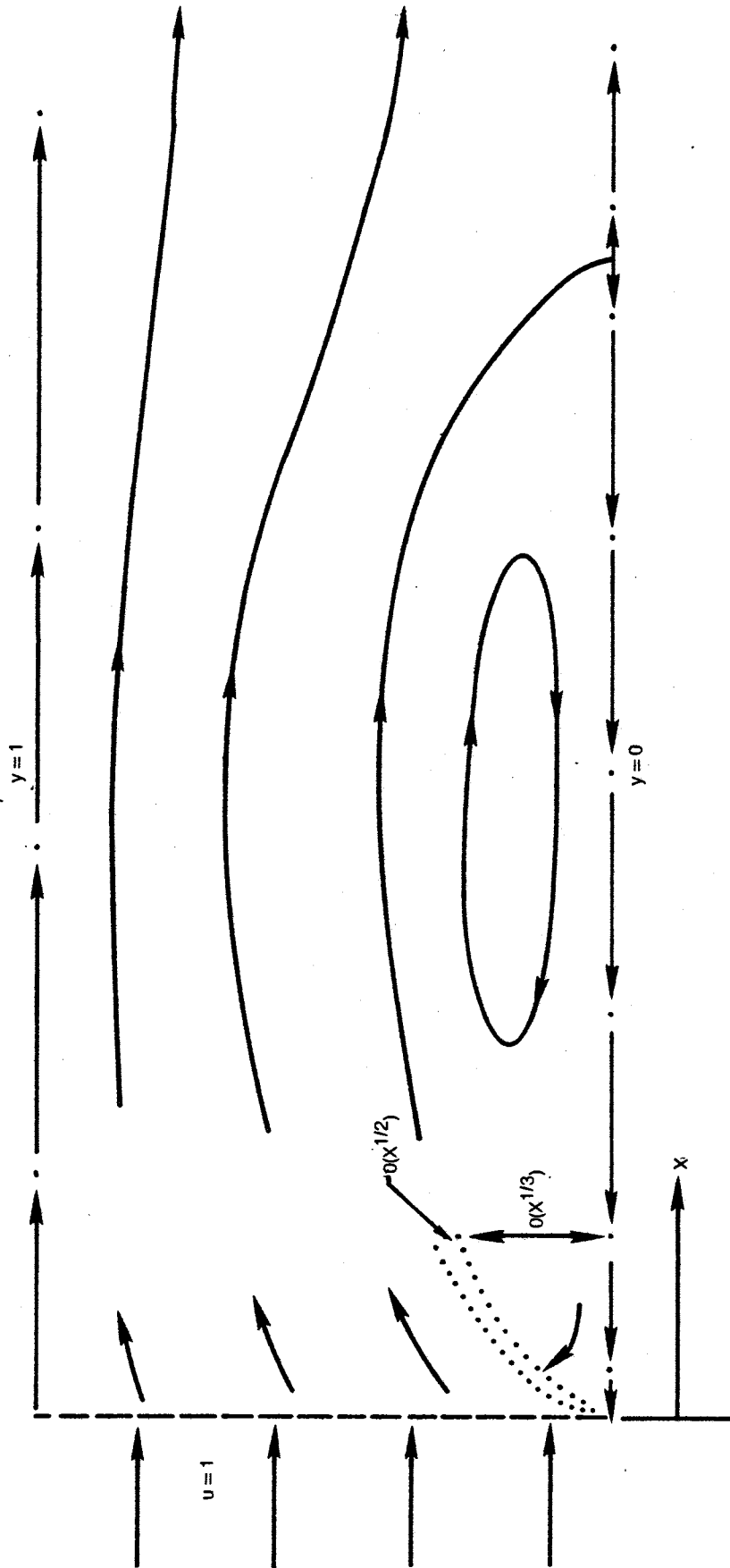


Figure 7 Nonuniqueness in Cascade Flow
(b) Branching From Pure Uniform State

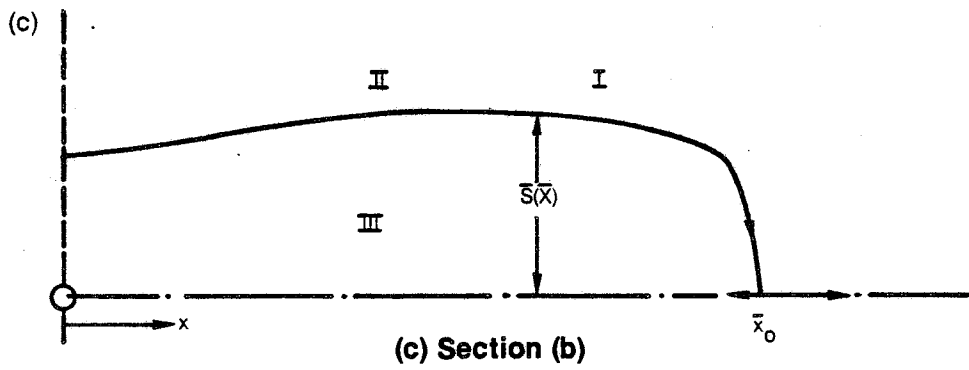
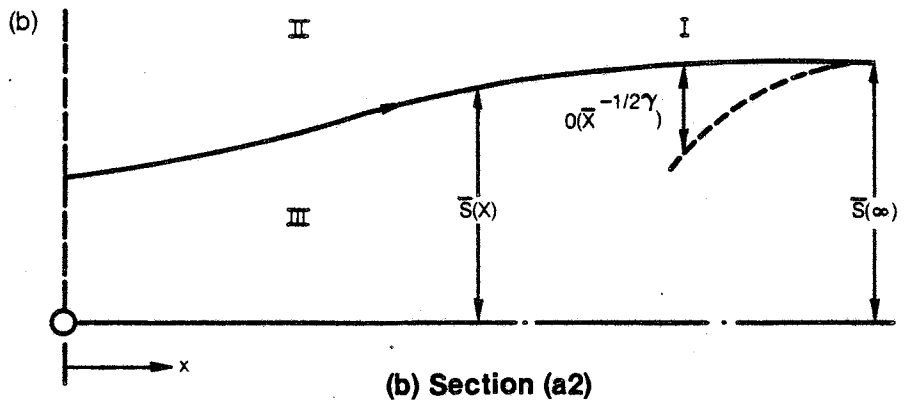
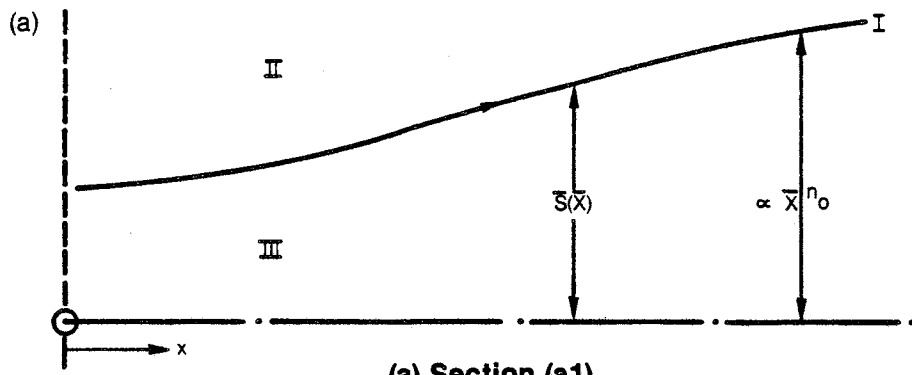


Figure 8 Eddy Properties

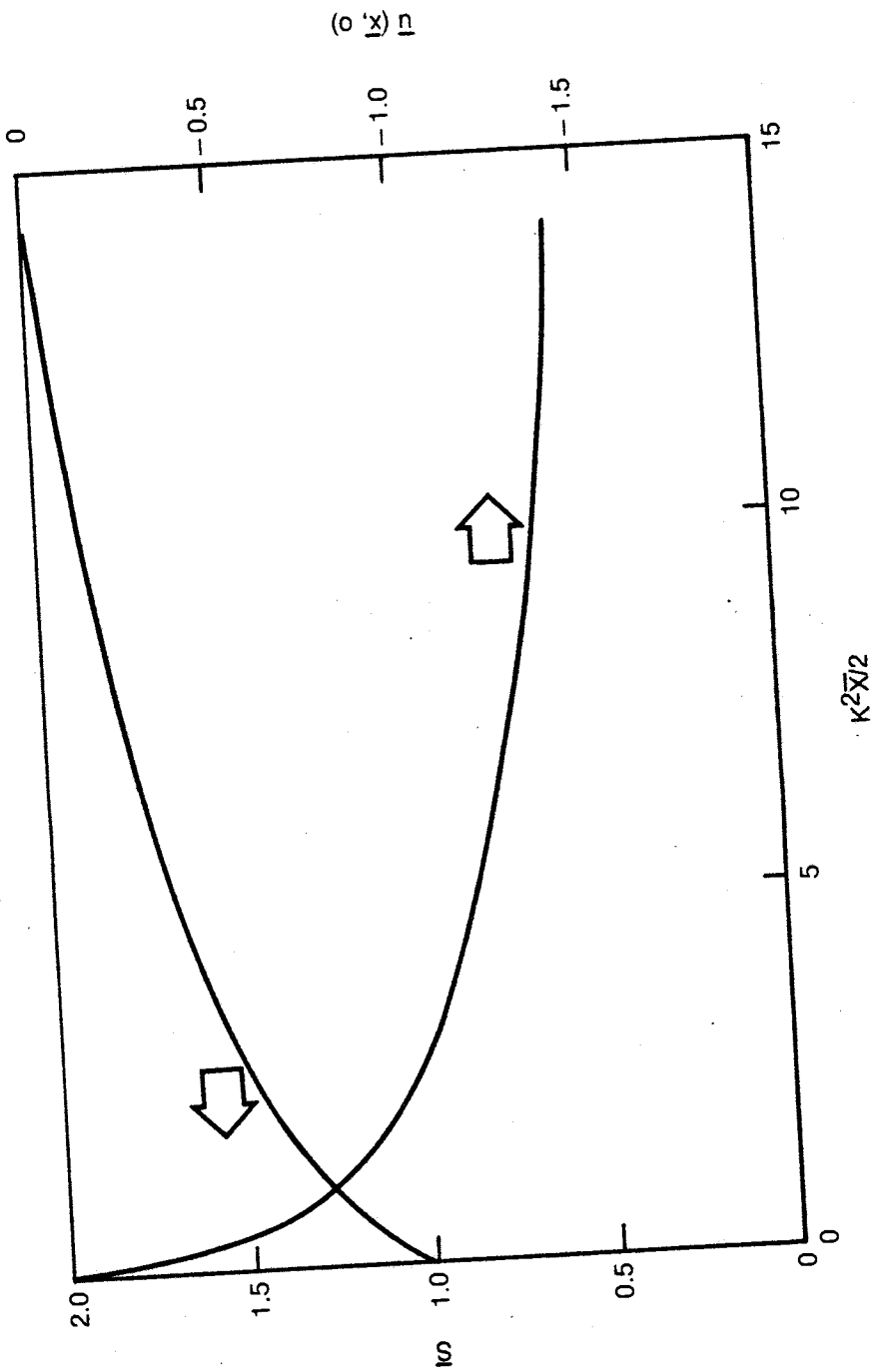
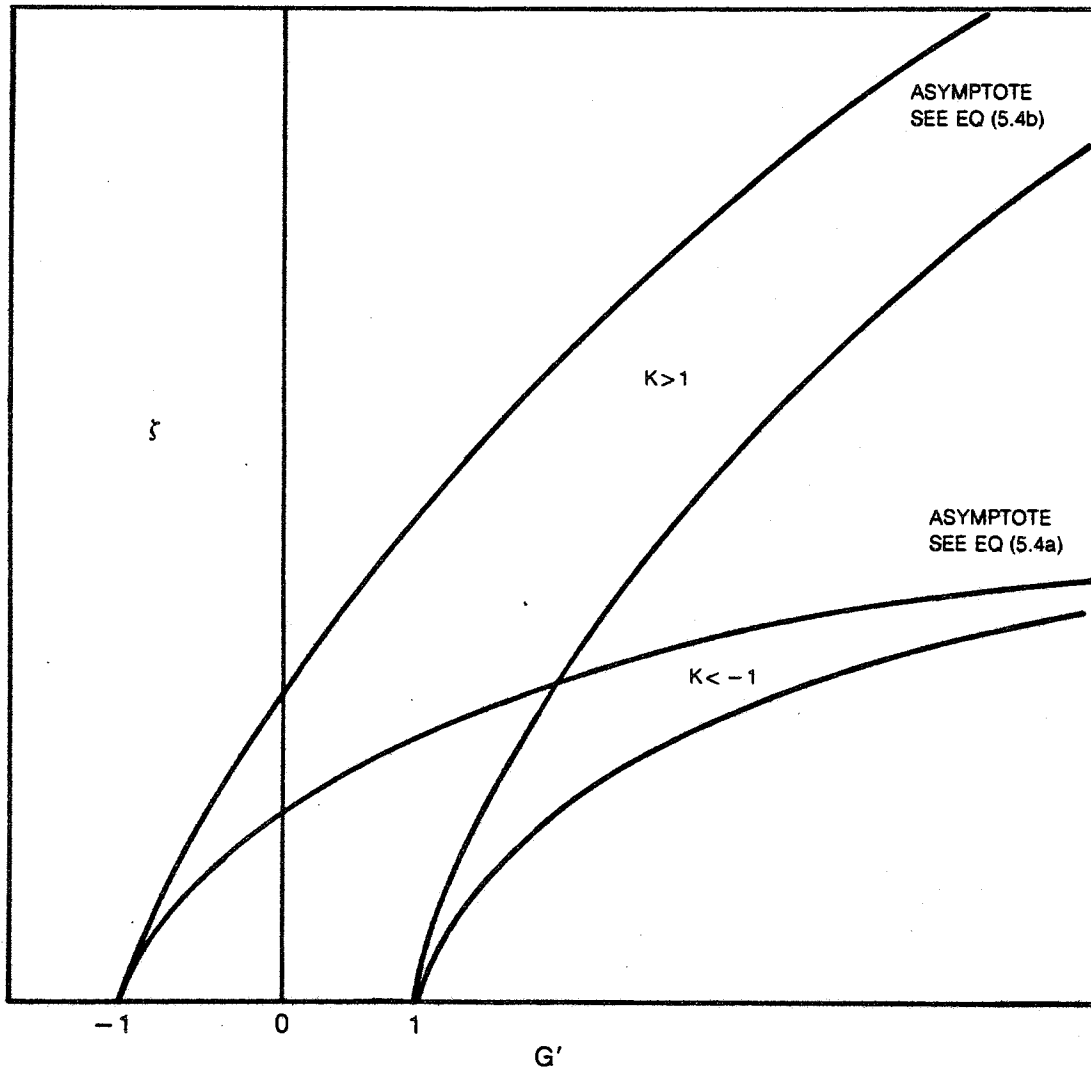


Figure 8 Eddy Properties
(d) Eddy Shape and Centerline Velocity, $\lambda = 1$



**Figure 9 Nonuniqueness in Wake Flows
(a) Near Field Velocity Functions**

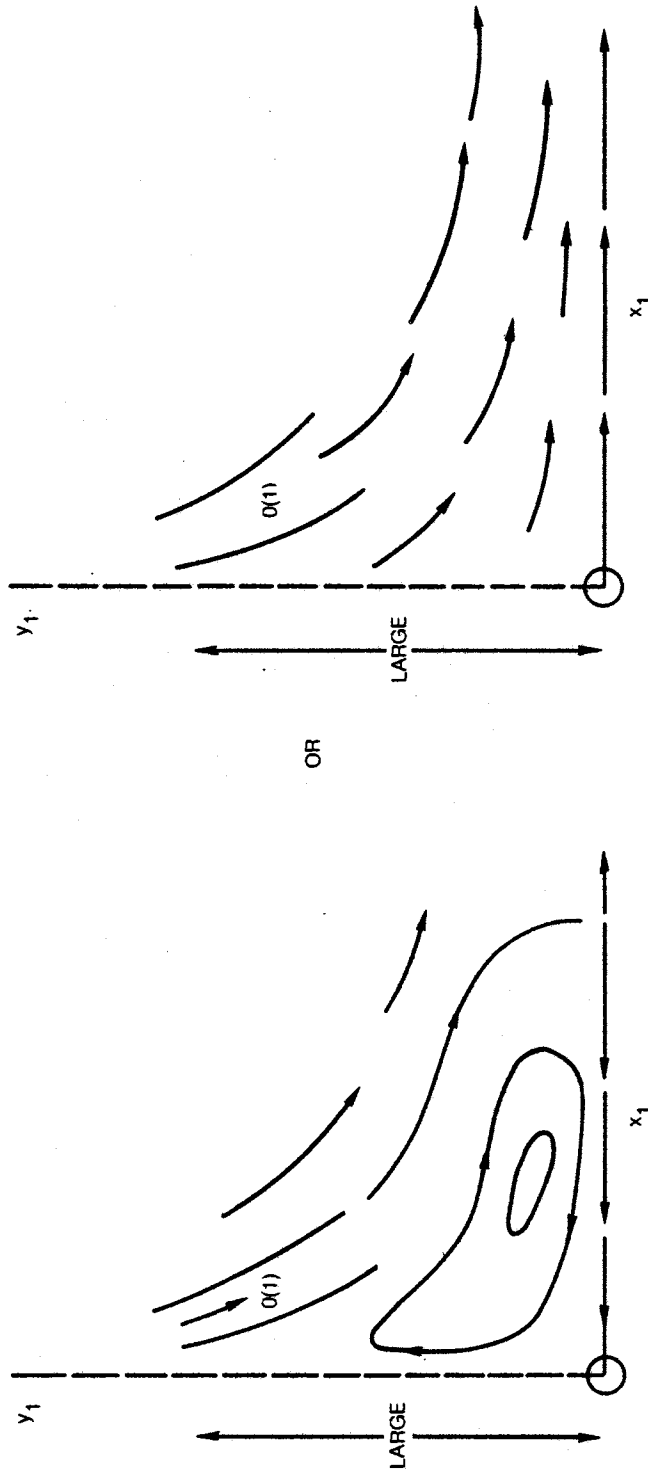
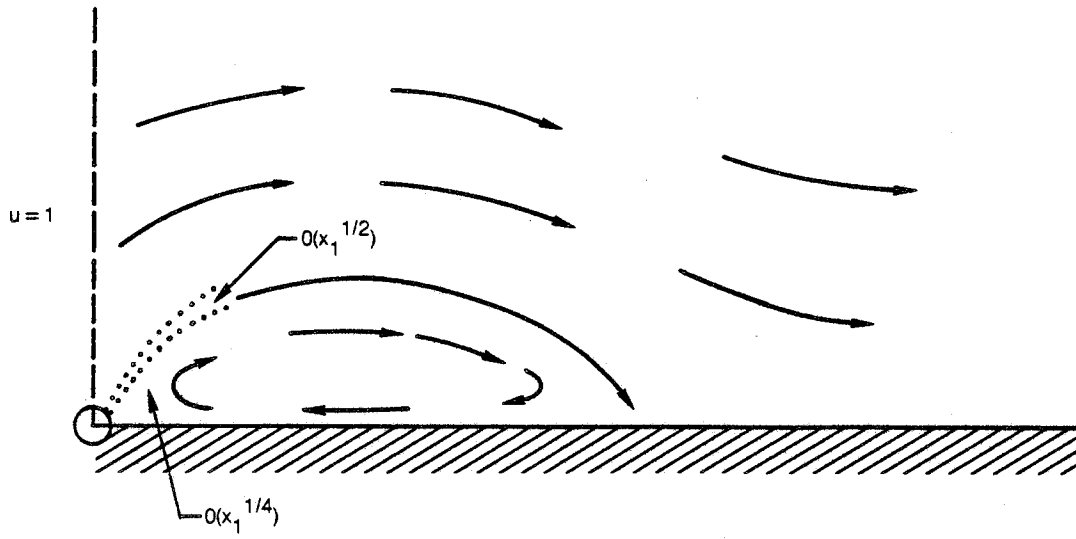
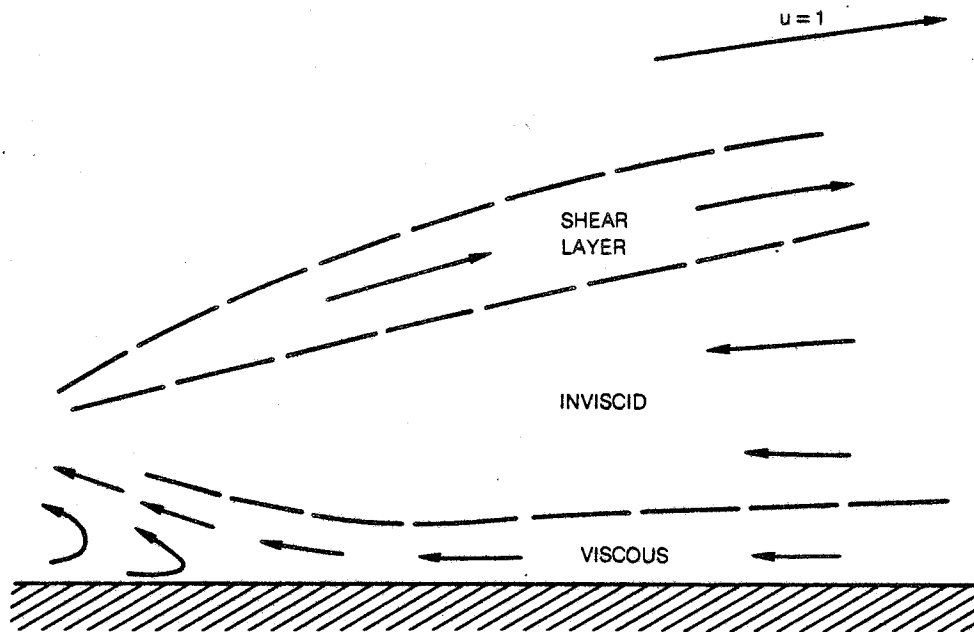


Figure 9 Non-uniqueness in Wake Flows
(b) Flow Structures for $K < -1$

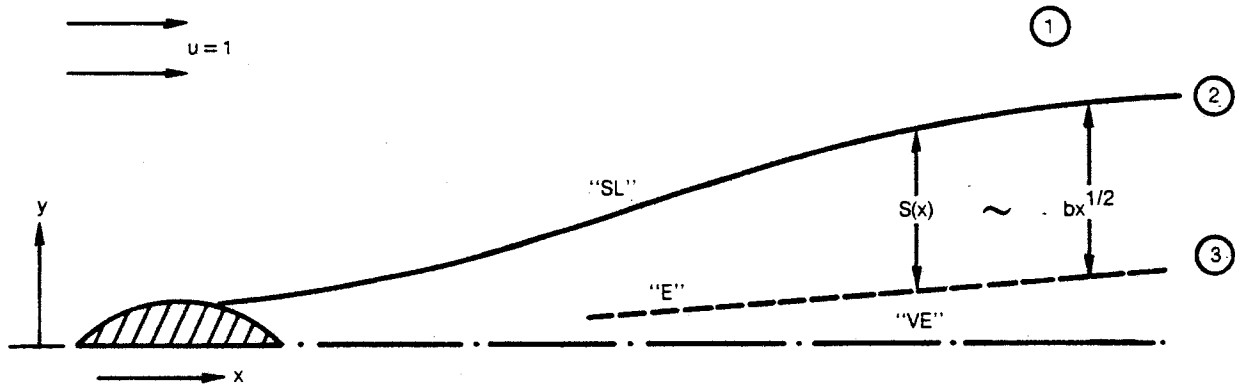


(a) Viscous Eddy Closure

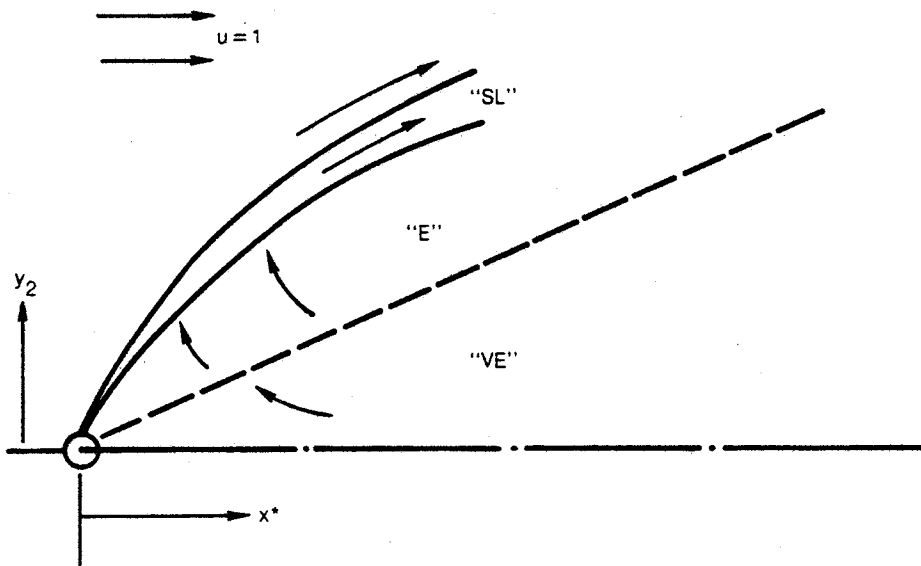


(b) Short Scale Flows — Secondary Separation

Figure 10 Solid Surface Reattachment



(a) Body Scale Motion



(b) Large Distance Structure $\sigma(Re)$

Figure 11 Large-Scale Separation Structure

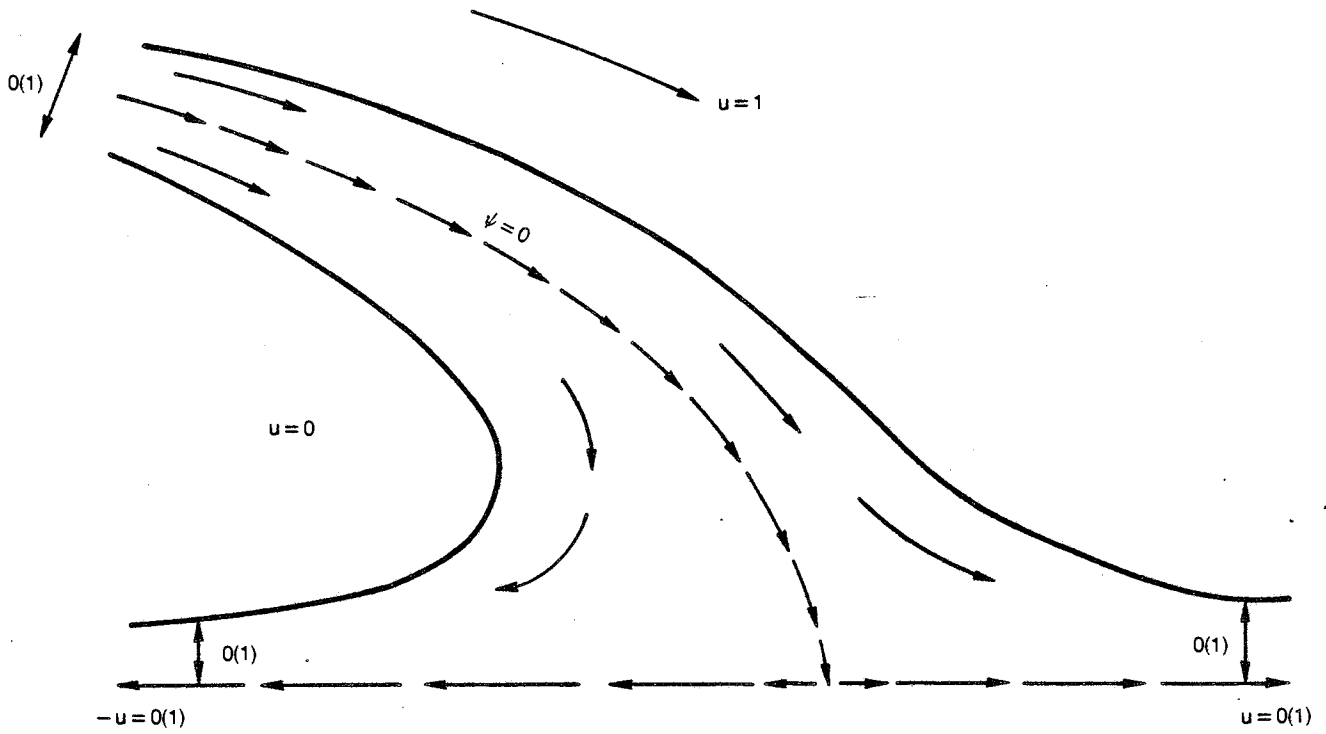


**Figure 11 Large Scale Separation Structure
(c) Inviscid Wake Closure Model**

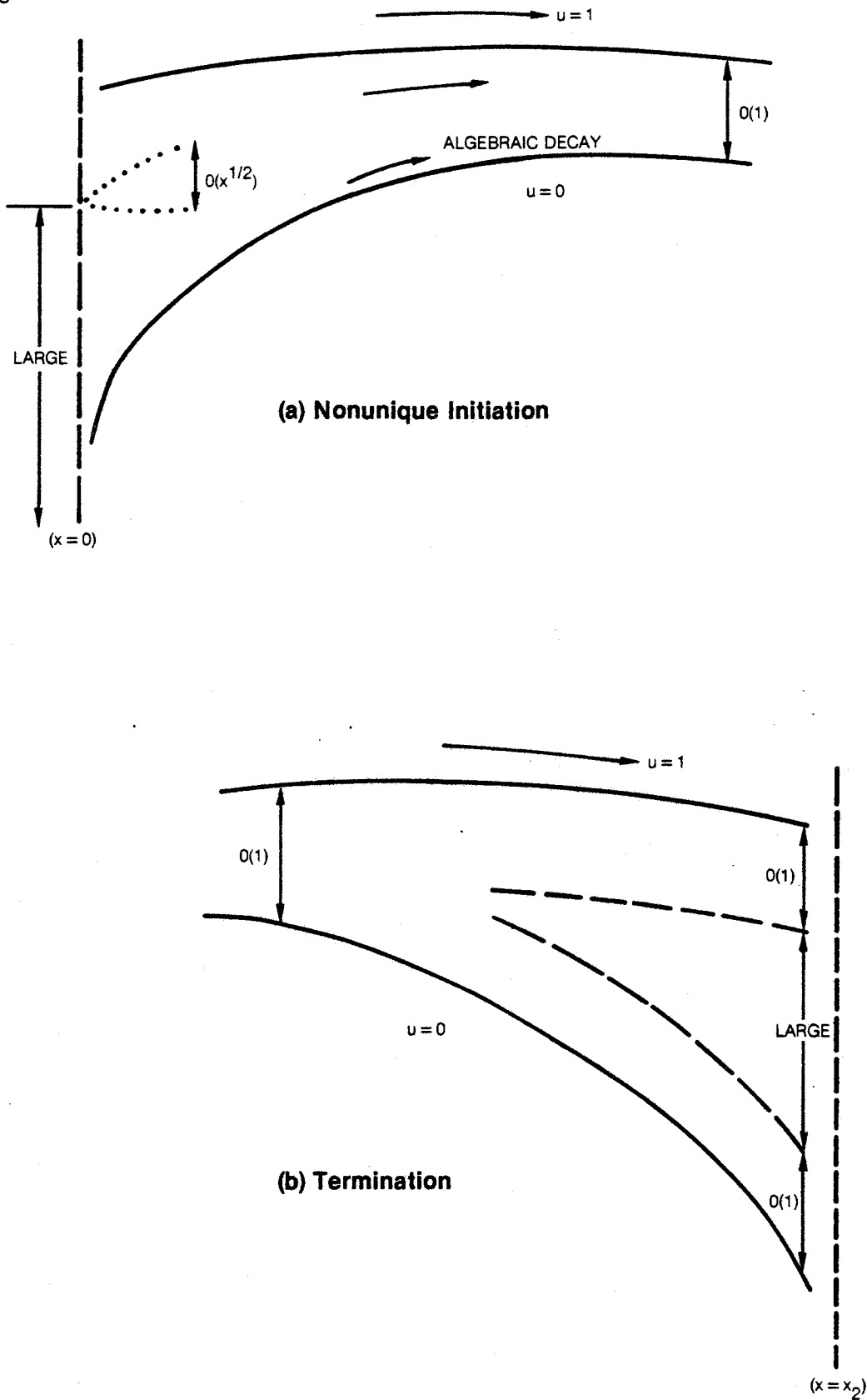


Figure 12 Non-entraining Shear Layer Structure

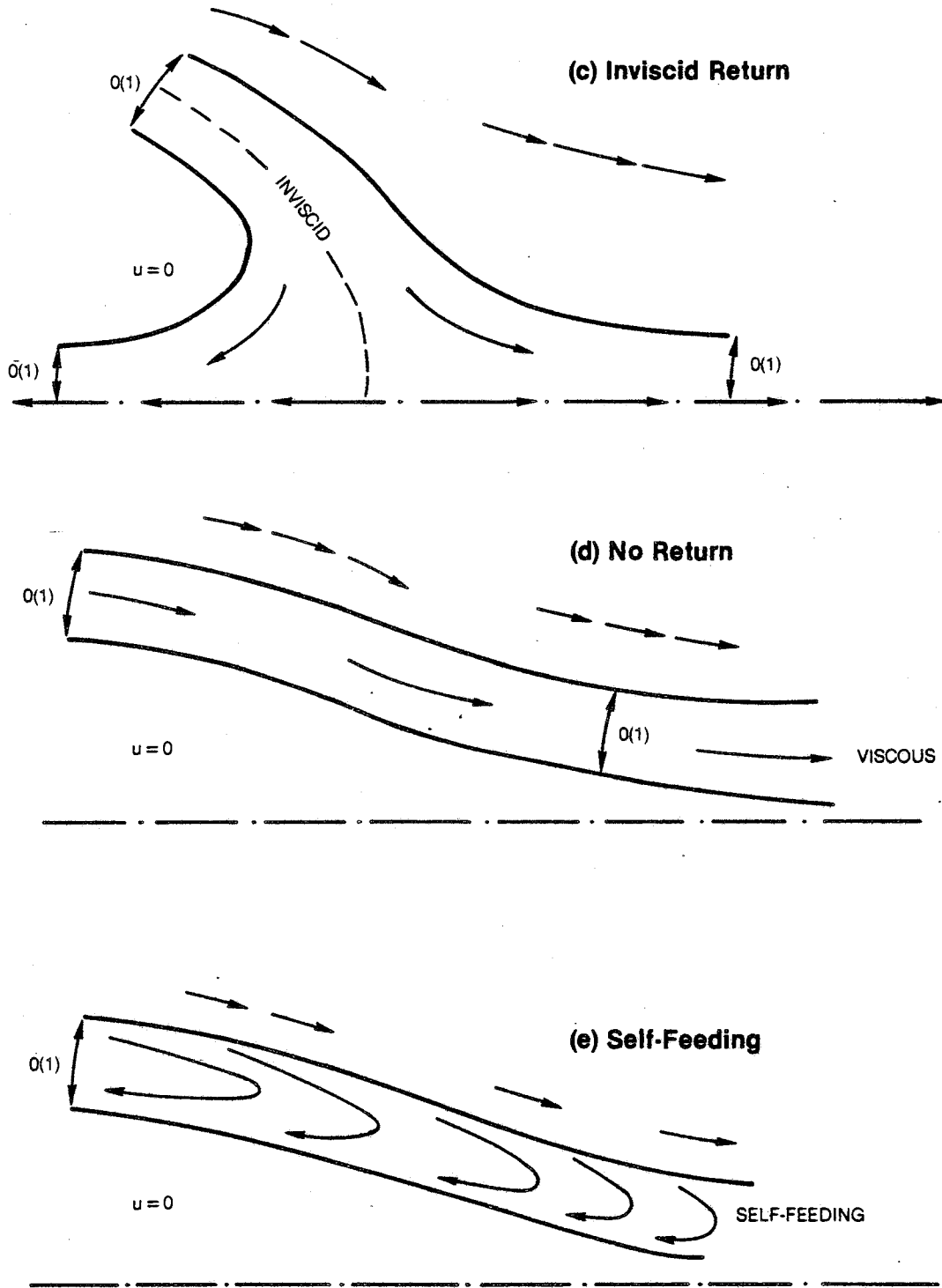


Figure 12 Non-entraining Shear Layer Structure